

**AD-A268 053****ATION PAGE**Form Approved  
OMB No. 0704-0188**1**

Average 1 hour per response, including the time for reviewing instructions, searching existing data sources, gathering the collection of information. Send comments regarding this burden estimate or any other aspect of this collection of information, including suggestions for reducing this burden, to Washington Headquarters Services, Directorate for Information Operations and Reports, 1215 Jefferson Avenue, Washington, DC 20540-6001, and to the Office of Management and Budget, Paperwork Reduction Project (0704-0188), Washington, DC 20503.

DATE

April 1993

3. REPORT TYPE AND DATES COVERED

THESIS/DISSERTATION

## 4. TITLE AND SUBTITLE

Application of a NEPTUNE Propulsion Concept to a Manned  
Mars Excursion

## 5. FUNDING NUMBERS

## 6. AUTHOR(S)

1st Lt Charles J. Finley

## 7. PERFORMING ORGANIZATION NAME(S) AND ADDRESS(ES)

AFIT Student Attending: The Ohio State University  
Graduate School8. PERFORMING ORGANIZATION  
REPORT NUMBER

AFIT/CI/CIA- 93-111

## 9. SPONSORING/MONITORING AGENCY NAME(S) AND ADDRESS(ES)

DEPARTMENT OF THE AIR FORCE  
AFIT/CI  
2950 P STREET  
WRIGHT-PATTERSON AFB OH 45433-776510. SPONSORING/MONITORING  
AGENCY REPORT NUMBER

## 11. SUPPLEMENTARY NOTES

## 12a. DISTRIBUTION/AVAILABILITY STATEMENT

Approved for Public Release IAW 190-1  
Distribution Unlimited  
MICHAEL M. BRICKER, SMSgt, USAF  
Chief Administration

## 12b. DISTRIBUTION CODE

## 13. ABSTRACT (Maximum 200 words)

**DTIC**  
**ELECTE**  
**AUG 17, 1993**  
**S B D****93 8 16 3****93-19024**  

## 14. SUBJECT TERMS

## 15. NUMBER OF PAGES

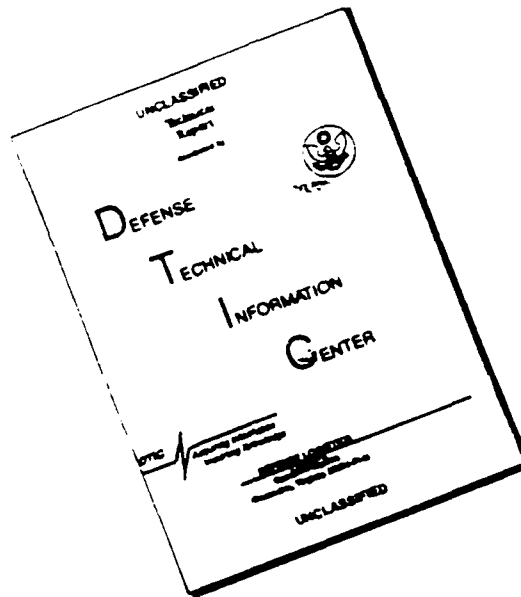
126

## 16. PRICE CODE

17. SECURITY CLASSIFICATION  
OF REPORT18. SECURITY CLASSIFICATION  
OF THIS PAGE19. SECURITY CLASSIFICATION  
OF ABSTRACT

## 20. LIMITATION OF ABSTRACT

# DISCLAIMER NOTICE



THIS DOCUMENT IS BEST  
QUALITY AVAILABLE. THE COPY  
FURNISHED TO DTIC CONTAINED  
A SIGNIFICANT NUMBER OF  
PAGES WHICH DO NOT  
REPRODUCE LEGIBLY.

92-11

# THESIS ABSTRACT

## THE OHIO STATE UNIVERSITY GRADUATE SCHOOL

**NAME:** Finley, Charles, Joseph

**QUARTER/YEAR:** Spring, 1993

**DEPARTMENT:** Aeronautical and Astronautical  
Engineering

**DEGREE:** M.S.

**ADVISER'S NAME:** Turchi, Peter, J.

**TITLE OF THESIS:** Application of a NEPTUNE Propulsion Concept to a  
Manned Mars Excursion

NEPTUNE is a multimegawatt electric propulsion system. It uses a proven compact nuclear thermal rocket, NERVA, in a closed cycle with a magnetohydrodynamic (MHD) generator to power a magnetoplasmadynamic (MPD) thruster.

This thesis defines constraints on an externally sourced propulsion system intended to carry out a manned Martian excursion. It assesses NEPTUNE's ability to conform to these constraints. Because an unmodified NEPTUNE system is too large, the thesis develops modifications to the system which reduce its size. The result is a far less proven, but more useful derivative of the unmodified NEPTUNE system.

<b>Accession For</b>	
NTIS GRA&I	<input checked="checked" type="checkbox"/>
DTIC TAB	<input type="checkbox"/>
Unannounced	<input type="checkbox"/>
Justification	
By	
Distribution/	
Availability Codes	
Dist	Avail and/or Special
A-1	

\_\_\_\_\_  
Adviser's Signature

DTIC QUALITY INSPECTED 3

**APPLICATION OF A NEPTUNE  
PROPULSION CONCEPT TO A  
MANNED MARS EXCURSION**

**A Thesis**

**Presented in Partial Fulfillment of the Requirements for the Degree  
Master of Science in the Graduate School of The Ohio State University**

**by**

**Charles Joseph Finley III, B.S. Astronautical Engineering**

**\* \* \* \* \***

**The Ohio State University**

**1993**

**Master's Examination Committee:**

**Approved by**

**Dr. P. J. Turchi**

**Dr. H. A. Oz**

---

**Adviser**

**Department of Aeronautical  
and Astronautical Engineering**

**to the greatest family and greatest friends in the world  
(and to whoever the lucky guy is that gets to enjoy them)**

## VITA

April 28, 1968 .....	Born - Boston, Massachusetts
1990 .....	B.S., United States Air Force Academy, Colorado Springs, Colorado
1990-1991 .....	Undergraduate Pilot Training, Laughlin Air Force Base, Texas
1992 .....	Astronautical Engineer, Air Force Phillips Laboratory, Albuquerque, New Mexico

## FIELD OF STUDY

Major Field: Aeronautical and Astronautical Engineering  
Studies in Electrical Engineering, Nuclear Engineering,  
and Plasma Physics

## TABLE OF CONTENTS

DEDICATION .....	ii
VITA .....	iii
LIST OF TABLES .....	vi
LIST OF FIGURES .....	vii
CHAPTER	PAGE
I. INTRODUCTION	1
1.1 Problem Statement .....	3
1.2 Nature of the Problem .....	3
II. BACKGROUND	6
2.1 The Elements of NEPTUNE .....	6
2.2 NEPTUNE as a System .....	15
III. APPROACH	22
3.1 Specific Mass Budget .....	23
3.2 Delta-V for Impulsive Mars Mission .....	26
3.3 Specific Mass Formula .....	36
IV. ANALYSIS OF TRIP-TIME AND SPECIFIC MASS	41
4.1 Delta-V for Impulsive Mars Mission .....	41
4.2 Specific Mass Budget .....	44
4.3 Specific Mass Values .....	52
4.4 Solving the Problem .....	55
V. NEPTUNE DEVELOPMENT AREAS	56
5.1 Nonequilibrium MHD .....	57
5.2 Particle Bed Reactor .....	72

VI.	ANALYSIS OF NEPTUNE SYSTEM	76
6.1	Thermodynamic Analysis of the NEPTUNE Loop . . . . .	76
VII.	CONCLUSIONS	89
APPENDICES		
A.	Routine for Calculating Delta-V Values for Round Trip Mars Scenarios	92
B.	Output for Short and Long Mars Options	98
C.	Feasibility of Schwing Trajectory for NEPTUNE	107
D.	Routine for Calculating Delta-V Values for Mars Mission with Schwing Trajectory	111
E.	Feasibility of Nonequilibrium MHD for NEPTUNE	119
	LIST OF REFERENCES	123



## LIST OF TABLES

TABLE		PAGE
4.1	Minimum delta-v round-trip Mars trajectories for each option . . . .	43
4.2	NEPTUNE specific mass budget . . . . .	44
5.1	Ionization energies of NEPTUNE fuel possibilities . . . . .	63
6.1	Thermodynamic data of NEPTUNE loop . . . . .	88

## LIST OF FIGURES

FIGURES		PAGE
2.1	Prismatic reactor .....	7
2.2	MHD fields .....	9
2.3	Induced E.M.F. ....	11
2.4	Schematic diagram of MHD .....	12
2.5	MPD thruster .....	14
2.6	Ion/electron reactions to Lorentz force .....	14
2.7	NEPTUNE .....	16
3.1	Hohmann trajectory .....	30
3.2	Block diagram of NEPTUNE loop .....	36
4.1	Variance of delta-v with mission time of flight for short option .	46
4.2	Variance of delta-v with mission time of flight for long option .	47
4.3	Variance of specific mass budget with mission time of flight for short option .....	48
4.4	Variance of specific mass budget with mission time of flight for long option .....	49
4.5	Effect of burn time on specific mass budget for short option ...	50
4.6	Effect of burn time on specific mass budget for long option ...	51
5.1	Creating a nonequilibrium gas .....	71
5.2	Particle bed reactor .....	73

6.1	Points of thermodynamic evaluation of NEPTUNE cycle . . . . .	77
6.2	Carnot cycle . . . . .	78
6.3	PV diagram of NEPTUNE loop . . . . .	79
C1	Swingby velocity savings . . . . .	107
E1	Series of MHD generators . . . . .	122

## **CHAPTER I -- INTRODUCTION**

NEPTUNE<sup>1</sup> is Nuclear Electric Propulsion Technology Using NERVA. Its main components consist of the NERVA nuclear thermal rocket, acting as the power source in a closed cycle system, a magnetohydrodynamic (MHD) electricity generator, a magnetoplasmadynamic (MPD) thruster, and the associated devices to remove waste heat from the system (i.e. radiator). It is intended as a step towards a high power nuclear electric propulsion technology.

The competition between conventional chemical propulsion technologies and less established, yet potentially more rewarding, nuclear thermal rocket engines began in the late sixties and continues to the present. So far, chemical systems have carried the burden successfully. They have met the needs of the missions they've been designed to support. They have been proven safe, reliable, high-thrust propulsion options, and this has always been good enough.

NEPTUNE represents a new class in the competition for high-thrust propulsion. It introduces electric propulsion for applications in ambitious high-thrust missions. Immediately the question arises -- if nuclear thermal propulsion was not necessary, why is nuclear electric propulsion necessary?

The answer is simple. Though the space race stagnates at times, the future will certainly bring with it more ambitious and more frequent departures from earth. The past

has shown that chemical propulsion is a good enough way to meet new goals, but eventually there will be a calling for the "best" way.

Is nuclear electric propulsion the best way to propel a spacecraft? It is unlikely. There is a lot of physics to be resolved before words like "best" will become appropriate. For now, however, it is sufficient to say nuclear electric propulsion is a better way than either chemical or nuclear thermal propulsion.

This presently unsupported statement will hopefully gain support in this thesis, but the basics are clear. The breaking of nuclear bonds generate more energy than the breaking of chemical bonds. More energy is available from less material if nuclear energy is harnessed. If ever there was a forum where mass must be minimized, it is space. Nuclear energy is made for space.

The comparison of nuclear thermal to nuclear electric technologies must focus on the better way to use nuclear energy. It is natural to first consider nuclear thermal rockets. Nuclear thermal rockets represent the use of nuclear power to imitate chemical rockets -- the basic difference being the origin of the energy.

But this should not be the only difference. Nuclear energy manifests itself in a very different manner than the energy available in chemical rockets and it is made for the closed cycle. That is its nature. The nuclear fuel does not become the coolant that carries the energy out of the system. The coolant can be cycled past the source, as it is in ground-based plants. It is different from a chemical source in that capacity, and it creates the opportunity to use the energy in a different way -- the most effective way.

It is unnecessary to use a nuclear sourced system to mimic chemical systems. The energy should be used in the best way to apply a large acceleration to a reasonable mass. The following chapters will explain why electromagnetic forces are the best way to use this energy.

### **1.1 -- PROBLEM STATEMENT:**

This thesis will deal with the problem of using the NEPTUNE propulsion concept as the primary propulsion source for a manned Martian excursion. It will define a round trip Martian trajectory of less than two years based on the delta-v parameter of that mission. It will derive a budget for the mass of a nuclear electric propulsion system to undertake that mission, and it will analyze NEPTUNE's ability to accommodate that budget.

In the event that NEPTUNE, in its purest form, is unable to meet the budgetary constraints on its mass, suggested modifications to the system will be presented and analyzed which will allow it to meet them.

### **1.2 -- NATURE OF THE PROBLEM**

Although creating a propulsion system specific to a mission seems to add an element of complexity to the analysis, it actually adds system constraints that make analysis possible. This strategy allows the problem to be approached from two directions. First, the mission is known. A round-trip mission to Mars is the goal. Moreover, it is a manned venture, putting definite constraints (less than two years) on the mission length.

There are characteristics of a round-trip Martian trajectory, lasting less than two years, that are independent of the propulsion system used. Therefore, NEPTUNE must first conform to these constraints.

The problem may be attacked from a second direction because the propulsion system to be used in the mission is also known. NEPTUNE has definite limitations. The NERVA source is limited in its capacity to produce power. Its electrical generator is limited in its capacity to convert power, and its electric thruster is limited in its ability to use the power. Enough is known about NEPTUNE's components to dictate mass estimates for the system based on the mission demands. However, enough is left unknown about NEPTUNE's components to allow for a manipulation to accommodate an ambitious mission.

NEPTUNE is a nuclear electric propulsion system. Nuclear electric propulsion (NEP) concepts have a number of advantages over traditional chemical and even nuclear thermal systems, or other electric propulsion systems. Because they use electromagnetic field forces to accelerate propellants, extremely high exhaust velocities are possible. Additionally, relatively few moving parts are involved in thrust production, so a definite reliability is inherent. Most importantly, however, NEP systems bridge the gap between electric propulsion and thermal systems because of the high power source that anchors them. The power going into the thruster can be higher than otherwise sourced electric propulsion systems (i.e. battery, solar) and can therefore accelerate more propellant. As a result, the range of their usefulness might not exclude higher thrust missions if sufficiently high power nuclear sources are available.

The manned Mars mission from low earth orbit (LEO) is one of a class of missions in the intermediate thrust range. It does not originate from the earth's surface, so it does not require so much instantaneous thrust as missions having to overcome surface gravity. However, the "manned" aspect of the mission limits the allowable time for the mission, which leads to significant thrust requirements.

This thesis will analyze NEPTUNE's ability to fulfill the requirements of this class of mission. In terms of specific impulse, it operates as an electric propellant accelerator, capable of exhaust velocities above 50,000 m/s. In terms of thrust, it has a source powerful enough to produce multimewatts of power. NEPTUNE would seem to accommodate that intermediate region (which encompasses most manned planetary space transfers) in which the craft is moved only from planetary orbit to planetary orbit.



## **CHAPTER II – BACKGROUND**

Although the merits of NEPTUNE are fully understood only when the system is considered as a whole, it is useful to first describe the elements of the system as they stand alone to provide sufficient background as to how they succeed together.

### **2.1 – THE ELEMENTS OF NEPTUNE:**

#### **REACTOR SOURCE:**

The subsystem that anchors the NEPTUNE concept is a compact, high power nuclear rocket. As the name implies, the concept would ideally employ a NERVA-style nuclear thermal rocket as the power source. It is a tested reactor and rocket engine combination, projected to be able to generate flow stagnation temperatures of 2500 K, thrust levels up to 75000 lbs, and specific impulse values above 750 seconds.<sup>2</sup>

The NERVA reactor is of prismatic type. In it a gaseous hydrogen coolant flows longitudinally through eight canals surrounded by a homogeneous mixture of uranium fuel and moderator. As the hydrogen gas passes over the fissioning fuel, the heat byproduct of the nuclear reaction taking place is transferred to the hydrogen working fluid.

If the engine is acting in its intended capacity, as a nuclear thermal rocket, the hot working fluid then passes through a nozzle, transferring the heat energy into kinetic energy of flow, and is expelled out of the system. The momentum transfer of the high

velocity hydrogen produces thrust just as the expulsion of the byproducts of chemical propellants do when they are thrown from traditional chemical systems. Because the molecular mass of  $H_2$  is low, the specific impulse of this type of system is high. However, the momentum flux (i.e. thrust) of the flowing gas is reasonably high as well because the reactor is able to add heat energy to a substantial total mass flow of hydrogen gas.

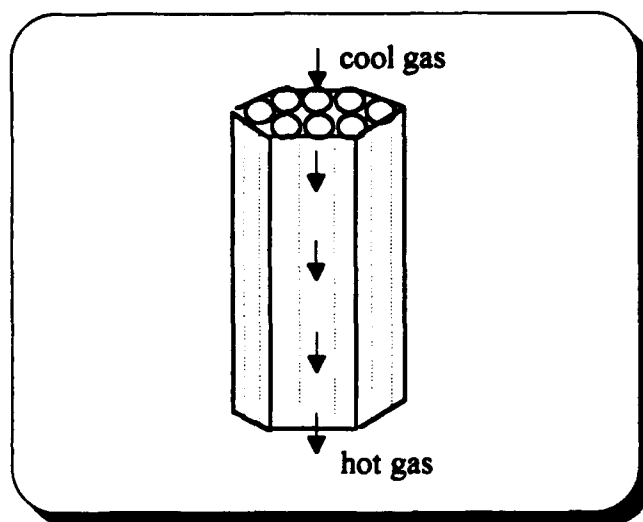


Figure 2.1 -- Prismatic Reactor<sup>3</sup>

Basically, NEPTUNE has two requirements in its power source. It must have the capability to transfer heat energy at the rate of 100 to 1000 MW to a gaseous coolant, and secondly, it must be compact enough for space travel. NERVA was designed with these very same goals in mind, making it a natural selection for the NEPTUNE system.

## MHD GENERATOR:

Normally, a NERVA nuclear rocket would expel its high energy propellant through a nozzle to produce thrust in an open thermodynamic cycle. However, in NEPTUNE, the rocket must be operated on a closed-cycle. The gaseous coolant exits NERVA's nozzle and enters a magnetohydrodynamic (MHD) generator.

Magnetohydrodynamic power generation is the conversion of the kinetic energy carried by a moving, electrically conducting fluid (e.g. plasma) into electrical energy by interaction of the fluid with a magnetic field. The velocity and the conductivity each tell something about the gas in an MHD system. The velocity indicates how much energy the gas has. The conductivity,  $\sigma$ , is one of the parameters used to determine the magnetic Reynolds Number:

$$Re_m = \sigma \mu u L \quad (2.1)$$

The magnetic Reynolds Number is a parameter that helps to define the ease with which the energy in the fluid can be extracted in the form of electric power. As a result, the most efficient system will involve a gas with not only high velocity, but high conductivity.<sup>4</sup>

The drawing of the fluid element uses vector geometry to describe the electromagnetic phenomenon that will be encountered in an MHD generator. In the volume element, consider a flowing plasma gas with velocity,  $u$ , and scalar conductivity,  $\sigma$ . As such a gas passes through a magnetic field of strength  $B$ , a current density is induced according to the formula:

$$\vec{j} = \sigma (\vec{E} + \vec{u} \times \vec{B}) \quad (2.2)$$

$j$  : current density  
 $\sigma$  : conductivity  
 $u$  : flow velocity

B : magnetic field

E : electric field

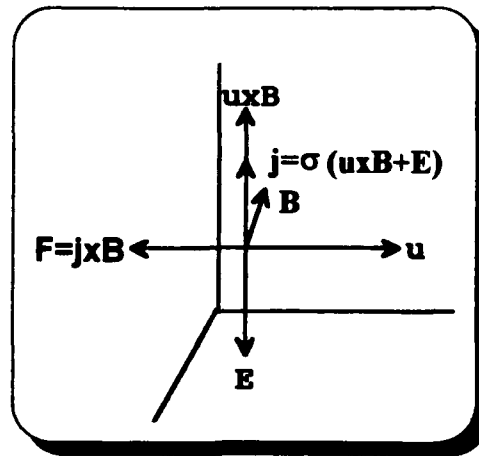


Figure 2.2 -- MHD Fields<sup>5</sup>

where **E** is the internal electric field induced to support the load. If a parameter **K** is defined as:

$$K = \frac{E}{uB} \quad (2.3)$$

then the current density can be rewritten:

$$j = (1 - K)\sigma uB \quad (2.4)$$

The intent of an MHD generator is to create power to support a load. The amount of power it can produce is related directly to the current density via the formula:

$$P_0 = jE = K(1 - K)\sigma u^2 B^2 \quad (2.5)$$

$P_0$  : generator power density

If the above relations are rearranged, the output electric field and power per unit volume as a function of current are defined as:

$$E = uB - \frac{j}{\sigma} \quad (2.6)$$

$$P_0 = juB - \frac{j^2}{\sigma} \quad (2.7)$$

Therefore, the voltage varies linearly and the power quadratically with current (as is the case with most power sources).<sup>4</sup>

The vector diagram pictures a  $j \times B$  force acting in a direction opposite the gas flow:

$$F = jB = (1 - K)\sigma u B^2 \quad (2.8)$$

This force slows the gas because it acts opposite to the direction of motion. It requires only a basic understanding of the law of conservation of energy to see that as the gas slows and the corresponding kinetic energy decreases, the energy must manifest itself in some other form, rather than just disappear. In the case of the MHD generator, it is manifested in the form of an electric field.

Having analyzed the electromagnetic events which are taking place in an MHD generator, the next step is to consider the device as a working system. A basic MHD generator system can be broken into three regions. The first of these expands a high-temperature gas through a nozzle to a high velocity. The high-temperature gases may be produced by a gaseous fission or fusion reactor or by a high-energy combustor. From there, the necessary level of ionization is added to the gas. To increase the electrical conductivity of the gases, they are often seeded with an easily ionizable substance, such as potassium or cesium. This region may or may not be included with the first. It will depend upon the amount of energy initially in the gas and the difficulty with which the gas achieves ionization.

Finally, the gas enters into a third region where the actual power generation takes place. In this region the flowing plasma is passed through a magnetic field region which contains a series of pairs of electrodes at either side of the magnetic channel. The electrode pairs face each other and lie in the plane parallel to the plane described by the flow and magnetic field directions, which are at right angles to each other.

When the conducting fluid enters the magnetic field, interaction will occur and an induced electric field is established normal to the flow and magnetic field directions and

between the electrode pairs. This field can then be used to drive a current via the electrodes to an external load where it is allowed to perform work. In doing so, the kinetic or potential energy of a gas is converted into electrical energy.

Consider a flowing gaseous conductor in a uniform magnetic field  $B$ . An e.m.f. ( $u \times B$ ) is set up at right angles to the velocity vector and the field as shown in the previous diagram. If the Hall number (the tendency of the electrons to carry current in the direction of the flow) is very small, then a current will flow parallel to the induced e.m.f. The induced e.m.f. is the charged particle separating force caused by the magnetic field.

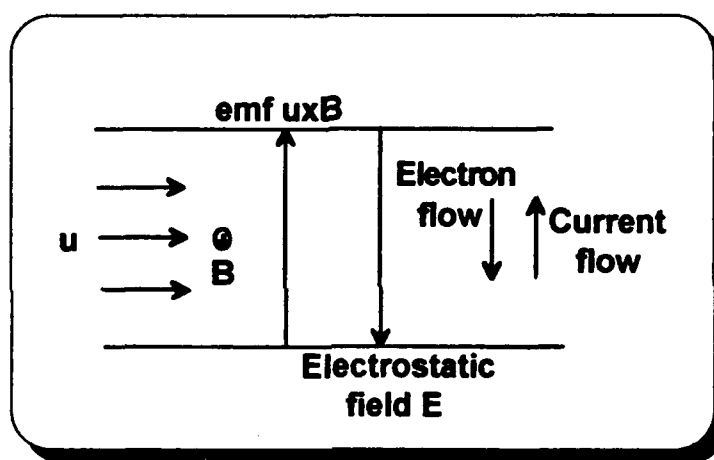


Figure 2.3 -- Induced E.M.F.<sup>4</sup>

In the absence of electrodes, as in the above diagram, open circuit conditions prevail and the electrons will flow downwards and the positive particles will flow upwards. As the charges separate, there results a distribution of charge (electrostatic field) which opposes the induced e.m.f. and eventually is sufficient to balance the tendency for charge separation. Therefore, e.m.f. and further current flow is prevented,  $E = -u \times B$ .

In order to allow the e.m.f. to drive a current through an external load, it is necessary to reduce the strength of the electrostatic field. This is achieved by immersing electrodes, which are connected to a load, into the fluid as shown in the second diagram. A restricted flow of electrons then occurs from the cathode through the fluid to the anode returning to the cathode via the external load. The driving force on the electrons is equal to the difference between the induced e.m.f. and the electrostatic field  $E$  and is called the total e.m.f. The actual value of the total e.m.f. depends on the value of  $E$ , which depends, by Ohm's law, on the total resistance of the electron circuit.<sup>5</sup>

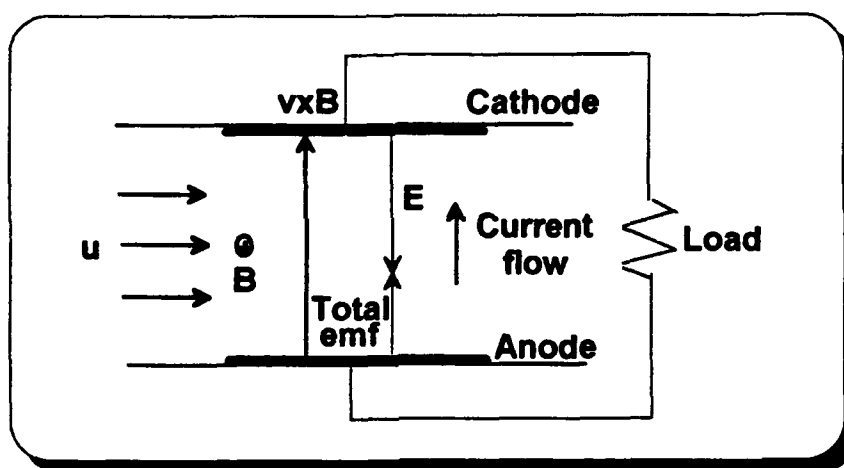


Figure 2.4 -- Schematic diagram of MHD<sup>4</sup>

In principle, MHD converters draw a simple analogy to conventional electric generators. A rotating-type generator produces electric power by moving a metallic conductor across a magnetic field. In a plasmadynamic converter, a conducting gas moves through a magnetic field. An electric potential difference develops across two electrodes which are placed perpendicular to the flow direction and to the magnetic field. The power output of the generator, like that of the conventional rotating-type generator, is a function

of the magnetic field strength, of the velocity of the conducting gas through the field, of the linear dimensions of the device, and of the conductivity of the working medium.<sup>4</sup>

Ideally, all of the energy taken from the slowing down of the flow would be transferred to electrical energy manifested in MHD power to drive the load. In reality, energy must go to generating the magnetic field and powering an ionizing source to create the working plasma. This adds new loads to the circuit, in addition to the thruster. Energy is also lost to resistive heating stemming from obstructions in the plasma as the current moves through.

In simple terms, an MHD generator is little more than a plasma accelerator acting in reverse. In the generator, the inlet velocity of the gas is greater than  $E/B$ . In this situation, the flow will be decelerated, and current will be driven through an external load by the motional electromotive force. Reversing the conditions would accelerate the flow.

Because the MHD and magnetoplasmadynamic (MPD) accelerators are so similar, they potentially mate into attractive and complementary systems for electric space propulsion. Since the spacecraft must already be set up to handle plasma (possibly seeded to aid ionization) flow through its channels if it uses an MPD accelerator, little modification will be necessary to accommodate the MHD generator to support the thruster. This kind of component coupling is an example of how careful engineering eliminates complexity and the associated system mass. This same combination of components is considered in the NEPTUNE concept.



# MPD THRUSTER:

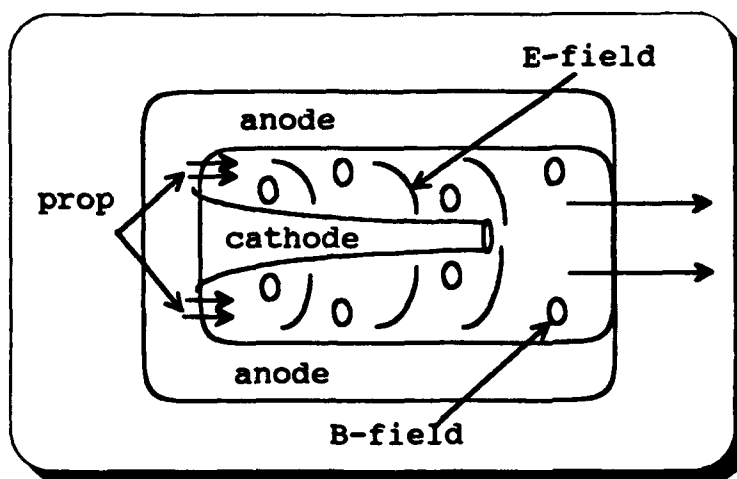


Figure 2.5 -- MPD thruster

The third major subsystem associated with NEPTUNE is the thruster. A magnetoplasmdynamic (MPD) thruster is an electric thruster which employs the same cross-field electromagnetic theory used by the MHD generator. However, the thruster reverses the processes and takes electric energy from a DC source and uses it to accelerate plasma electromagnetically for the purpose of producing thrust.

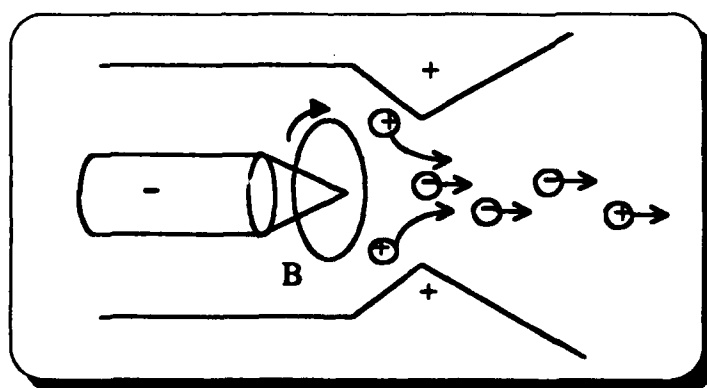


Figure 2.6 -- Ion/electron reactions to Lorentz force

MPD thrusters hold a major advantage over other types of electric thrusters because they use the Lorentz force to produce thrust:

$$\vec{F}_{thrust} = \vec{j} \times \vec{B} \quad (2.9)$$

In so doing, the plasma, with its component electrons and ions, though responding to fields oppositely, are accelerated in the same direction and exit the craft together. Though the gas has free charges, it is electrically neutral and problems associated with charge build-up are nonexistent.

In principle, MPD thruster performance should improve with increased power because thrust density and specific impulse are increasing functions of arc current<sup>6</sup>:

$$\vec{F}_{thrust} = \frac{\mu_0}{4\pi} \left( \ln \frac{r_a}{r_c} + \frac{3}{4} \right) J^2 \quad (2.10)$$

J : thruster current  
 $r_a$  : anode radius  
 $r_c$  : cathode radius  
 $\mu_0$  : permeability of free space

## 2.2 – NEPTUNE AS A SYSTEM:

Chemical propulsion systems have traditionally carried the burden of high thrust space ventures because they are able to expel a large amount of mass at a reasonable exhaust velocity. Consequently, the change in momentum, the thrust force, is high enough to kick spacecraft in the right direction to its destination, despite the forces of gravity resisting that change. Electromagnetic field based propulsion systems are traditionally designed for less ambitious missions. In the past, the power contained in the field accelerator has been too small to accelerate enough propellant to produce high thrust. What makes this a shame is the fact that field thrusters can accelerate propellants to much higher velocities than conventional thermodynamic accelerators on chemical systems. If

these fields were only powerful enough to apply their force to a larger amount of propellant, the momentum changes they could create would quickly establish them as the more desirable system, in terms of efficiency.

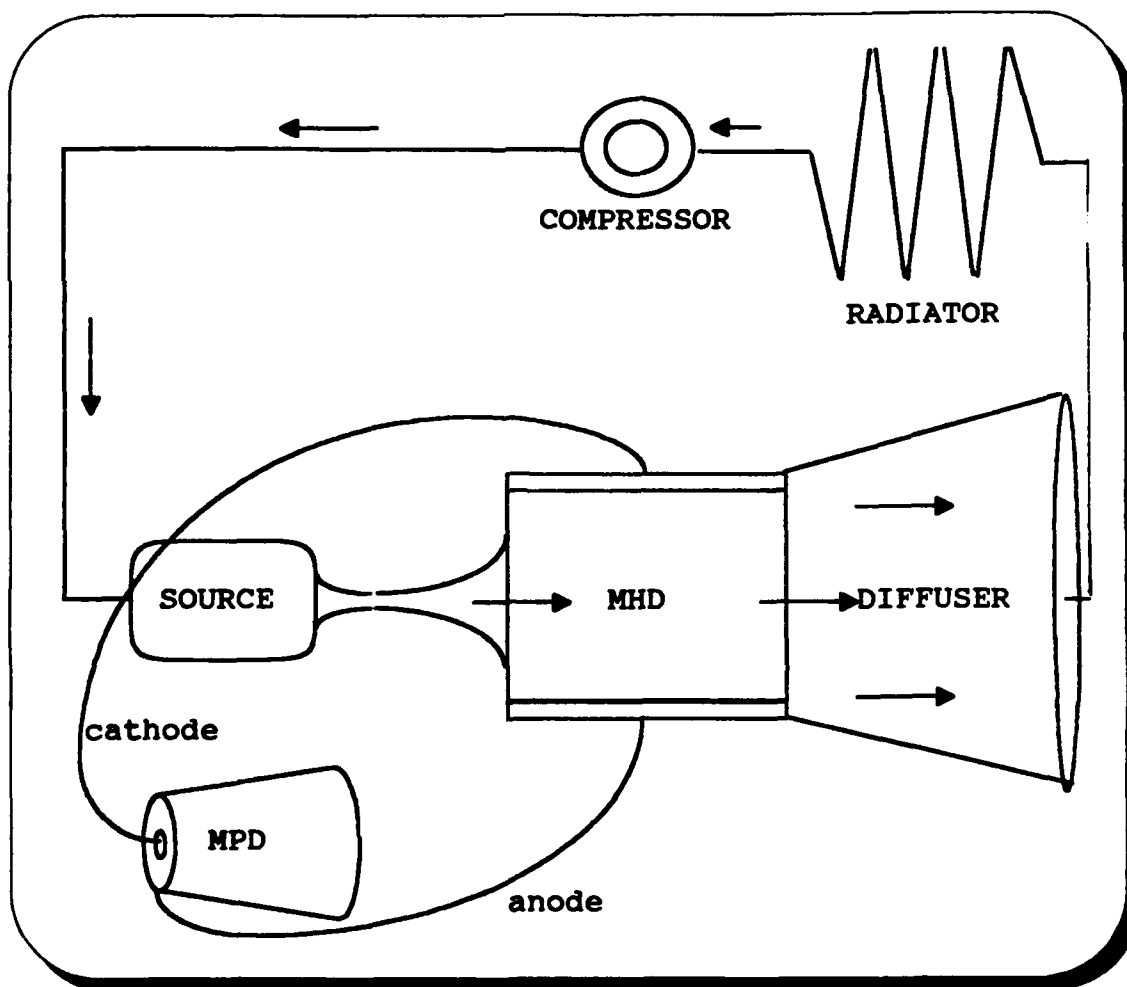


Figure 2.7 -- NEPTUNE

NEPTUNE calls for the application of the theory of electric acceleration of propellants to a high thrust impulsive mission. Just as the ally to chemical thrust production is high mass output, the ally to the electrical system must be high velocity output, coupled with just enough mass output to provide the required amount of thrust. Even at its best, NEPTUNE will not be suited for truly impulsive missions. The thrust is

not applied impulsively, or very nearly so, as is the case with conventional chemical schemes. Due to the relatively small mass output and despite the high velocity of this output, the electric thruster will only be capable of a reduced amount of thrust and if it were only allowed an instant of firing, its effect on the spacecraft trajectory would be negligible. But how reduced must this thrust level be? If we are able to dump more power into the fields of acceleration potential than they generally encounter, can we approach the momentum change of a chemical system? If we apply the thrust at a constant, reasonably high level for a longer period -- a period just short enough to make the firing time look impulsive when compared to the extended transfer time of its Mars mission -- can NEPTUNE rival chemical systems? This section describes the unique combination of NEPTUNE components that will allow an electric propulsion system to operate in a high thrust impulsive domain.

The thrust for NEPTUNE is provided by a multimegawatt MPD thruster, capable of generating fields with enough strength to accelerate a large mass flow of propellant. The last section described how the MPD thruster operates. It involves no moving parts in its purest sense and avoids any complications. Since complexity often leads to inefficiency, it would be useful to keep the thruster in its purest state in NEPTUNE. Since, the electric field of an MPD thruster is a static field simply running from an annular anode to a cylindrical cathode it needs simple DC power to create a difference in potential across its curved "plates". However, to be useful for the NEPTUNE mission, the fields in the thruster must be powerful and the source to drive them must be likewise. Therefore,

NEPTUNE needs a device to supply a large magnitude of DC power to mate with its unique MPD thruster.

This leads us a step backward along NEPTUNE to the MHD generator. The MHD generator electromagnetically decelerates a high velocity conducting fluid and converts the flow energy to direct current electrical energy. Obviously, if the amount of energy contained in the flow is sufficient, this DC source will lead perfectly into the MPD thruster. Absent are the converters, the moving parts, and the inefficiencies.

The key, however, is to ensure that enough DC power is coming from the MHD generator. So we take yet another step backward along the NEPTUNE cycle. What is needed is a device that efficiently creates a very high energy flow conducting gas. The conductivity part of this requirement is handled by an arc discharge just prior to the entrance of the generator. This ionizes the previously neutral gas. Additionally, the arc is composed of a DC field which can be supported by the same DC generator which it helps to run. The key being the coupling of devices that work naturally together.

The second part of the requirement is for a high velocity gas. Chemical reactions can result in high temperature gas to be expanded to a high velocity, but the magic of the chemical reaction is not something that can be repeated in the closed cycle. It calls for something more simple -- something to act as a very powerful stovetop burner, so as the fluid passes by it, multimegawatt heat transfer occurs. That is what a nuclear reactor does. It adds energy to a fluid in the form of heat and, because of the potential of the nuclear bond, the magnitude of this energy is very high. Furthermore, by using the

NERVA engine, the compact reactor is included to supply the energy in the form of heat and a nozzle is attached to transfer the heat into kinetic energy in the flow.

The NERVA rocket's intended application was as a nuclear thermal rocket. In this class of propulsion device, propellant/coolant is taken from a storage tank, passed over the very hot nuclear reactor source, taking with it the source's heat, and finally accelerated with a nozzle which converts the heat energy in the gas to kinetic energy of the flow.

Now the flow of this high velocity fluid, normally expelled to the environment and leading directly to thrust, may be contained and used on the closed cycle. It turns out that this is just the type of very high energy content gas that can be exploited by an MHD generator to create very high levels of electrical energy. This can, in turn, be exploited by the MPD thruster, using large electric fields to expel moderate amounts of propellant at very large velocities and producing thrust.

NEPTUNE as a propulsion system represents the combination of components described above. It is founded on three basic advantages that will be noted throughout the thesis. The first is the incorporation of the same high power producing technologies that are performing on the ground, condensed for use in space. The second and, in my opinion, most significant is the manipulation of field theory for our own benefit. This represents the manipulation of nature, or the use of force in the form nature creates it. Finally, NEPTUNE is about efficiency -- simply assembling pieces that belong together and creating success through simplicity.

However, NEPTUNE is only one combination of these ideas. They are by no means limited to NEPTUNE. If not in NEPTUNE, these ideas will surface in whatever propulsion system develops to support the needs of the future.

NEPTUNE's use of a nuclear source represents how it exploits the first advantage. Whether or not NERVA is the source of choice, the harnessing of nuclear energy is a clear improvement over the use of chemical energy. The forces holding the nucleus of an atom in place are simply stronger than the bonds between chemicals. As a result, it makes sense that more energy can be derived from the process of splitting the nucleus, than the molecule. Energy density is key in space because mass is such an overriding concern. The same bulky systems which have great success on land do not translate to the realm of space. While high power is still important, low mass is key. Nuclear power represents very concentrated energy. For this reason, it belongs in space.

The second advantage is more abstract. It involves a subject that is easily the most poorly understood by the scientific community. Field forces represent action at a distance. They are excited by mass, in the case of gravity, or charge, in the case of electromagnetism. The final understanding of the relationship between mass and charge will be the final understanding of matter and the universe, but what is important to know in the interim is that nature has organized the universe with the use of fields. They are a natural occurrence. They are how nature wants energy to exist.

In NEPTUNE, the NERVA rocket is used very differently than intended, to create a field based system. A closed cycle of gas is the platform in which energy is carried. It is loaded on at the reactor in the form of heat. It is rearranged by the nozzle into kinetic

energy of flow. Then it is off-loaded in the MHD generator as electricity, only to return to the reactor source and complete the cycle. This energy then leads to another device that uses electromagnetic field forces to accelerate an ionized gas (plasma) from the system to produce thrust. Because nature must undergo no conversion when fields are used, electromagnetic forces can attain much higher exhaust velocities than are possible by expanding a fluid thermodynamically, as in nuclear thermal or chemical systems.

The magic of field forces is key to systems of the future because the understanding that will come with time seems to lead to unheard of potential. As stated earlier, the breakthrough that explains why they can act as they do is the breakthrough that explains what makes up our surroundings.

The final key to NEPTUNE is basic, but important because of its range of usefulness. This is the idea that waste may be removed from a system if the time is taken to create a system from components that belong together. Absent from NEPTUNE are the moving parts characteristic of most propulsion systems. This translates into system efficiency and reliability. But even more importantly, what is absent from NEPTUNE are unnecessary energy conversion devices and the reductions in efficiency they carry with them. Because a high thrust MPD device requires a powerful DC source, an MHD generator is used. Because the generator needs high speed flow, the NERVA engine is used. The moral of the story is that maximum efficiency is achieved through optimum component matching.



### **CHAPTER III -- APPROACH**

The intent of this chapter is to present, in detail, the methodology used in determining NEPTUNE's ability to support a manned Mars venture. Although this chapter will not contain any of the actual calculations or results, the exact processes to obtain the results will be explained in detail.

The methods used to evaluate NEPTUNE's ability to support a manned Mars mission can be broken into three parts, each explained in a separate section of this chapter. The ultimate goal is to define a maximum mass for the NEPTUNE propulsion concept if it is to be expected to carry out a given round trip Mars mission scenario. In order to define this upper limit, an equation to relate the propulsion system mass to parameters describing the mission is necessary. This equation is the subject of the first section of this chapter.

The next step is to calculate the key parameter, used in the mass equation, describing the mission, based on the allowable mission time of flight. This parameter is the delta-v and it represents the magnitude of the velocity change required to carry out the Mars transfer. The method by which this parameter is determined will be the subject of the second part of this chapter.

Finally, the third section will derive an equation to analyze the elements of NEPTUNE and evaluate their ability to meet the mass budget defined by combining the first two sections of the chapter. In other words, it will compare what must be possible

for the mission to succeed to what is actually possible based on the components which are NEPTUNE.

The methods are described in a sensible order in this chapter -- starting with the primary unknown for NEPTUNE, the system mass, and moving to those parameters necessary to solve for this unknown. However, in the actual calculation process, it is more convenient, in order to test every possible scenario, to use a different order. More specifically, the following process outline will guide the calculations for the first part of this thesis:

- 1 -- calculate the delta-v required for the mission
- 2 -- solve for the specific mass of a system with the capabilities of NEPTUNE to perform the mission
- 3 -- compare this specific mass value to another compiled from the specific masses of the component parts of NEPTUNE

In performing this process, we may compare how "good" NEPTUNE must be to how "good" NEPTUNE is. The results from this analysis will answer the question presented in the problem statement -- is NEPTUNE able to support a manned Mars venture?

### 3.1 -- SPECIFIC MASS BUDGET:

The previous section draws a relationship between mission time of flight to delta-v for the mission. Now a relationship to propulsion system mass must be added. This basis for the relation of delta-v, and therefore, time of flight, to propulsion system mass is the rocket equation<sup>7</sup>:

$$\frac{m_0}{m_f} = e^{\Delta v / u_{ex}} \quad (3.1)$$

$m_0$  : initial mass of spacecraft

$m_f$  : spacecraft mass after firing

$\Delta v$  : change in velocity required  
 $u_{ex}$  : exhaust velocity of propellant

However, in NEP systems, this equation holds different meaning than in traditional chemical systems. In chemical engines, the difference between the initial mass and the final mass is the mass of the propellant and propulsion system, since the propellant dominates the mass of the propulsion system. In NEPTUNE, however, the propulsion system mass cannot be neglected compared to the mass of the propellant. In other words, the initial mass can be defined:

$$m_0 = m_{\text{propellant}} + m_{\text{propulsion system}} + m_{\text{payload}} \quad (3.2)$$

and the final mass:

$$m_f = m_{\text{propulsion system}} + m_{\text{payload}} \quad (3.3)$$

This leads to a new rocket equation, designed for concepts with power sources separate from propellant<sup>7</sup>:

$$\Delta v = u_{ex} \ln \left( \frac{m_{\text{prop}} + m_{\text{prop syst}} + m_{\text{payload}}}{m_{\text{prop syst}} + m_{\text{payload}}} \right) \quad (3.4)$$

Consider a vehicle that will travel to Mars in a short time. If the amount of thrust it is capable to apply is defined, it would like to maintain the vehicle weight at the lowest value possible so that thrust force will have more of an effect in accelerating it. In other words, it is important to attain a high thrust-to-weight ratio. The thrust will ideally be high and the weight low. It is obviously an advantage if the amount of propellant used to create the thrust is low. In order for that to happen, the velocity at which the propellant is expelled must be very high to compensate. This describes the theory behind electric propulsion, but the theory is complicated by other considerations. In order to support the electric propulsion, some kind of electricity generator must be a part of the propulsion

system. Obviously, if the mass of this electricity production plant is large, it will negate the savings achieved by the lower propellant mass requirement.

The factor of interest in this thesis is the mass of the propulsion system. It is what will make NEPTUNE different than other systems designed for interplanetary travel. Typically, the mass of the electricity plant has significantly diminished the benefit of the electric thruster. However, also typically, electric propulsion has not been applied to high thrust endeavors. Fortunately, scaling to these high thrust and high power missions is not linear and if electric thrusters can be designed to handle the higher power, a space electricity generator is conceivable with low enough weight to make the resulting vehicle a definite advantage.<sup>5</sup>

Because scaling will be such a factor in the analysis, the mass of the propulsion system is broken into mass per unit power, or the specific mass:

$$m_{\text{propulsion system}} = P_{\text{prop syst}} \beta_{\text{prop syst}} \quad (3.5)$$

$\beta_{\text{prop syst}}$  : specific mass of propulsion system  
 $P_{\text{prop syst}}$  : power of propulsion system

In this manner, the power requirements for the mission can simply be coupled with the specific mass to lead to a overall propulsion system mass.

If the substitution is made for the propulsion system mass in the external source rocket equation, terms can be rearranged to obtain:

$$m_{\text{prop}} = (m_{\text{pay}} + \beta_{\text{ps}} P_{\text{ps}})(e^{\Delta v / u_{\text{ex}}} - 1) \quad (3.6)$$

Over the life of the propulsion system, it will be expected to apply a total impulse, or change in velocity, to complete the mission. This will equal the thrust that will be produced, throughout the entire mission, by the propulsion system:

$$I_t = \int_0^t F dt \quad (3.7)$$

$I_t$  : total impulse

$t$  : thruster firing time

$F$  : thruster force

This total impulse can also be related to specific impulse, a parameter of the thruster to be used<sup>3</sup>:

$$I_t = I_{sp} g_0 \int_0^t \dot{m} dt \quad (3.8)$$

$I_{sp}$  : specific impulse

Note that the mass flow rate integrated over the entire time of burning will simply be the mass of the propellant. The propellant mass is seen also in the rocket equation, so a new equality is set up:

$$I_t = I_{sp} g_0 [(e^{\Delta v/u_{ex}} - 1)(m_{pay} + \beta_{ps} P_{ps})] \quad (3.9)$$

Next, if we consider the propulsion system in its basic form as a machine that is not throttleable, meaning a machine that applies only one constant level of thrust whenever it is burning, the relationship with the total impulse is exploited to get an equation for thrust:

$$F_t = \frac{I_{sp} g_0}{t} [(e^{\Delta v/u_{ex}} - 1)(m_{pay} + \beta_{ps} P_{ps})] \quad (3.10)$$

Finally, since the power of the thruster is related to its thrust force by:

$$P_t = \frac{1}{2} F_t u_{ex} \quad (3.11)$$

a substitution into the thrust equation derived above returns a relation for the thruster power:

$$P_t = \frac{u_{ex}^2}{2t} ((e^{\Delta v/u_{ex}} - 1)(m_{pay} + \beta_{ps} P_{ps})) \quad (3.12)$$

This power relationship is very useful since a great deal is known about the power source in the NEPTUNE system. NERVA is a compact nuclear reactor with definite capability limitations. Its maximum power level is established. Therefore, knowing how much power is produced by the source, a fairly strong estimate may be made as to how much power will eventually reach the thruster and be available to produce thrust. This estimate

will come from general understandings of the electricity generator and the electric thruster and their associated efficiencies:

$$P_{gen} = \epsilon_{gen} P_{source} \quad (3.13)$$

$$P_{mpd} = \epsilon_{mpd} \epsilon_{gen} P_{source} \quad (3.14)$$

Having derived the basic equations used, the procedure to calculate a specific mass budget, or the highest total specific mass allowable for the NEPTUNE propulsion system to complete the intended mission, combining the parameters of the mission with the characteristics of the propulsion system is outlined below:

- 1 -- Define the available power. This is dependent upon the power production capabilities of the NERVA source. It is a known parameter.
- 2 -- Use the efficiencies of the thruster and generator subsystems of the propulsion system to calculate the power that will be available for the thruster.
- 3 -- From a knowledge of the exhaust velocities obtainable by the thruster to be used, calculate the required mass flow rate of the propellant.

$$P_{mpd} = \frac{1}{2} \dot{m}_{mpd} u_{ex}^2 \quad (3.15)$$

- 4 -- Determine the total mass of the propellant by combining the mass flow rate with the total time during which the propulsion system will be applying thrust. The firing time is defined by a percentage of the total transfer time, to maintain an impulsive trajectory. It does not take into account capabilities of NEPTUNE to operate on a continuous basis, although electric thrust systems are generally used in this capacity.

$$m_p = \dot{m} t_{burn} \quad (3.16)$$

- 5 -- Plug values into the external source rocket equation and solve for the specific mass budget,  $\beta_{ps}$ .

$$\epsilon_{mpd} \epsilon_{gen} P_s = \frac{u_{ex}^2}{2I_b} [(e^{\Delta v/u_{ex}} - 1)(m_{pay} + \beta_{ps} P_{ps})] \quad (3.17)$$

### **3.2 – DELTA-V FOR IMPULSIVE MARS MISSION:**

In any impulsive transfer calculation it is always important to minimize the delta-v required for the mission. In manned transfers, however, it is just as important to minimize the transfer time for the mission. The two parameters are directly related and clearly competing. A short transfer time calls for a more direct trajectory, leaving less work to the forces of gravitational attraction between the bodies and more for the propulsion system. This translates directly into a high delta-v requirement for the mission and a larger propulsion system or longer firing time. Since the firing time is limited by the assumption that the transfer must be legitimately considered impulsive, the obtainable delta-v is limited, in large part, by the thrust capability of the propulsion system.

Different mission scenarios are examined in the program MARSTRIP (Appendix A). The mission delta-v's calculated vary with the transfer time and planetary geometry. Because the planetary geometries repeat periodically (particularly when considered in two-dimensional space), the program is set up to evaluate the mission at the entire cycle of geometries for a given transfer time. Transfer time limits are imposed to make the mission realistic for manned travel and realistic for propulsion system capabilities. The mathematical technique used in the program is outlined below.

The trajectory analyzed in defining the Mars transfer is basic. The mission begins from a low earth parking orbit. From this orbit, an impulsive burn is applied to set the spacecraft on its way towards Mars. The magnitude of the thrust is dependent on the amount of time allowed for this outbound transfer. As the craft approaches the Martian sphere of influence on a trajectory that is hyperbolic with respect to the planet, a second

burn is used to insert the vehicle into a closed orbit of Mars. During the time that the landing party is on the planet's surface, the transfer craft continues to orbit. After the stay time has passed, a final burn sends the spacecraft on its return transfer.

Obviously, the geometry of the Sun-earth-Mars system plays a major factor in the magnitude of the delta-v necessary to complete the round-trip venture.

Specifically the analysis process can be broken down as follows:

#### **Delta-v at point A:**

Point A is defined as the point in low earth orbit (LEO) of initial impulsive burn. The burn is performed in a 400 km parking orbit of earth. The desired velocity vector is calculated using a simple relation:

$$\underline{v}_{sat/sun} = \underline{v}_{sat/geo} + \underline{v}_{geo/sun} \quad (3.18)$$

$\underline{v}_{sat/sun}$  : velocity of satellite with respect to the sun  
 $\underline{v}_{sat/geo}$  : velocity of satellite with respect to earth  
 $\underline{v}_{geo/sun}$  : velocity of earth with respect to the sun

All velocities may be considered in this fashion if standard units are used.

In the above relation,  $\underline{v}_{sat/sun}$  may be considered the velocity of the spacecraft at the perihelion of its transfer orbit to Mars in an heliocentric or sun-centered reference frame. This point will always be the perihelion and as time of flight restraints dictate more direct missions, the size of the elliptical outbound transfer will grow so that Martian orbit radius is reached earlier in the orbit. This vector may be calculated according to the formula:

$$\underline{v}_{sat/sun} = \sqrt{\frac{\mu_{sun}}{p}} \sin(v_a) \hat{P} + \sqrt{\frac{\mu_{sun}}{p}} [e + \cos(v_a)] \hat{\zeta} \quad (3.19)$$

$\mu_{sun}$  : gravitational parameter for the sun  
 $p$  : semi-latus rectum  
 $v_a$  : true anomaly at point a  
 $e$  : eccentricity



In order to define this vector, the parameters  $p$  and  $e$  of the transfer orbit must be known. This proves to be a profound problem, solved using an iterative process in subroutine ECCENT (Appendix A).

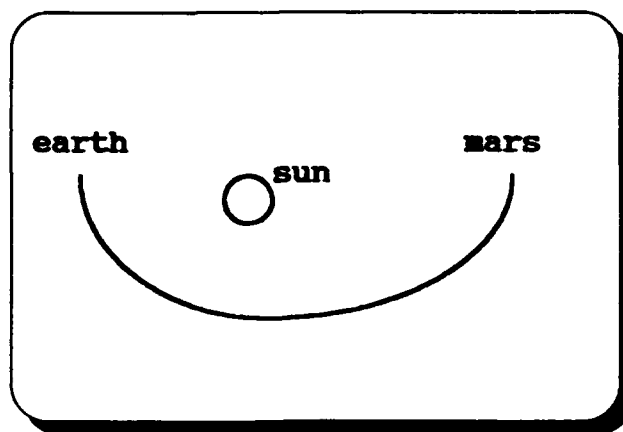


Figure 3.1 -- Hohmann Trajectory<sup>9</sup>

Subroutine ECCENT addresses the problem of determining the size of an orbit necessary to meet limits imposed by outbound trip times to Mars. The first step is to assume a value for eccentricity of the transfer orbit,  $e$ . We could begin with a value of zero for eccentricity, corresponding to a circular orbit. However, this would result in more iterations than necessary and a longer computer run time. If the initial eccentricity guess is instead based upon a Hohmann transfer eccentricity, calculations may be reduced. A Hohmann transfer represents the lowest energy impulsive trajectory that will allow the spacecraft to go between earth and Mars. If this trajectory were followed, the earth would be at the point of perihelion of the orbit, while Mars would be at the apohelion point just as the spacecraft arrives, as shown in the diagram of a Hohmann transfer.

This orbit has a definite eccentricity:

$$e = \frac{(r_a - r_b)}{(r_a + r_b)} \quad (3.20)$$

$e$  : eccentricity

$r_a$  : distance from sun to point a  
 $r_b$  : distance from sun to point b

Using this eccentricity as an initial guess, the semi-major axis is found:

$$a = \frac{r_a}{(1-e)} \quad (3.21)$$

Also, the semi-latus rectum is found:

$$p = a(1 - e^2) \quad (3.22)$$

Now, find the angle between  $r_a$  and the radius vector for the spacecraft when it reaches Mars at point B (in this case, at the apohelion):

$$\cos v = \frac{p-r_b}{(e)(r_b)} \quad (3.23)$$

From the true anomaly, it is helpful to model the transfer orbit as a circular orbit and calculate a new angle, the eccentric anomaly, based on this model<sup>9</sup>:

$$\cos E = \frac{\cos v + e}{1 + e \cos v} \quad (3.24)$$

$E$  : eccentric anomaly

Now a time of flight corresponding to the eccentricity guess is calculated:

$$TOF = \frac{a}{\mu_{sun}} [E - e \cos E] \quad (3.25)$$

Finally, this new time of flight is compared to the allowed time of flight. If they are the same, this is the orbit to use for the transfer. If they differ, the eccentricity must be increased by some amount to make the transfer orbit larger so that the spacecraft reaches Martian radius earlier in the orbit and the time of flight between the planets is lower. This subroutine will accept orbit parameters as correct once they predict the time of flight within half of one earth day.

The next step is to calculate the energy necessary to create a transfer orbit of appropriate size. Obviously, lower trip times will require more eccentric parabolic or hyperbolic orbits and more energy. The problem is broken up so that the velocity change

is calculated at two points. The first is the point where the transfer orbit begins (the periapsis of the orbit) and the other is the point where the transfer ellipse intersects the circular orbit of Mars. Since a parabolic orbit retains constant energy along its path, calculations at other points are unnecessary.

Now the parameters for the outbound Martian transfer are known and the vector velocity that the spacecraft must have at earth departure in order to undertake this transfer can be calculated. The coordinate system being used is defined by the plane of the transfer orbit from earth to Mars. The P direction is defined as the direction of periapsis in this orbit, which is also a position vector to pt. A. Consequently,  $v_a = 0$  radians.

The second vector to be found is  $v_{geo/sun}$ . The same formula is employed:

$$v_{geo/sun} = \sqrt{\frac{\mu_{sun}}{r_a}} \sin(v_a)P + \sqrt{\frac{\mu_{sun}}{r_a}} \cos(v_a)Q \quad (3.26)$$

In the previous equation, since the orbit of the earth about the sun is considered circular,  $p = r_a$  and  $e = 0$ .

Now these vectors are simply subtracted to determine the velocity that the satellite must have with respect to earth at the periapsis point of its heliocentric transfer orbit to Mars.

Originally, the satellite will have a velocity at point A of:

$$v_{cs} = \sqrt{\frac{\mu_{geo}}{r_{cs}}} \quad (3.27)$$

$r_{cs}$  : radius of circular orbit about earth

$v_{cs}$  : velocity of satellite in circular earth orbit

$\mu_0$  : gravitational parameter of earth

To escape the influence of the earth, it will need to first attain escape velocity, but this will not be enough. Escape velocity is defined as the exact velocity necessary for the craft to escape earth's gravity. As the distance from the earth becomes infinite, the velocity of the

craft will be exactly zero. However, for our purposes, the craft must have a velocity of  $\underline{v}_{sat/sun}$  as the gravity of earth is overcome. Consequently,  $\underline{v}_{sat/sun}$  is our hyperbolic excess velocity, or the velocity of the craft when the distance from the earth to the craft may be considered infinite. We may calculate that velocity necessary in LEO to give us  $\underline{v}_{sat/sun}$  outside the earth's sphere of influence by the following relation:

$$v_{bo}^2 = v_{esc}^2 + v_{sat/geo}^2 \quad (3.28)$$

$v_{bo}$  : required burn-out velocity

$v_{esc}$  : earth escape velocity at LEO

$$\bar{v}_{sat/sun} = \bar{v}_{sat/geo} + \bar{v}_{geo/sun} \quad (3.29)$$

Then the delta-v that will be necessary is a simple matter:

$$\Delta v_a = |\underline{v}_{bo} - \underline{v}_{cs}| \quad (3.30)$$

#### Delta-v at point B (#1):

For the Hohmann transfer problem, this delta-v at point B is easily calculated much as the delta-v at A was, but the problem is more complex for the case of more direct transfer orbits. This is because the vector direction of the transfer orbit velocity at point B is not in the same direction as the circular satellite, or Martian, orbit velocity direction for this case. Instead, the two velocity vectors will be off by an angle  $\delta$ , determined by the position in the elliptical transfer orbit where the spacecraft encounters Mars. This angle may be calculated with the formula:

$$\cos \delta = \frac{r_a v_a^2}{r_b v_b^2} \quad (3.31)$$

Now, the thrust must not only be applied to slow down and circularize the orbit, but to manipulate the velocity vector into the proper direction for a circular satellite.

This constitutes the second burn of the NEPTUNE mission, when the spacecraft encounters the vicinity of Mars. In order to determine the magnitude of this delta-v, it is important to first determine the exact location in the transfer orbit when the spacecraft reaches Mars. In other words, find the true anomaly of Mars encounter. The true anomaly is the angle between the perihelion direction (in this case, point A) and the position vector to the spacecraft at any point. The true anomaly at point B can be found:

$$\cos v_b = \frac{p - r_b}{(e)(r_b)} \quad (3.32)$$

where  $r_b$  is the magnitude distance from the sun to point B, or Mars. Now the position and velocity vectors of the spacecraft, at the point of Mars encounter, may be calculated using the familiar relations:

$$r_b = r_b \cos(v_b)P + r_b \sin(v_b)Q \quad (3.33)$$

$$\underline{v}_{(sat/sun)b} = \sqrt{\frac{\mu_{sun}}{p}} \sin(v_b)P + \sqrt{\frac{\mu_{sun}}{p}} [e + \cos(v_b)]Q \quad (3.34)$$

Additionally, the velocity vector,  $\underline{v}_{mars/sun}$ , may be found with the same formula as above, assuming  $p$  is replaced with  $r_b$  and  $e$  is assumed to be zero since the Martian orbit is nearly circular about the sun.

The unknown is the velocity of the spacecraft with respect to Mars at point B.

This may be found with simple vector addition:

$$\underline{v}_{(sat/sun)b} = \underline{v}_{(sat/Mars)b} + \underline{v}_{(Mars/sun)b} \quad (3.35)$$

Now, it's a matter of working in reverse of the process used at earth departure to calculate the delta-v. The burnout velocity at earth may be analogized to the desired reentry velocity at Mars and calculated as follows:

$$v_{re}^2 = v_{(sat/Mars)b}^2 + v_{mars esc}^2 \quad (3.36)$$

The delta-v to enter a low Mars orbit is simply the difference between this reentry velocity and the circular satellite velocity of the desired Martian orbit:

$$\Delta v_{b1} = |v_{re} - v_{(sat/sun)b}| \quad (3.37)$$

The spacecraft will continue to orbit Mars for as long as the astronauts remain on the surface. All the while, both Mars and earth continue to revolve about the sun, so when the departure time arrives, new calculations of position and velocity vectors are necessary.

#### **Delta-v at point B (#2):**

The first and most important step in determining the magnitude of this third burn is to define the return orbit. Once again, the orbit will be derived from the time of flight constraint imposed on the return. The problem consists of two position vectors to be traversed in a given time. The first position vector is the location of Mars at the time of departure, while the second position vector is the location of the earth at the time when the spacecraft reaches an earth radius from the sun. When considered in this way, the problem may be identified properly as a Gaussian problem.<sup>9</sup> The two position vectors accompanied by a time of flight exactly define two closed transfer orbits, one with a true anomaly less than 180 degrees and one with an anomaly greater than 180.

Subroutine Gauss tackles the problem at hand, accepting the two position vectors and time of flight, performing an iterative process, and returning the accompanying velocity vectors at points B and A. The vector at point B may be thought of as  $\underline{v}_{sat/sun}$ , while the vector at A is the velocity the spacecraft will have upon earth arrival. Knowing the heliocentric velocity vector at Mars necessary for the return orbit enables you to treat this third burn just as you would treat the original burn at earth.

The total delta-v to be supplied by the propulsion system is simply the sum of the changes necessary at these three points and represents the cost of the time of flight for the mission.

### 3.3 – SPECIFIC MASS FORMULA:

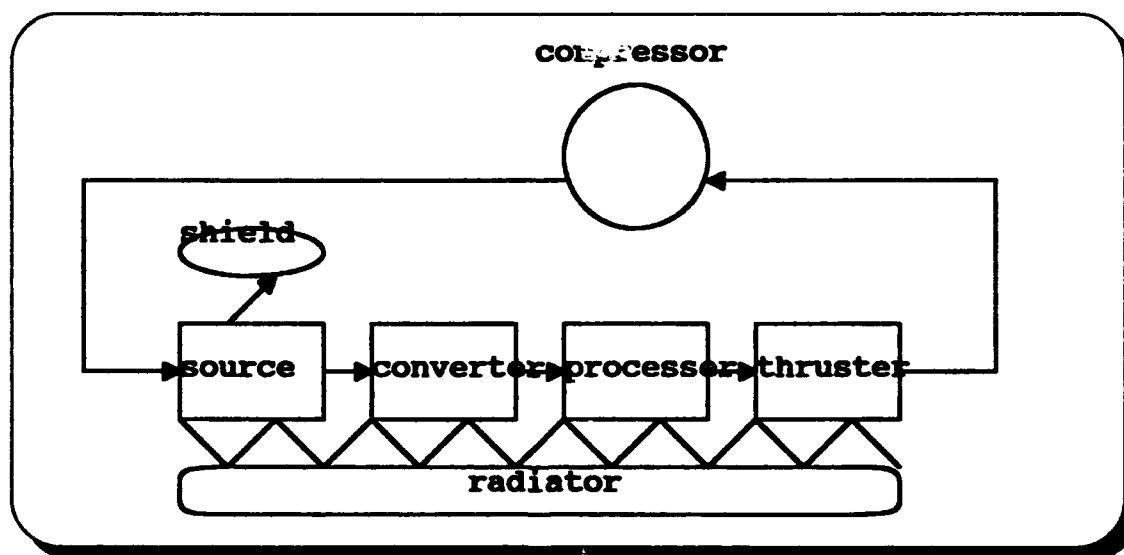


Figure 3.2 -- Block diagram of NEPTUNE loop

The purpose of the above sections was to create a picture of what NEPTUNE must look like, based on the mission it is to perform. This section will help to define what

NEPTUNE will look like, based upon its components. It will attempt to define the whole as a sum of its parts. The NEPTUNE flow is represented by the block diagram that follows.

The total mass of the propulsion system is no more than the mass of its parts. For our purposes these parts include:

$$M_{\text{neptune}} = M_{\text{source}} + M_{\text{shield}} + M_{\text{conv}} + M_{\text{pwr proc}} + M_{\text{thrust}} + M_{\text{rad}} \quad (3.38)$$

What we are therefore dealing with is the problem of assigning values to this symbolic formula. Obviously, the masses will be different and dependent upon how demanding the propulsion requirements are. In order to standardize the elements, we work in specific masses so that the new formula becomes:

$$M_{\text{neptune}} = (\beta_s + \beta_{sh})P_s + \beta_c P_c + \beta_{pp} P_{pp} + \beta_t P_t + \beta_r P_r \quad (3.39)$$

Considering the NEPTUNE mass equation, some variables are taken from previous analysis. The source power is defined based on maximum NERVA capabilities. The power that will arrive at the converter and power processor is the source power, minus that power lost to inefficiencies in the system. This is considered in the efficiency parameter,  $\epsilon$ . Likewise, the power that will arrive at the thruster is the converter/processor power, reduced for inefficiencies in those subsystems. Finally, the power that reaches the radiator is that waste power lost to inefficiency throughout the system. It is the "other" power.

The NEPTUNE mass equation may be broken down to incorporate the efficiency terms. Consider the converter subsystem, changing heat from the source to energy for an electric system. The amount of mass this will contribute to NEPTUNE will look like:

$$M_{\text{conv}} = \beta_c P_c + (1 - \epsilon_c) (\beta_s) P_s \quad (3.40)$$



$\epsilon_c$  : converter efficiency

A similar formula can be written for the power processor, which would transform the power to the exact form needed for the load, the thruster. However, this is where one of the possible advantages to the NEPTUNE system comes into play. It has been explained that NEPTUNE derives efficiency through optimum component coupling. The MHD converter may also be considered the processor because it produces electric power in exactly that form required by its load, the MPD thruster. As a result, the mass contribution of the processor might be eliminated. The mass addition of the processor waste power to the radiator would then also be avoided.

The thruster subsystem is a unique situation. While the radiator is responsible for maintaining steady-state conditions in the closed cycle NEPTUNE generator and source subsystems, it does not have to include losses in the thruster that are carried away by the exhaust flow, or radiated by the thruster itself.

The reactor shield is obviously a direct factor of the amount of power supplied by the source reactor. For the purposes of this study, the specific mass of the shield will be combined with the source specific mass.

A specific mass term for the radiator may be derived from an equation for the area of the radiator. The area required to radiate any amount of power at a fixed temperature is given by the equation<sup>10</sup>:

$$A_{rad} = \frac{P_{rad}}{\sigma T_{rad}^4} \quad (3.41)$$

$T_{rad}$  : temperature at which power is radiated

$P_{rad}$  : power to be radiated

$\sigma$  : Boltzmann constant

Obviously, as more power must be radiated, the area of the radiator must increase to accommodate it. However, the equation illustrates the tremendous importance temperature has on radiator area, and therefore, radiator mass. The fourth power dependence upon temperature means that the radiating temperature must be kept to a minimum at all costs to avoid a mass explosion.

From the radiator area and a knowledge of the general properties of the material from which the radiator is to be made, a radiator mass can be related to the area:

$$m_{rad} = \mu A_{rad} \quad (3.42)$$

$\mu$  : specific mass of radiator (kg/m<sup>2</sup>)

Substituting the equation for radiator area, a true specific mass is:

$$\beta_{rad} = \frac{\mu}{\sigma T^4} \quad (3.43)$$

In order to develop a single formula for the overall mass of the propulsion system of NEPTUNE, all of the terms must be combined. This equation can be reduced so that all powers are defined in terms of the known source power:

$$m_{neptune} = [\beta_{NERVA} + \beta_{gen}\epsilon_{gen} + \beta_t\epsilon_{gen}\epsilon_t + (1 - \epsilon_{gen})\frac{\mu}{\sigma T^4}]P_s \quad (3.44)$$

The above equation is very useful. The mass resulting from the equation for  $m_{neptune}$  may be compared to the results of the rocket equation. By multiplying the maximum allowable NEPTUNE system specific mass, from the mission analysis, by the NERVA source power, we define a maximum allowable mass for the NEPTUNE system. By summing actual specific masses of the various components, we can estimate the actual mass of the NEPTUNE system. Ideally, we seek the inequality:

$$m_{neptune} < \beta_{prop\ sys} P_{source} \quad (3.45)$$

The results of this inequality will derive the ideas presented in the second part of the thesis. If the combined mass of the components of NEPTUNE falls within the mass

budget, the problem of applying NEPTUNE to a manned Mars mission is solved.

However, if the system mass is above the allowable maximum, improvements to the system must be engineered in order to bring the mass within limits.

## **CHAPTER IV – ANALYSIS OF TRIP-TIME AND SPECIFIC MASS**

### **4.1 – DELTA-V FOR IMPULSIVE MARS MISSION:**

The goal of program MARSTRIP (Appendix A) was to model all possible round trip impulsive Mars trajectories. In order to cover all possible planetary geometries coming from different combinations of outbound transfer time, surface stay time, and return transfer time, the program performs delta-v calculations at small increments of each. The procedure outlined in the previous chapter was adhered to completely. The resulting trajectory model is easily sufficient to generate the rough figures necessary for this project, but it clearly incorporates assumptions that separate it from reality. These assumptions are summarized below:

- 1 -- Launch time is flexible. It is possible to wait a launch opportunity so that Mars will arrive at point B (initial Mars encounter) just as the transfer craft does.
- 2 -- The problem is analyzed in two dimensions.
- 3 -- A three body (Sun, Mars, earth) scenario is considered.
- 4 -- The mission begins from a 400 km earth orbit. The craft enters a 400 km orbit of Mars.
- 5 -- No final burn is included to enter earth orbit on return.
- 6 -- Trajectory calculations are performed at twenty day increments. This is assumed sufficient to get clear picture of delta-v trends.
- 7 -- Payload mass is set at 20,000 kg.

MARSTRIP was set up to calculate the delta-v requirements for round trip Mars missions at twenty day increments in outbound transfer time, Martian surface stay time, and return transfer time. The transfer times were considered for periods between 70 and 250 days. The stay times lasted from 10 to 110 days. This resulted in minimum mission time of 150 days round trip and a maximum of 610 days. The minimum was governed by the fact that transfers of shorter times than these lead to unreasonably high delta-v requirements and hyperbolic trajectories with respect to the sun. The maximum is imposed due to the fact that this is a manned mission and space travel nearing two years would be excessively demanding.

Figure 4.1 and 4.2 summarize the results of MARSTRIP when an exhaust velocity of 98.1 km/s ( $I_{sp} = 10,000$ ) is used. The curves are the result of a series of arcs. Because of the possibility for a return trip in either direction about the sun, the program calculates the delta-v for both options. Therefore, as the geometry of the sun-earth-Mars system changes, the direction for the "short" return transfer about the sun reverses. This leads to the discontinuities in the graphs. The graphs, however, clearly highlight the maximum and minimum delta-v's and make it possible to couple a delta-v value with a trip-time value for either the long or short option. For more specific numbers, refer to Appendix B, which contains the actual values used to generate these graphs.

Specifically, the delta-v requirement for the fastest mission (150 days) considered was 42.9 km/s. The longest mission, on the other hand required a delta-v of only 29.7 km/s. Although it would seem that the delta-v and time of flight would have a direct inverse relationship, this was not the case. As the missions became less demanding in

terms of transfer time, a general trend in decreased delta-v requirement was apparent, however, the dependence upon convenient planetary geometry was just as large a factor.

The return trajectory was solved to consider the option of a return in either direction about the Sun. The "long option" as it was called in the program favored longer trajectories and returned the lowest delta-v's. However, the "short option" could also find small delta-v's with the definite advantage that missions under this option were much shorter. The optimum missions identified by MARSTRIP are summarized in the table below:

Table 4.1 -- Minimum delta-v round trip Mars trajectories of each option

Transfer Time (days)	Outbound (days)	Surface Stay (days)	Return (days)	Mission $\Delta V$ (km/sec)
290	130	10	150	22.5
470	230	10	230	11.4

Although the above trajectories result in the lowest possible delta-v's, they are not necessarily the optimum trajectories for the mission. In fact, the surface stay time is likely too short to warrant a manned Mars excursion. The complete results of program MARSTRIP are given in the following graphs. They plot delta-v as a function of total transfer time. Use the graphs by first deciding on a desired round-trip mission time. Follow the horizontal axis on either the short or long option graph to that time. Then proceed vertically until a curved line is intersected. For most mission times, several curves will correspond. Each represents a different combination of outbound transfer, surface stay time, and return transfer time. The discontinuities (straight lines connecting the curves) in the graphs come at the point where the "short" trajectory changes to a return in

the opposite direction about the sun. This is a result of dynamic planetary geometry during the outbound transfer and surface stay. Do not confuse these lines with the delta-v curves matched to the mission time. For a specific mission scenario, made up of an outbound transfer, surface stay, and return transfer, refer to Appendix B. This is the actual output data from program MARSTRIP and is not confused by the discontinuities.

The true usefulness of the graph is found in the minimums it highlights. The minimum delta-v's may be matched with their corresponding mission times. The delta-v parameter may then be used set up a specific mass budget in the manner considered below.

#### 4.2 -- SPECIFIC MASS BUDGET:

Next, the process outlined in the previous chapter was used to calculate a budget for the specific mass of the propulsion system. This budget represents the largest value to which the specific mass of NEPTUNE per unit power may grow before the mission becomes impossible. As explained, the budget will vary with a number of factors, such as total burn time for the propulsion system, efficiency of the generator and thruster, and power supplied by the source. Results are summarized for likely cases below:

Table 4.2 -- NEPTUNE specific mass budget

$\Delta V$ (km/sec)	$P_{\text{source}}$ (MW)	$u_{\text{ex}}$ (km/sec)	$\epsilon_{\text{MHD}}$	$\epsilon_{\text{MPD}}$	$t_{\text{burn}}$ (% $t_{\text{trans}}$ )	$\beta_{\text{NEPTUNE}}$ (kg/MW)
22.5	1,732	98.1	0.5	0.5	0.5	13.7
11.4	1,732	98.1	0.5	0.5	0.5	74.1
22.5	1,732	98.1	0.5	0.5	1	39
11.4	1,732	98.1	0.5	0.5	1	159.7
22.5	1,732	98.1	0.5	0.5	2	89.5
11.4	1,732	98.1	0.5	0.5	2	330.9

The source power value used in the calculations comes from an understanding of the power producing capacity of the NERVA engine. The exhaust velocity for the MPD thruster is based on projections of their abilities to produce  $I_{sp}$ 's up to 10,000 seconds. Efficiencies are very rough estimates of the abilities of MHD and MPD technologies. In the case of the MHD generator, these values may be considered conservative, while in the instance of the MPD thruster, they lean more toward the liberal side. General goals necessary to make NEPTUNE useful would be to lose no more than half the power in transition. Finally, the burn time is a factor more of the trajectory class considered than the ability of the NERVA engine. Because NEPTUNE is anchored by a nuclear source which is more tailored to a closed-cycle (as used on earth) than open, it should have little problem applying its power over the longer term. After all this time period is still very short when compared to the time that nuclear generators are expected to work on earth. For this project, the burn times were limited by the fact that the trajectories followed are impulsive and the application of thrust must therefore be impulsive.

A full plot of specific mass budget variance with the time of flight data from program MARSTRIP is included in Figure 4.3 and 4.4 (for the short and long return trajectory option). The graph is obviously very rough because of the discontinuities in the output of MARSTRIP, but once again, the idea is to identify the maximum budget and these are clearly identifiable in the plot. The actual output data contained in Appendix B is useful to obtain numerical values of the specific mass budget.

The tradeoff between burn time and specific mass is an interesting one. The above table illustrates the increase in budget derived from a longer thrusting time. Figure 4.5



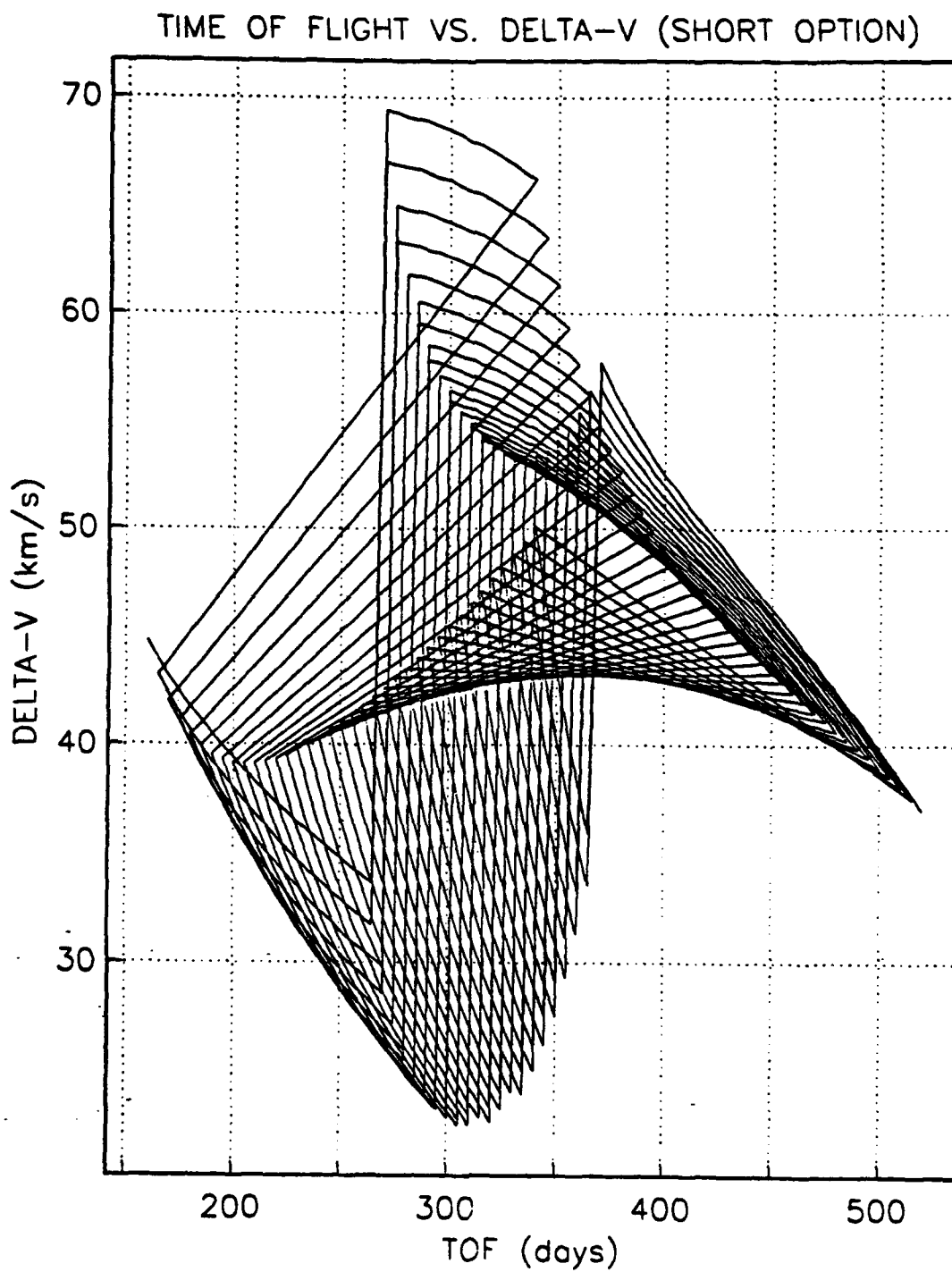


Figure 4.1 -- Variance of Delta-v with Mission Time of Flight for Short Option

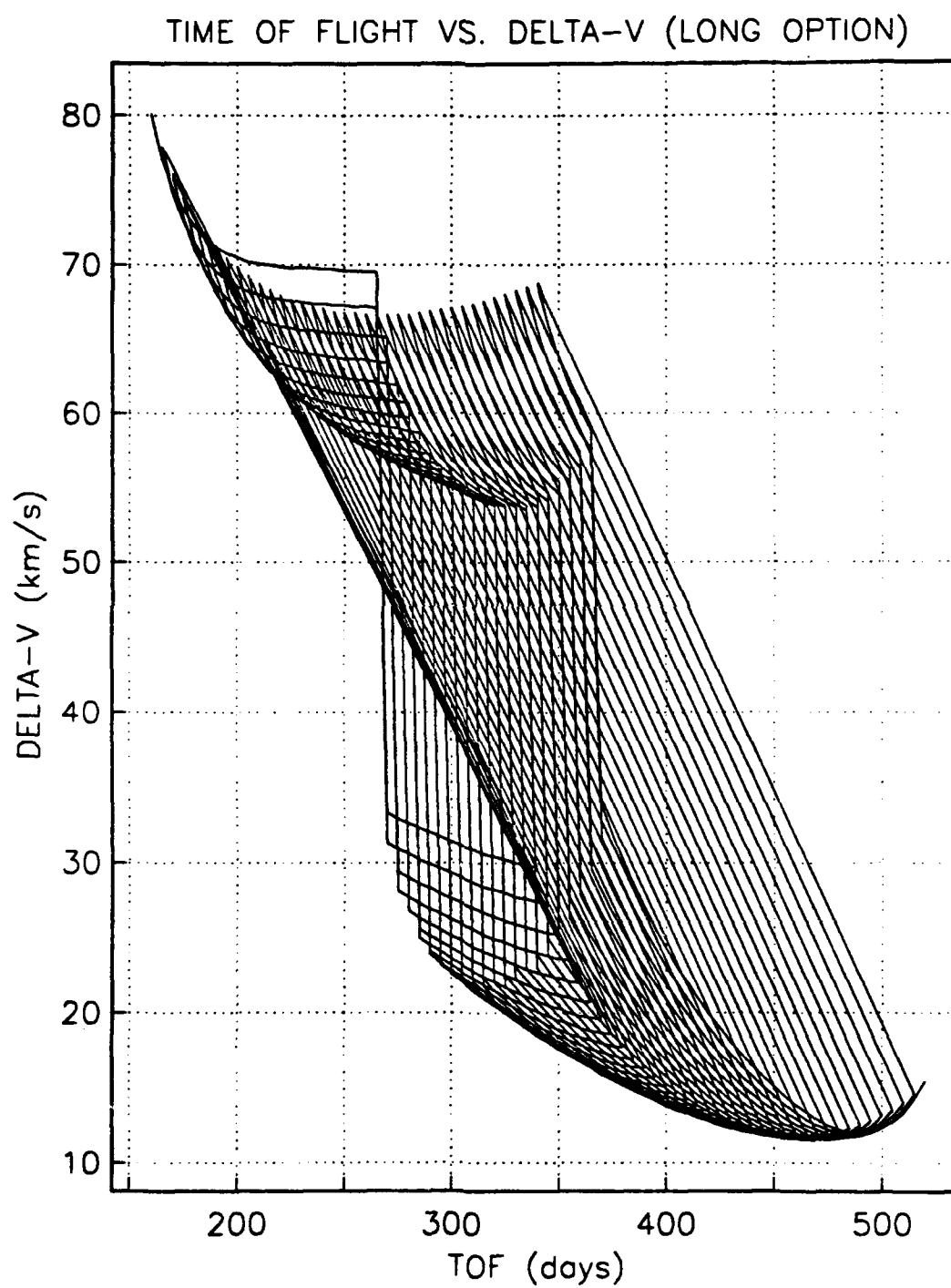


Figure 4.2 -- Variance of Delta-v with Mission Time of Flight for Long Option

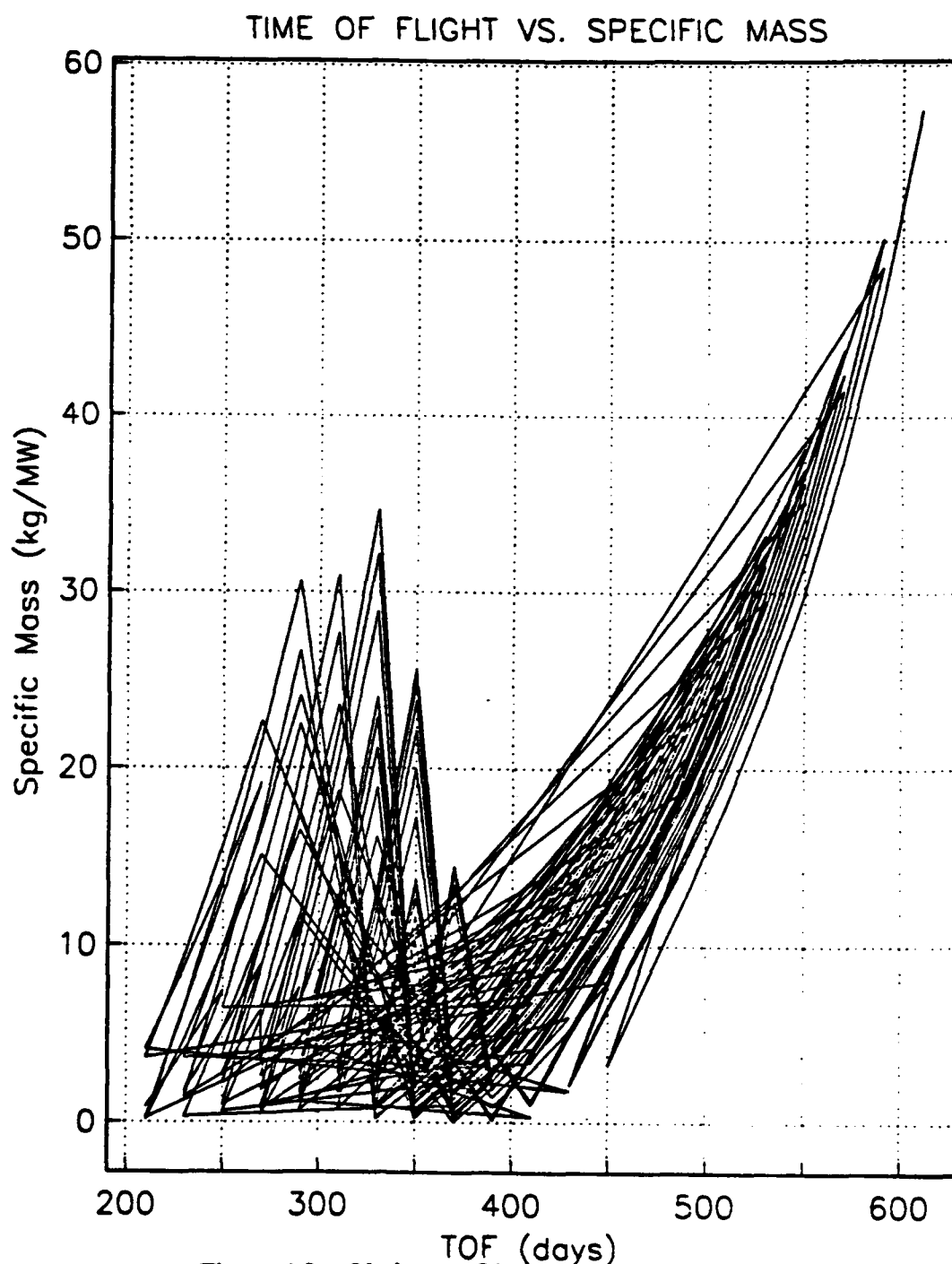
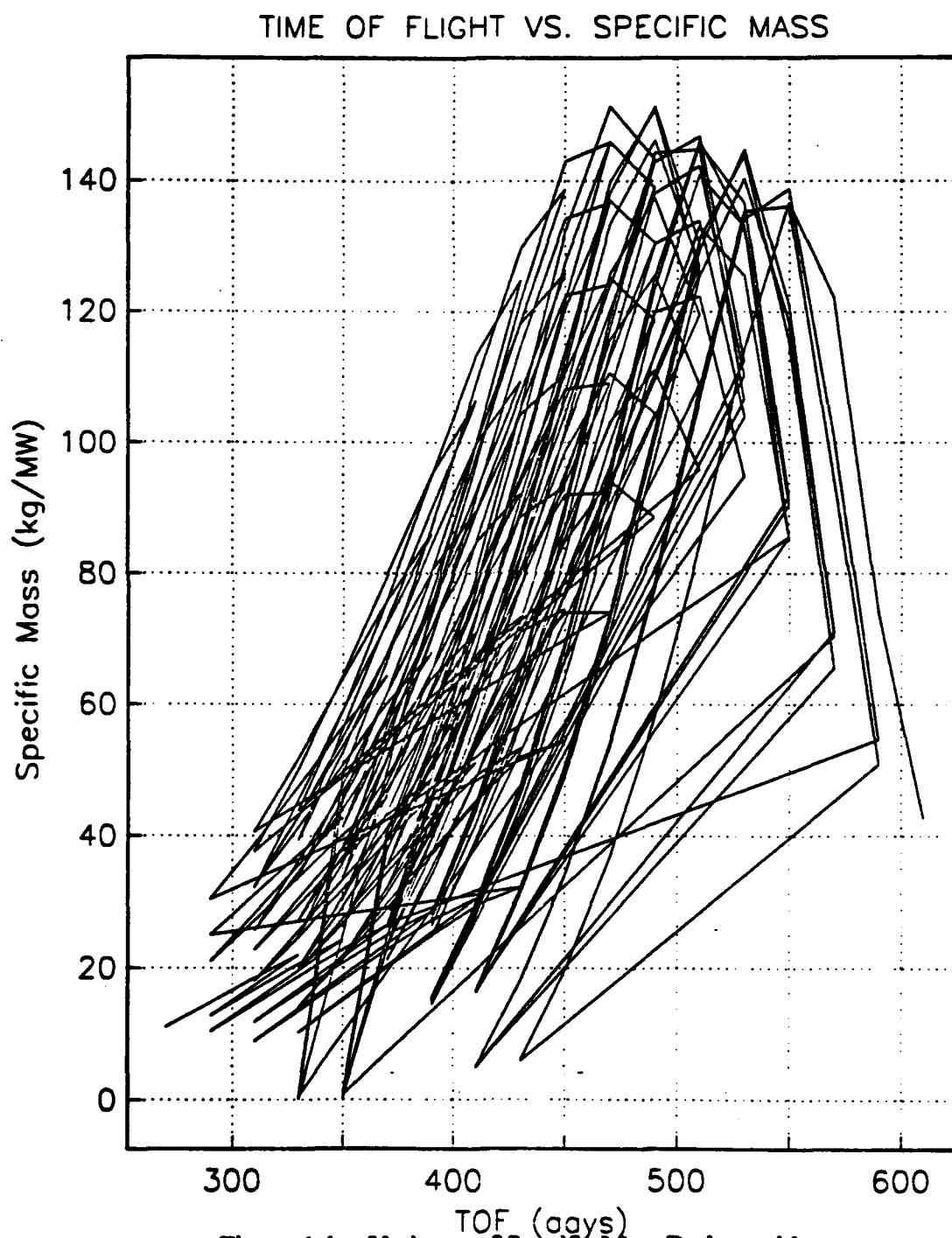
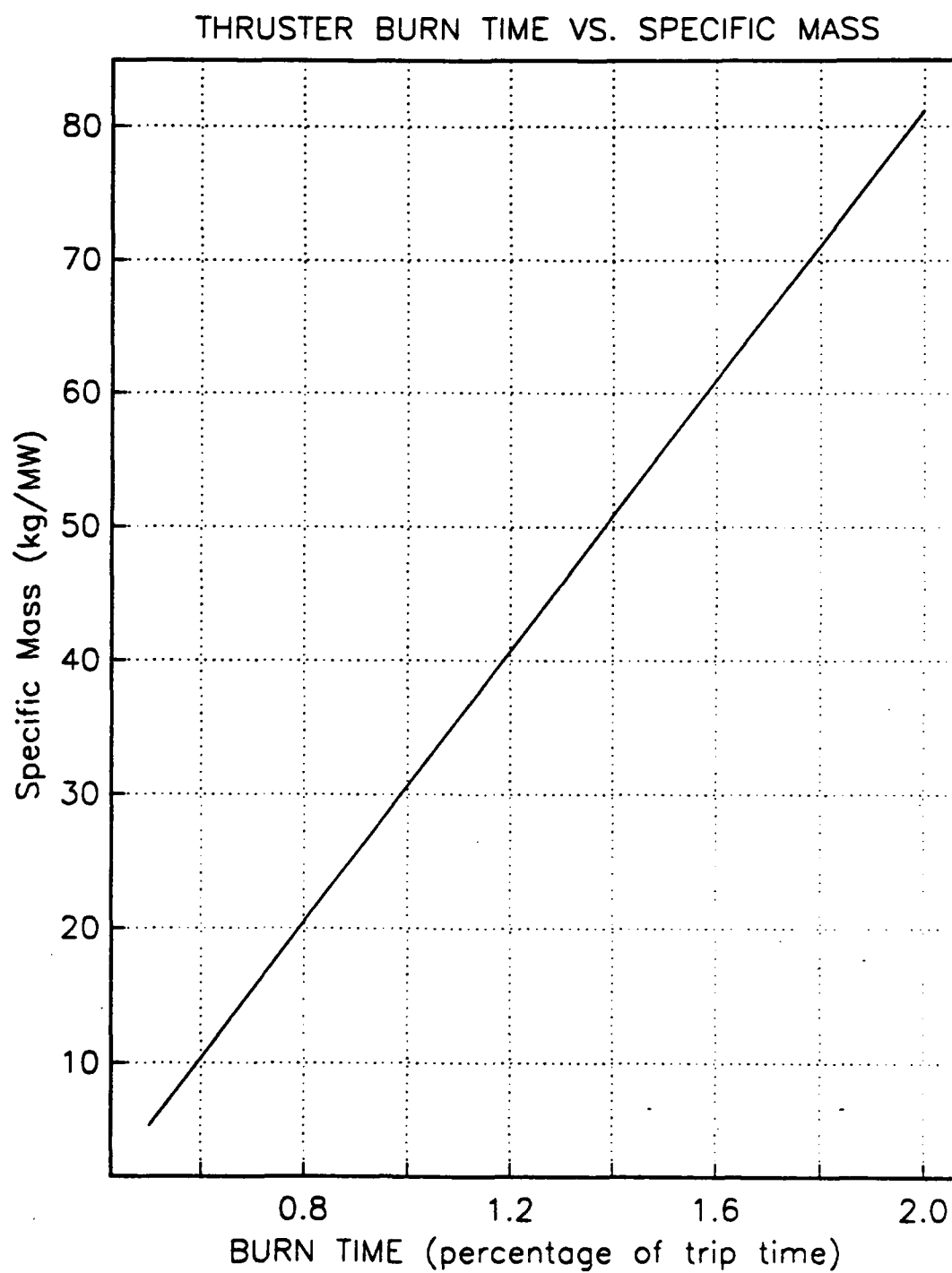


Figure 4.3 -- Variance of Specific Mass Budget with  
Mission Time of Flight for Short Option



**Figure 4.4 – Variance of Specific Mass Budget with  
Mission Time of Flight for Long Option**



**Figure 4.5 -- Effect of Burn Time on Specific Mass Budget for Short Option**

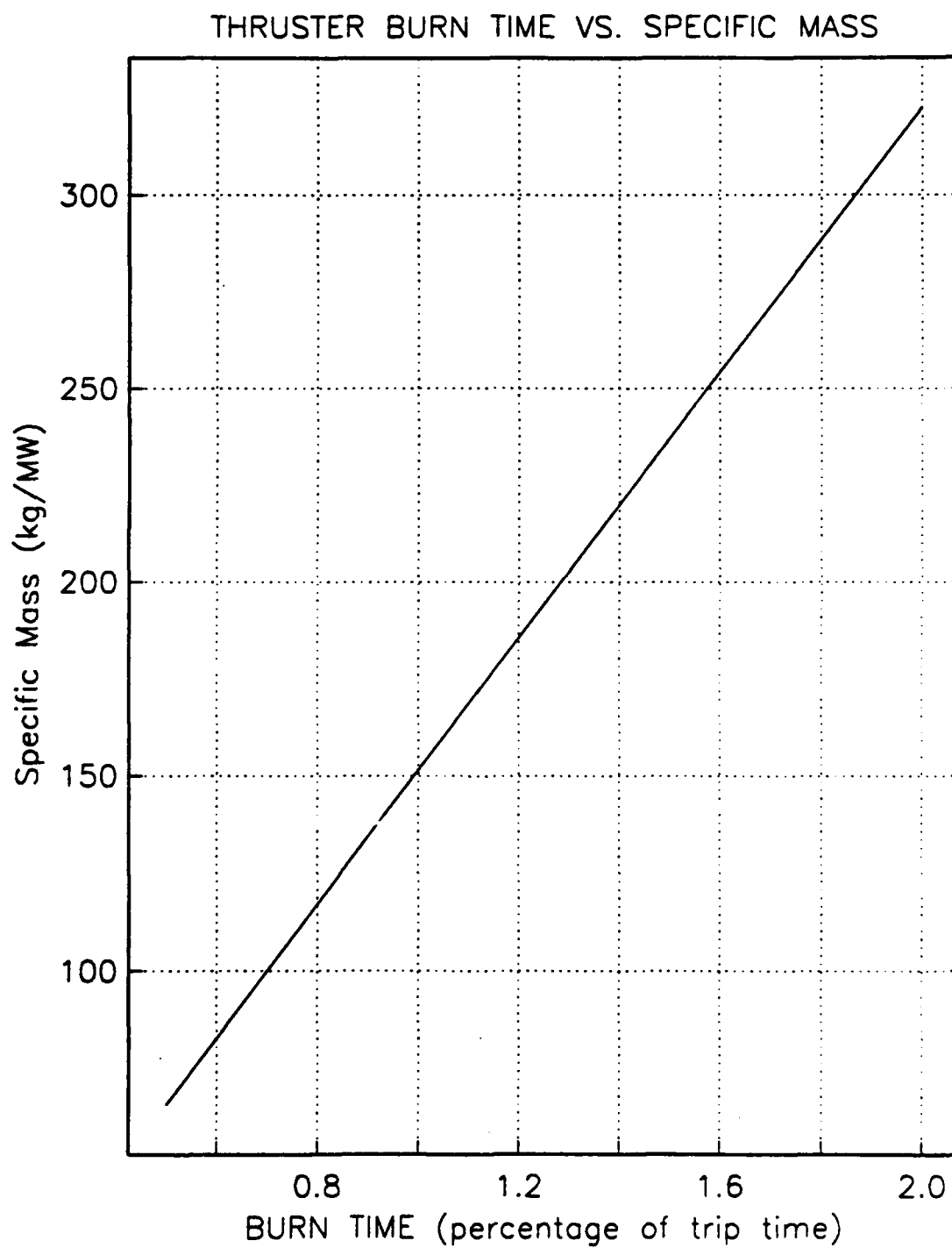


Figure 4.6 -- Effect of Burn Time on Specific Mass Budget for Long Option

highlights the linear relationship between these two parameters. This graph would seem to imply that the thrusting time should be increased as much as possible. It must not be forgotten, however, that the trajectories being analyzed are impulsive and, as such, the thrusting time must look instantaneous when compared to the time for the transfer. This fact clearly limits the acceptable amount of time during which the propulsion system may apply its thrust.

#### **4.3 -- SPECIFIC MASS VALUES:**

This section summarizes research on existing systems which would serve as components of NEPTUNE. MHD generators and MPD thrusters working with continuous levels of power as significant as those intended for NEPTUNE are yet to be developed. However, through the use of the specific mass, systems designed with less ambitious uses in mind may be applied to multimewatt power levels. Obviously, since the existing technology is not developed for very high powers, there is a great deal of uncertainty as to how the technology will transfer. This can be either a positive or negative aspect. It encompasses phenomenon, such as the onset condition, which could make high power applications impossible. However, more than likely, a system designed to deal with multimewatt power levels will have a lower specific mass than their smaller relatives. The mass of the system will undoubtedly grow, but not in a linear fashion with the power. As a result, the conclusions from this section are relatively predictable. Masses within the budget cannot be expected until the subsystems are reconfigured to deal with very high power systems, such as NEPTUNE.

Because the source is set up for very high powers, it is useful to start with a consideration of NERVA. NERVA, acting in its capacity as a nuclear thermal rocket, can possibly attain specific impulses as high as 1000 seconds, translating to exhaust velocities of 9810 m/s. It does so by heating the coolant/propellant to a maximum temperature of 2500 K. In the past it has demonstrated an increase in efficiency with increasing power output. Although NERVA never supplied power above a couple hundred megawatts, thrust projections for the system were as high as 330 kN.<sup>11</sup> Combining this with the specific impulse of up to 1000 seconds would lead to a maximum power of over 1600 MW, which is well above the 1000 MW demands estimated for this study.

A number of different figures can be found for NERVA's mass. They vary depending on the output power, and subsidiary devices included. However, the specific mass of NERVA is about 220 kg/MW.<sup>8</sup> This factor again is based on NERVA tests conducted at lower power levels than expected for NEPTUNE.

The NERVA source, because it is developed to operate at fairly high power levels, has a lower specific mass than the other subsystems that make up NEPTUNE and already it is apparent that NEPTUNE's system mass, when developed as a combination of the component masses will be larger than allowed by the budget constraints. This will become even more obvious when the specific masses for existing MPD thrusters and MHD generators are included.

In the area of MPD thrusters, the specific mass values vary greatly, due to the different models created. The self-field vs. the applied-field thrusters are two completely different types of device, which react very differently to high currents. They are estimated



to be capable of operating in the specific impulse range of 1000 to 10000 seconds, but seem to work at power levels only between 100 and 1000 kW.<sup>12</sup> Fortunately, however, their efficiency has displayed a trend of improvement at the higher power levels (0.1-10 MW). The highest demonstrated performance for a self-field MPD thruster was a specific impulse of 5000 seconds when operating at 1.5 MW. The thruster displayed an efficiency of 40 %. At 30 kW, however, the thruster worked at an efficiency of 70 % with an  $I_{sp}$  of 7000 seconds.<sup>13</sup>

Conceptually speaking, MPD thrusters are thought to be possible with specific masses of 0.2 kg/kW.<sup>12</sup> This would translate to 200 kg/MW and, once again, push the envelope for NEPTUNE's budget, even under best conditions. This subsystem of NEPTUNE is by far the least understood and warrants further study. There is no readily apparent reason why MPD thrusters can not be used in a high power system, and, if that is the case, their specific impulse values make them too attractive to overlook.

The MHD generator has been applied widely to ground based power producing systems, so a great deal about the devices is known. Unfortunately, since system mass is a relatively minor constraint on the ground, mass values are still questionable. The MHD generator is composed of many of the same parts as the MPD thruster and can be expected to adopt similar specific masses. Once again, specific masses for these systems will undoubtedly improve with power level. In fact, in the case of the MHD generator, it becomes a far more attractive system at higher power levels. MHD generators mate extremely well with nuclear sources because of the high energy fluids they can generate. Although characteristic values for specific masses of these generators are normally around

4 kg/kW<sup>8</sup>, one estimate puts them as low as 0.45 kg/kW.<sup>14</sup> The efficiency of the generators vary wildly. The working fluid and the ease with which it ionizes are major concerns. Projections of efficiencies of 80 % with cesium gas and 55 % with xenon are notable.<sup>14</sup>

#### **4.4 – SOLVING THE PROBLEM**

Combining only the best specific masses of the generator, thruster, and NERVA source results in a NEPTUNE specific mass of 870 kg/MW. This already exceeds the budget defined earlier. This is a problem (although not unexpected) considering the fact that the radiator mass has not been included in the estimate and, because of the inefficiencies expected in the system, this mass could be significant. Fortunately, the values used in the analysis, as mentioned previously, are for systems operating at much lower power levels. Improvements in both system efficiency, leading to lower radiator mass, and specific mass will undoubtedly come with the high power systems.

The question of NEPTUNE's ability to accommodate a manned Mars mission has been answered. In its most basic state, using component specific mass parameters intended for low power applications (and restricting the burn time to 2 percent or less of the trip time), NEPTUNE can not support this mission. The question now becomes -- can alterations to NEPTUNE be made which might allow it support the manned Mars mission? This question is the topic of the remainder of the thesis.

## **CHAPTER V -- NEPTUNE DEVELOPMENT AREAS**

The conclusions from the previous chapter must be that if NEPTUNE is to be expected to accommodate a manned Mars venture, one of two things will have to occur -- either the mission must become less demanding (in terms of delta-v requirement) or the system must become more apt to undertake a demanding mission.

The idea of reducing the delta-v requirement for an impulsive Mars mission, while maintaining a fixed time of flight is a challenging astrodynamics problem. One popular technique used to reduce the delta-v burden on the propulsion system is the planetary swingby. The gravity of large bodies can be used to create a velocity change on the spacecraft. Moreover, if done cleverly, this velocity change can be appropriate to the transfer for which the craft is intended. One scenario for obtaining a "free" delta-v using a Martian swingby is addressed in Appendix C. Additionally, a computer routine to calculate the effects of the swingby is in Appendix D. This is a formidable problem and deserves further consideration.

This section will consider two developments that could aid the NEPTUNE propulsion system, itself, in better using its power. The technologies discussed are intended to reduce the mass of NEPTUNE without detracting from its capacity to produce thrust. The first section considers an alternative MHD generator, in which a

nonequilibrium plasma is used to carry the flow energy. The second section considers the development of a different nuclear rocket source, employing a particle bed reactor.

### **5.1 – NONEQUILIBRIUM MHD:**

The dimensions of the MHD device used in NEPTUNE will be larger than any device previously studied for space purposes because of the magnitude of the power requirements for an MPD thruster intended for interplanetary space exploration. However, just as NEPTUNE evolved as an alternative to the brute force method of continually increasing the size of established chemical systems, the more powerful MHD generator will be of little use if it simply scales with the smaller ones that preceded it. Therefore, since it is an intention of this project to improve rather than to scale, we must exploit characteristics of an MHD generator that affect its power output, that are more subtle than its size.

This section will present the theory behind a nonequilibrium MHD generator and explain why it is able to drive a high current, using minimal energy. The explanation will describe the benefits of the generator by addressing a series of related questions about the physics of a working fluid as it interacts, first with an arc discharge, then with electromagnetic forces in the MHD generator.

The first issue is to address the respective importance of electrons versus ions in the working plasma in carrying current through the generator. Two questions should be answered. Why are the electrons in a plasma almost completely responsible for carrying the current in the MHD generator and what relates the electric field created in the

generator to the amount of current that the generator can drive? These questions introduce the issue of conductivity of the working fluid and the parameters of the plasma that influence it. Next, once it is established that a high conductivity plasma is necessary to produce high current, and having shown that it is the electrons that are carrying the current in the plasma, how is it possible to increase the conductivity of those elements of the plasma which are responsible for carrying the current?

First, consider a plasma flowing through an MHD generator. As the conducting fluid runs normally to the applied magnetic field an electric field is created:

$$\vec{E}_{total} = \vec{E}_{applied} + (\vec{u} \times \vec{B}) \quad (5.1)$$

$u$  : flow velocity

Assume the net electric field generated has a strength,  $E$ . Then the force applied by the field on the electron will have a magnitude,  $eE$ , and will be directed in the same direction as the field. Likewise, an ion in the plasma, under the influence of the same field will feel an equal magnitude force in the opposite direction due to the field, as it possesses equal, but opposite charge. However, since the electron mass,  $m_e$ , is much smaller than the ion mass,  $m_i$ , the acceleration on the electron, due to the electric field,  $eE/m_e$ , will be much larger than the acceleration on the ion,  $eE/m_i$ .

This describes the situation in the plasma as it passes through the MHD generator. After a fixed time,  $t$ , the electrons have reached a velocity, based on their higher acceleration, which is much larger than that reached by the ions. In comparison, the ions achieve practically no directed drift velocity due to the electric field.

Now, consider the most fundamental description of current density. It is simply the amount of charge passing through a unit area per unit time -- a charge flux.

Microscopically, it may be expressed as a vector summation of all the individual charge motions:

$$\vec{j} = \sum_i n_i q_i \vec{v}_i \quad (5.2)$$

$n$  : number density

$q$  : charge

$v$  : particle velocity

Using the plasma assumption (that the electron and ion number densities are equal) and recalling that the charges on both ions and electrons have the same magnitude, the majority of the current density will be due to the motion of the faster particles, the electrons, in the direction of the electric field. In fact, because the electrons are so much smaller than the ions, almost all of the current will be carried by the free electrons in the plasma.

The above description answers the first question. It explains why the electrons, rather than the ions, carry the current through the MHD generator. Now, consider the relationship between the net electric field and the current density generated. The parameter that relates them is the bulk conductivity of the gas:

$$\vec{j} = \sigma (\vec{E} + \vec{u} \times \vec{B}) \quad (5.3)$$

$\sigma$  : conductivity

This equation, which is analogous to Ohm's Law, demonstrates the importance of high conductivity in creating current. The calculation of the conductivity of the gas is a calculation of the vector-averaged velocities of the elements which make up the gas. This is no trivial problem because of the many internal and external forces that direct them. In all, the mass and charge of the particles considered, their state of random thermal motion (temperature), the frequency and detailed characteristics of their collisions with themselves

and with all other particles in a gas, and the prevailing gasdynamic flow all affect the migration velocity of each charged particle and the bulk property called conductivity.<sup>15</sup>

The motion of the fluid through the generator will provide an electric field in the generator. The purpose of the generator is to drive current. In the case of a multimegawatt MPD thruster load, this current is significant. Therefore, it is essential that the plasma attain a high conductivity. Because the electrons are influenced much more heavily than the ions by field forces, the conductivity of a gas is primarily due to the motions of the electrons through it.<sup>16</sup> It is specifically these particles that must have a high conductivity.

Consider one of the characteristics of the gas, the temperature, and why it contributes to the gas conductivity. Conductivity may also be described as the ratio of the current density to the rate at which electrons in a unit volume gain momentum by impact with positive ions:

$$\sigma \propto \frac{j}{d(mv)_{coll}} \quad (5.4)$$

Consider the denominator of this ratio for two plasmas, one at high temperature and one at low, and determine the effect of the temperature of the gas on conductivity. In the low temperature plasma, the electron will impact ions and exchange some amount of momentum in the collision. As the temperature is raised to the second situation, the energy is increased in the gas uniformly, so the velocity increases in the electrons more than the ions (since it is a squared relationship in energy). Now when an electron collides with an ion, since momentum is linear with velocity, a larger amount of momentum is imparted on the ion and less momentum is gained by the electron in the collision (where

momentum is conserved). As a result, the denominator of the conductivity ratio becomes smaller with higher temperature and the conductivity becomes larger.

A relationship for the conductivity of a fully ionized gas flowing transverse to a strong magnetic field (as is the case in the MHD generator) can be written<sup>17</sup>:

$$\sigma = \frac{T^{3/2}}{1.29 \times 10^4 (Z \ln \Lambda)} \quad [\text{mho/cm}] \quad (5.5)$$

$Z$  : atomic number

$\ln \Lambda$  :  $h/p_0$

$h$  : Debye shielding distance

$p_0$  : close-collision distance

This relationship reflects the fact that the conductivity is directly related to the temperature of gas.

Now, the importance of the electrons to carry the current in the generator has been established. Also, the importance of high conductivity and the corresponding high temperature that helps to create it has been shown. All that remains is to find a way to exploit these qualities of a plasma to make the most efficient generator. How is it possible to create a plasma where the temperature of the electrons and the associated conductivity is high enough so that they may carry the necessary amount of current, but keep the bulk temperature of the gas low to avoid the excess energy input necessary for uniform heating and ensure that it can be contained by the materials in the generator?

The problem of creating a plasma with a much higher electron than ion temperature should begin with a discussion of how a plasma is created, in general. Consider the working fluid in the NEPTUNE system as it exits NERVA's nozzle. The energy added by the nuclear source to the working fluid is used to create a high velocity flow. As a result, by the time the fluid reaches the generator subsystem, the heat energy



has been converted, for the most part, to fluid velocity and the gas temperature is too low for ionization. The extent to which magnetic body forces can be exerted on an ionized gas depends on the ability of that gas to conduct electric current. Obviously, for the gas to carry current, free charges must exist in the gas. Processes that provide these free charges in the gas are ionization processes.

Ionization occurs when an amount of energy is added to that atom that surpasses its ionization potential. In a gas, the energy increment necessary to ionize a constituent atom may be delivered in a number of different events. The atom may undergo an inelastic collision with another particle (an ion, electron, or another atom) of sufficiently high kinetic energy:



Since the collision is inelastic, the colliding particle does not leave with as much kinetic energy as it came with. Instead that energy goes into the receiving gas atom to create the desired ionization.

A second event might involve the atom absorbing an electromagnetic photon of adequately high frequency:



Alternatively, an electron may be forcibly extracted from the atom by a strong electric field, as may be the case in a radio-frequency propagating electromagnetic wave train<sup>15</sup>:



The energy increment required to ionize varies from element to element. The ionization potential of NEPTUNE's working fluid, hydrogen, is given below.<sup>16</sup>

Table 5.1 -- Ionization energies of NEPTUNE fuel possibilities

Gas	Resonance potential eV	Ionization potential eV	Probable Ionization Process
H <sub>2</sub>	7.0	15.38	H <sub>2</sub> --- H <sub>2</sub> <sup>+</sup>
		18.0	H <sub>2</sub> --- H <sup>+</sup> +H
		26.0	H <sub>2</sub> --- H <sup>+</sup> +H+KE
		46.0	H <sub>2</sub> --- H <sup>+</sup> +H <sup>+</sup> +KE
He		24.58	He --- He <sup>+</sup>

Although several factors influence the ionization process in fluids (e.g. pressure), the most significant of these is the type of fluid to be ionized and its associated ionization energy. Unfortunately, the ionization potential of hydrogen is higher than most elements, thus making ionization more difficult to achieve.

Fortunately, there are intermediate stages of ionization. The degree of ionization,  $\alpha$ , of a plasma is defined by:

$$\alpha = \frac{n_e}{n_0} \quad (5.9)$$

$\alpha$  : degree of ionization

$n_0$  : number density of particles

$n_e$  : number density of electrons

It makes sense that a plasma with an abundance of free charges, a highly ionized plasma, would be able to carry more current than one with a lesser degree of ionization. To some extent this is true. At degrees of ionization less than  $10^{-3}$ , the electron-ion collisions are negligible and the conductivity increases as a function of energy content, reflected by the degree of ionization. However, at degrees of ionization above  $10^{-3}$ , the large coulomb cross-section for electron-ion collisions becomes dominant and, since it is assumed that  $n_e$  equals  $n_i$ , the conductivity is largely independent of electron density. Therefore, no significant gain in electrical conductivity, due to extra free charges, is made beyond the degree of ionization of  $10^{-3}$ .<sup>5</sup>

Additionally, there are ways to reduce the energy requirement for ionization. One of the most commonly used is "seeding", or enhancing the working fluid with some easily ionizable component that leads to further ionization. The addition of a seeding element, such as cesium, could take place just after the working fluid has passed through the core of the reactor. This would allow ionization to occur at temperatures as low as 2000 K, which is below the temperature of the gas coming out of the core.<sup>18</sup> Unfortunately, seeding carries with it certain drawbacks. It adds definite complexity to the system as it would require deseeding to occur prior to the inlet of the reactor.

In equilibrium, the degree of ionization in a gas is a function of the energy content. Therefore, the degree of ionization can be related to the gas temperature. This relation is the law of mass action<sup>4</sup>:

$$\frac{n_e n_i}{n_n} = \frac{(2\pi m_e k T)^{3/2}}{h^3} \frac{2g_i}{g_0} e^{\varepsilon_i/kT} \quad (5.10)$$

$n_e, n_i, n_n$  : number densities of electrons,  
ions, and neutrals, respectively  
 $k$  : Boltzmann constant  
 $g_i, g_0$  : electronic partition functions for ions  
and neutrals, respectively  
 $m_e$  : mass of electron  
 $T$  : electron temperature  
 $\varepsilon$  : ionization potential

The above equation is useful in highlighting the elements that go into the ionization process. Unfortunately, the above form of the law of mass action, complete with its electronic partition functions, makes calculations difficult. Consequently, for the calculations in this paper a form of the Saha equation to calculate the degree of ionization, is used<sup>19</sup>:

$$\log_{10} \left( \frac{x^2}{1-x^2} p \right) = \frac{-5050 V_i}{T} + 2.5 \log_{10} T - 6.5 \quad (5.11)$$

$x$  : degree of ionization  
 $p$  : fluid pressure

$V_i$  : ionization potential  
 $T$  : electron temperature

In NEPTUNE, the energy necessary to ionize the working fluid is added in a concentrated fashion by an arc discharge. The arc is created by applying a high enough current between two electrodes to break down the dielectric and allow a concentrated flow of electrons. As the originally inert working gas comes out of NERVA and encounters the arc discharge, it is bombarded by the flowing electrons. The energy transfer to the gas comes in the form of collisions between the electrons in the arc and the components of the working gas. Collisions with the comparatively massive nuclei in the gas are elastic, with electrons simply bouncing off and imparting little energy. Collisions with the smaller electrons result in significant energy transfers, sufficient to ionize the fluid. Through this process, the energy from the arc is consumed, almost exclusively, by the electrons in the working fluid and the temperature of the electrons increases.

The overall picture that emerges in the flowing plasma is the flow of two fluids entangled within one another. The first consists of the electrons, with a high temperature corresponding to the energy input from the arc ionizer. The second consists of the heavy particles.<sup>4</sup>

This description answers the last of the questions behind a nonequilibrium MHD generator. It explains how the temperature, and associated conductivity, of the electrons in the plasma may be increased with minimum energy input. It was shown earlier that the electrons in the complete plasma (or the electron gas in the two gas model) are the devices used to carry current. Moreover, the higher the energy content (the higher the temperature) of the gas, the higher the conductivity and the more current the gas can

carry. Therefore, if the gas flowing through the MHD generator maintains the flow velocity of the gas as a whole, and the electrons in the gas, which have soaked up all of the energy added in the ionization process, maintain their higher temperature, the conductivity of only those particles which are necessary to carry the current will have been increased. In creating this scenario, we will have deposited all the required energy for ionization and conductivity exactly where it is needed simply because that is the way the laws of nature (conservation of energy and momentum) say it must happen. This substantially increases the efficiency of the system. All the benefits of a high temperature, high conductivity gas are being achieved without the penalty of a high energy input.

Unfortunately, another question is introduced. In order to achieve sufficient power output in the generator, it is important that the nonequilibrium condition be sustained throughout the length of the generator. How long will this nonequilibrium condition, created by the arc discharge, exist? Will there not be a tendency for the fluid to move towards equilibrium?

It is here that a complete understanding of the relationship between collision rates and energy transfer per collision becomes important. Using the arc, an inert working fluid which may be described as the flow of two entangled gases at a common temperature, one consisting of slow moving nuclei and the other made up by faster bound electrons, has been separated and moved to a condition where the temperature of the heavy gas is essentially the same, while the energy of the electron gas is much higher. The gas is now a nonequilibrium gas. The electrons, with their freshly added energy, must undergo collisions between themselves to adjust to their new temperature in a Boltzmann

distribution. (In actuality, the heavy gas must also undergo collisions between its members to achieve a higher new temperature distribution, as it will soak up a minute amount of energy directly from the field as well.) However, at the same time the electrons are colliding with other electrons, there are also collisions occurring between the components of the two gases, electrons and ions, tending to equalize the temperatures between the particles.

In order to determine if it is possible to sustain a nonequilibrium gas through the generator, the competing effects which work to preserve or eliminate the nonequilibrium must be examined.

This problem may be addressed by analyzing the flow of energy through the electron gas. The nonequilibrium situation is defined by a high energy electron gas and a lower energy ion gas. As energy is added to the electron gas, the nonequilibrium becomes more pronounced. However, as energy flows from the electrons to the rest of the gas, equilibrium is approached.

First, consider the energy leaving the electron gas. The amount of power flowing from the gas is a function of both collision frequency and energy transferred per collision. The electrons will have collisions between themselves that force the electron gas to a Boltzmann distribution for its new energy content. The self-collision time between like particles may be written as:

$$t_c = \frac{11.44^{1/2} T^{3/2}}{n Z^4 \ln \Lambda} \quad (5.12)$$

A : atomic mass number

Intuitively, the terms in this expression make sense. As temperature increases, the energy and velocity of the particles will increase, making collision more likely and decreasing the

time between collisions. Also, notice the number density of the particles is in the denominator. Likewise, this makes sense since a dense concentration of particles will lead to more frequent collisions and a shorter time between collisions. It is interesting to note that, even in an equilibrium gas where the electrons and ions share a common temperature, the time between collisions for the electrons will be shorter than the heavy particles because of the  $m^{1/2}$  term in the numerator. As a result, if energy is input uniformly in the gas, the electrons will reach a Boltzmann energy distribution faster than the heavy particles since the amount of energy per collision will be directly scaled in collision between like particles.<sup>17</sup>

However, the collisions between electrons in the gas represent an energy transfer within the electron system. The intent is to consider the flow of energy out of the system. This will come as a result of collisions between the high energy electrons and the slower heavier ions. The amount of energy per unit time being transferred in these collisions is the power leaving the electron gas and working to erase the nonequilibrium.

Spitzer defines the relationship:

$$\frac{dT}{dt} = \frac{T_1 - T}{t_{eq}} \quad (5.13)$$

This equation describes how fast a two temperature gas equilibrates and assumes a common temperature. The result is the change in temperature per unit time. This can be related to the change in energy per unit time per unit volume between the electron gas and the heavy particle gas by substituting the known relationship for heat energy:

$$P_{out}/vol = \frac{3/2(n_e)k(T_e - T)}{t_{eq}} \quad (5.14)$$

The result of the above equation is called  $P_{out}/vol$ . This represents the flow of energy out of the electron gas. As it turns out, the energy is not leaving the gas, but to the electrons,

it looks as if it is. Notice, the parameter,  $t_{eq}$ . This is the characteristic time for equipartition of energy between the gases. It is defined by Spitzer as:

$$t_{eq} = \frac{5.87 A_e A}{n_e (Z_e^2 Z^2) \ln \Lambda} \left( \frac{T_e}{A_e} + \frac{T}{A} \right)^{3/2} \quad (5.15)$$

$A, A_e$  : atomic mass numbers of heavies  
electrons

$Z, Z_e$  : atomic numbers of heavies and electrons

$T, T_e$  : temperatures of heavies and electrons

$n_e$  : electron number density

The above describes the collisional process by which energy flows from the electron gas. Obviously, if this were the only input to the system, the gas would work towards equilibrium and the usefulness of the MHD generator would diminish.

Fortunately, there is a second factor to consider.

Although inefficiency is usually a negative side effect of electric power generation, it is a fortunate side effect in the case of a nonequilibrium MHD generator. Refer to the MHD generator power density equation:

$$P_0/vol = juB - \frac{j^2}{\sigma} \quad (2.7)$$

The second term in this equation represents the losses due to resistive heating. As the current is generated through the plasma, some of the energy is lost due to resistance (collisions between electrons) within the plasma. As a result, heat energy shows up in the electrons for the same reason it went to the electrons in the arc discharge. Normally, this would be considered a loss, since this energy will be unavailable to supply the load. However, in this unique case, this deposition of heat energy in the electrons helps to enforce the nonequilibrium situation that exists in the plasma. The input power per unit volume to the electron gas is therefore:

$$P_{in}/vol = \frac{j^2}{\sigma} \quad (5.16)$$

The conductivity of a plasma is a complicated variable. Fortunately, Spitzer has



developed a relation for the conductivity of a plasma flowing transverse to a strong magnetic field:

$$\sigma = \frac{7.702 \times 10^{-3}}{Z \ln \Lambda} T^{3/2} \quad (5.17)$$

The temperature in the above equation will be the electron temperature in a nonequilibrium gas because the electrons are the elements which carry the current.

In order to maintain or improve the nonequilibrium state in the plasma, the flow of energy into the electrons must exceed the flow from the electrons to the heavy particles. This sets up an inequality that can be rearranged to help identify those characteristics that aid in the maintenance of a nonequilibrium gas in the MHD generator:

$$\frac{(n_e)^2 T_e}{j^2} \leq \frac{(5.04 \times 10^{-4}) A}{k Z_e^2 Z(A_e)^{1/2}} \quad (5.18)$$

The right hand side of the inequality is made up completely of known terms for any gas.

The left hand side will be dependent on the characteristics of the generator.

The inequality defines those characteristics that help to maintain the nonequilibrium gas. A low electron density is desirable. This makes sense. Fewer electrons means fewer collisions, leading to lower energy transfer rate. Additionally, the lower the electron temperature the better. The low temperature difference leads to a smaller energy gradient driving the gas to equilibrium and a lower amount of energy being exchanged per collision. Finally, the high current density means that there is more loss due to resistive heating and, as stated earlier, the "loss" is a positive tool for preserving the nonequilibrium.

At this point, it is necessary to define what macroscopic properties are conducive to the creation of a nonequilibrium gas in the ionizer? Since it has been shown that energy added to the gas goes almost exclusively to the electrons, a good thing is high

energy input per unit time. This means little more than reasonably high electric field strength. Also, it was shown that energy is exchanged between like particles in the gas just as energy is exchanged between electrons and the heavy particles – through collisions. Therefore, a bad property is one that increases the collision frequency. Temperature is one of these parameters, but to keep it at low values would be to defeat the purpose of the system as a whole. However, what it is possible to keep low is the pressure and density of the flow. A more loosely packed gas means that the distance between collisions is greater and the time between collisions is longer. Therefore, the ratio of  $E/p$  becomes very important for the creation of a nonequilibrium gas as can be seen from the graph taken from Cobine.<sup>19</sup>

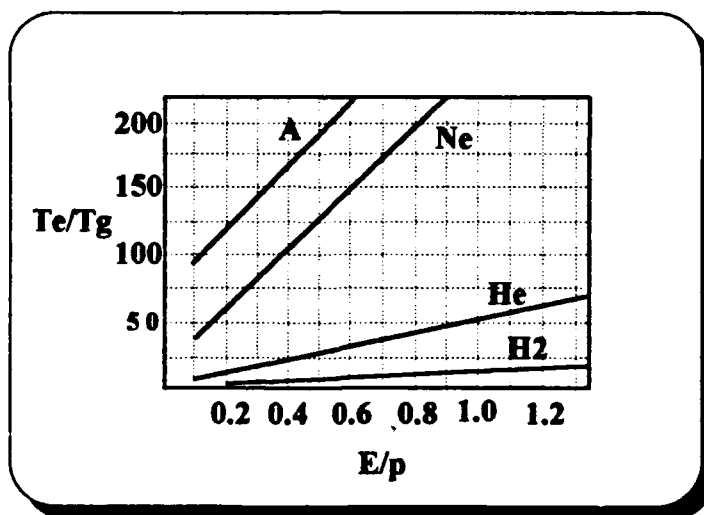


Figure 5.2 -- Creating a nonequilibrium gas

This relationship can be calculated numerically as well, by the equation<sup>20</sup>:

$$\frac{T_e - T_g}{T_e} = \frac{\pi m_g (\lambda_e e E)^2}{24 m_e (k T_e)^2} \quad (5.19)$$

$\lambda_e$  : mean free path length of electrons

$m_g$  : mass of heavy particle

The quantity  $\pi m_e / 24 m_e$  is already 240 for hydrogen and only gets higher for helium and other elements. Added to that, the temperature difference gets larger with the electric field, since the amount of energy that electrons pick up per path length is  $\lambda_e e E$ . The influence of the pressure in the gas comes from the mean free path, which is inversely proportional to pressure. Therefore, it is important to maximize the ratio of  $E/p$ .

This section has explained why a nonequilibrium MHD generator is an improvement upon MHD generators which do not employ nonequilibrium gases. Moreover, it has identified those conditions necessary to create and sustain nonequilibrium conditions in a MHD generator. The feasibility of supplying a nonequilibrium MHD generator with the exhaust gas generated by the NERVA rocket is assessed in appendix E.

## **5.2 -- PARTICLE BED REACTOR:**

The Air Force recently has supported two research programs to produce a nuclear thermal rocket to perform missions like the NERVA rocket of the late sixties and seventies. The first of these is a rejuvenation of the NERVA project. New technologies, particularly in the area of high temperature carbon composites, add new possibilities for an aging system. The second project involves the development of a compact particle bed reactor for space applications. This is called the Space Nuclear Thermal Propulsion (SNTTP) program.

The NERVA reactor is of prismatic form, as explained earlier. The coolant flows longitudinally through channels surrounded by rods of fissioning material. Heat is exchanged from the fission reaction to the flowing coolant.

A particle bed reactor derives benefits from the geometry it employs. The nuclear fuel is contained in small spherical shells, coated to withstand extremely high temperatures. The fuel spheres are dispersed in a porous bed through which coolant may flow.

The hydrogen enters the bed through a low temperature cold frit. It picks up heat, the byproduct of fission occurring in the fuel pebbles in the supporting bed, and is expelled through a very high temperature hot frit.

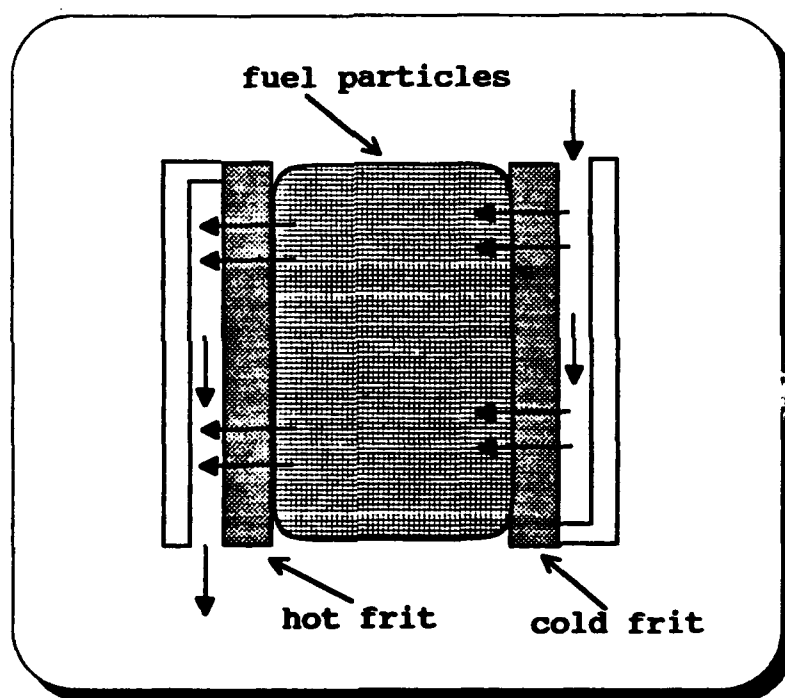


Figure 5.3 -- Particle Bed Reactor<sup>3</sup>

Because the spheres expose the maximum amount of area to the coolant, more heat can be transferred to the working gas than in a more conventional prismatic reactor.

Additionally, in the particle bed design, the moderator is separated from the fuel and

surrounds the bed along with a reflector. Its absence from direct contact with the fuel allows more direct contact of the hydrogen with the fuel.

Obviously, an important consideration in the development of this kind of reactor is the ability to produce materials which can be shaped as necessary, but at the same time, withstand temperatures as high as 3000 K. Research in carbon-carbon materials to replace graphite strengthen the concept. Although graphite can handle the high temperatures inherent to nuclear reactors, the carbon-carbon is a woven material that, if engineered properly, can be far stronger.

The result of these improvements is a more efficient reactor. SNTP is projected to produce coolant temperatures as high as 3000 K, specific impulses somewhat higher than NERVA (1000 seconds), and thrust of 353 kN, which is above NERVA's best projections. For our purposes, the increase in efficiency leads directly to a savings in mass. The mass of a particle bed reactor which can produce the same power as the NERVA reactor will undoubtedly be lower. Specific mass values identified for the modernized nuclear rocket sources are as low as 4.525 kg/MW.<sup>21</sup>

The advantages of the SNTP rocket are an improved reactor geometry and utilization of advanced materials. The drawback, however, is that this is not existing technology. Therefore, the parameters presented on SNTP are only projections. Much of the project is still classified and unavailable for presentation.

SNTP is another example of the benefits of creative engineering. It does not involve the discovery of some new energy source. It simply puts the available nuclear

energy source to better use through its ideal geometry. This is an underlying tone of the entire NEPTUNE system.

## **CHAPTER VI – ANALYSIS OF NEPTUNE SYSTEM**

The principles that make improvements on the NEPTUNE cycle possible were described in the previous chapter. Because the technologies involved, such as the particle bed reactor and nonequilibrium generator, are still in the theoretical stage of development, the success which they might have remains uncertain. Methods may be created, however, to analyze and evaluate the theory behind these technologies and determine if there is a possibility for them to work as intended. Appendix E contains an example of a theoretical analysis of the viability of a nonequilibrium generator supplied by standard NERVA exhaust.

In this chapter, however, the assumption is made that these improvements may be successfully integrated into the NEPTUNE cycle. The intent of this chapter is to analyze NEPTUNE by focusing on the gasdynamic flow.

### **6.1 – THERMODYNAMIC ANALYSIS OF THE NEPTUNE LOOP:**

NEPTUNE is about energy and the working fluid that carries it. It is about how energy shows up in the nuclear reactor and ends up in the electric thruster. The picture of a flowing gas is drawn from the definition of the gases' properties at key points within the loop. But what are the key points? The diagram of the NEPTUNE cycle is now labeled to identify the points of interest, between each of its components. The specifics of the

components themselves are not of primary interest. Instead, the intent is to describe the state of the gas after being acted on by the devices. These are the points where the complete state of the working fluid must be defined.

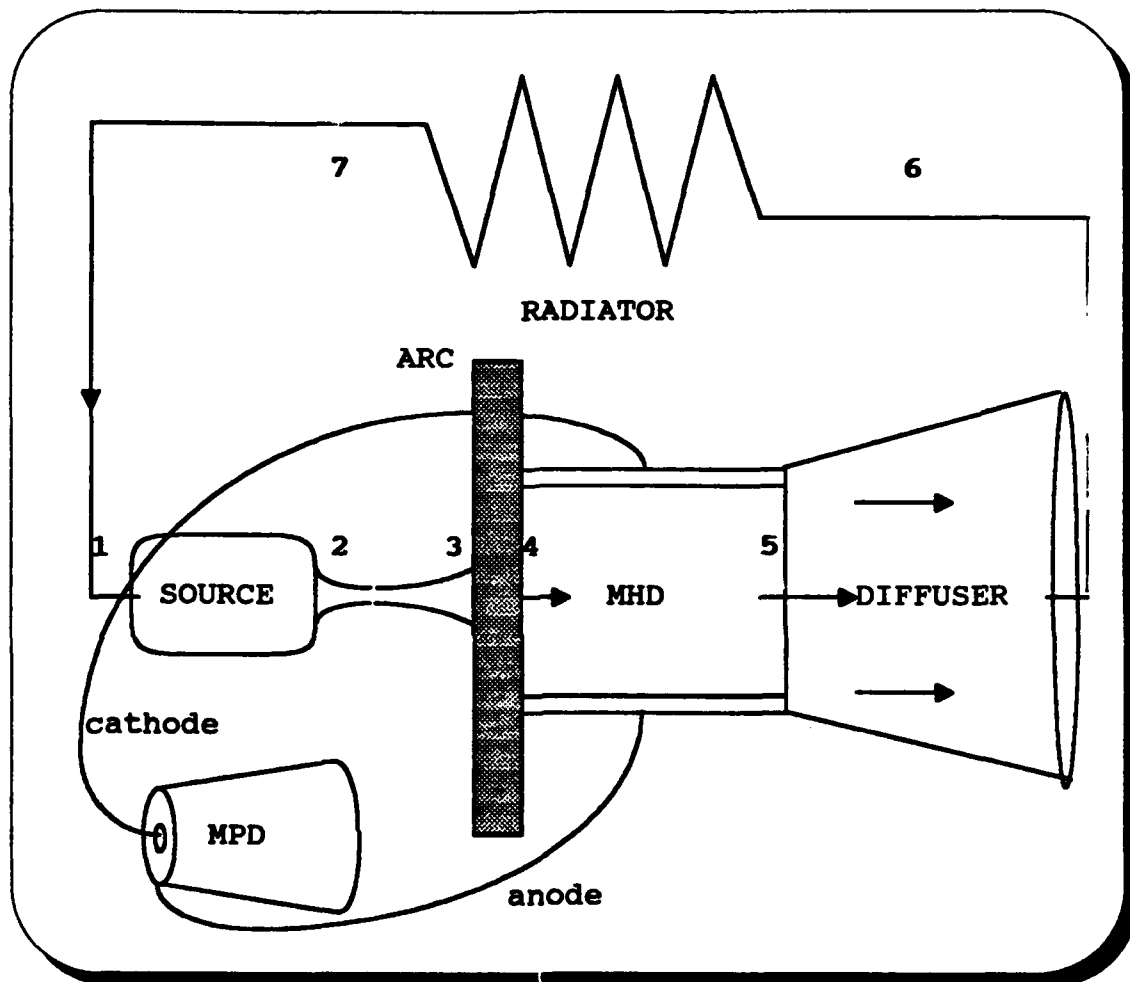


Figure 6.1 -- Points of thermodynamic evaluation of NEPTUNE cycle

NEPTUNE's fluid cycle can be compared to a Carnot cycle. A Carnot cycle is a fluid cycle consisting of two isothermal processes and two adiabatic processes. In the PV diagram, the work extracted from the fluid is represented by the area enclosed by the curves.



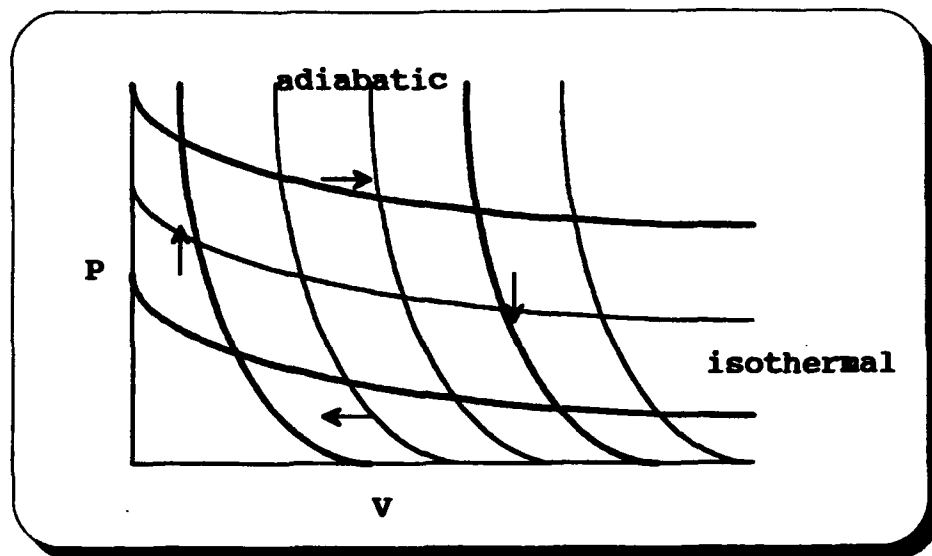


Figure 6.2 -- Carnot cycle<sup>22</sup>

Obviously, in order to extract a large amount of work, the temperature change over the highest and lowest point in the cycle should be large -- all of the energy available in the fluid should be used. This idea is captured in the Carnot efficiency, which determines how much of the available energy is extracted by the cycle<sup>22</sup>:

$$\eta = 1 - \frac{T_l}{T_u} \quad (6.1)$$

Modeling NEPTUNE by a thermodynamic cycle requires some variation from the Carnot cycle. The addition of heat energy in the nuclear source is practically isobaric, while the stagnation and static temperatures change. Consequently, the NEPTUNE cycle diverges from the Carnot cycle between thermodynamic points one and two (from the labeled NEPTUNE diagram). Next, comes an adiabatic expansion (like the Carnot cycle) through the nozzle on NERVA to exchange the heat energy for kinetic energy. Following this, the gas flows through the MHD generator where the conditions fit into none of the

simple categories. They are neither adiabatic nor isothermal. This section of the cycle is difficult to define and will be considered in depth later.

After the generator, the fluid must be brought to the radiator temperature by an adiabatic diffuser (points 5 to 6) and then the waste heat may be rejected at a constant temperature by an isothermal radiator. Ideally, after the radiator has done its job in rejecting losses in the system, the fluid will have been returned to its initial inlet conditions for NERVA at point 1.

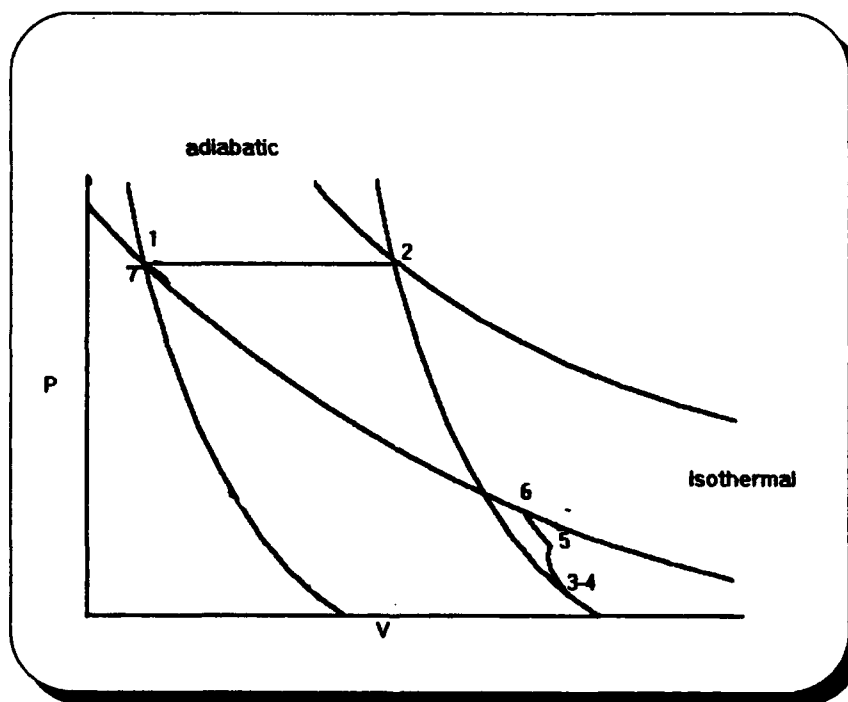


Figure 6.3 -- PV diagram of NEPTUNE loop

Some characteristics of the NEPTUNE system further constrain its representation by a PV diagram. For instance, there are definite advantages to maintaining a reactor inlet temperature (point 1) as high as possible. Radiator size, and therefore radiator mass, is largely dependent upon the temperature at which the energy is to be radiated:

$$A_{rad} = \frac{P_{rad}}{\sigma T^4} \quad (6.2)$$

Although it would be possible to achieve a higher cycle efficiency with a larger temperature spread, it is far more detrimental, due to the fourth power dependence of radiator area, to lower the minimum temperature any further than the reactor inlet requires.

This chapter seeks to explore an ideal NEPTUNE cycle in which the radiator temperature is held at the maximum value possible. This would be a case where the radiator temperature is equal to the reactor inlet temperature, requiring no adiabatic compression of the fluid to return it to reactor inlet conditions (i.e. pressure and density). Obviously, even this would be unacceptable unless the NERVA engine was modified for the closed cycle to allow a high enough inlet temperature to keep the radiator area at acceptable levels.

Normally, the coolant for NERVA comes from a cryogenic storage tank, where it is stored at a very low temperature. If the intent of the analysis is to complete the cycle with a isothermal expulsion of waste heat by the radiator, returning the fluid to its initial conditions, the inlet temperature must be considerably higher than normal. Only then will it permit the radiator to radiate its energy at an acceptably high temperature -- one that will keep the radiator area and mass within reasonable limits (which are defined by the specific mass budget derived in the first part of the paper).

Consider then, for this analysis, a modified nuclear rocket, with an inlet temperature of 1000 K and an outlet temperature of 3000 K. The reduced temperature spread does not prohibit the rocket from supporting the MPD load, as its extremes still surround the temperature for dissociation of hydrogen. Therefore, it can still store and

reclaim the energy involved in dissociation of the working fluid as the cycle proceeds, without making a large spread in the stagnation temperature of the fluid necessary.

The reduced change in stagnation enthalpy through the nuclear reactor creates a need for a somewhat higher mass flow rate for the coolant, in order to take out the heat energy. The original mass flow rate for the rocket may be calculated based on the known thrust force and exhaust velocities it provides.

Consider the SNTP rocket producing a thrust force of 353 kN.<sup>21</sup> The maximum specific impulse projection for the system is 1000 seconds, translating to an exhaust velocity of 9810 m/s. Therefore, using the equation:

$$F_t = \dot{m} u_{ex} \quad (6.3)$$

the mass flow rate may be calculated as 36 kg/s. However, for the modified rocket, with the reduced stagnation enthalpy spread, the mass flow must increase to 50 kg/s.

Additionally, approximate nozzle dimensions for NERVA's nozzle include a throat diameter of 0.19 m and an exit diameter of 4.3 m, which is a nozzle expansion ratio of 500:1.<sup>23</sup> Other parameters are specified for the reactor chamber (thermodynamic point 2). The chamber temperature is 3000 K and the pressure is  $6.895 \times 10^6$  N/m<sup>2</sup> (1000 psia).<sup>21</sup>

These numbers, coupled with assumptions made concerning the NEPTUNE cycle, are enough to completely define the thermodynamic state that must exist at the entrance to the reactor (point 1). As stated, the pressure will remain constant between points 1 and 2. Therefore,  $p_1$  equals  $6.895 \times 10^6$  N/m<sup>2</sup>. Additionally, stagnation conditions are assumed at the reactor inlet, so  $u_1 = 0$ . Finally, as stated earlier, the temperature at the reactor inlet will be 1000 K for this study. This presses the upper boundaries for material integrity for the reactor, but it is sufficiently high to maintain a low radiator mass and sufficiently low

so that the hydrogen coolant is completely recombined. The perfect gas law may be used to set the inlet density that corresponds to the other conditions.

$$p_1 = \rho_1 R_{H_2} T_1 \quad (6.4)$$

Next, use a combination of known data from NERVA and physical laws of gasdynamics to define the state of the gas at thermodynamic point 3, prior to the generator. The exhaust velocity for the rocket is  $u_3$ . Assume that it will remain constant across the ionizing source, so it may also be considered  $u_4$ , with a maximum value of 9810 m/s (corresponding to a specific impulse of 1000 seconds).

The rocket nozzle exit leads directly to the generator, so the cross-sectional areas at points 3 and 4 are the nozzle exit area, 14.5 m<sup>2</sup> for NERVA. This area will be taken as constant through the generator.

Since the mass flow, the area, and the velocity of the flow at the nozzle exit are known, they may be used to determine the fluid density at this point, from the law of conservation of mass:

$$\rho_3 = \frac{\dot{m}}{A_3 u_3} = \rho_4 \quad (6.5)$$

The temperature of the fluid at point 3 comes as a result of applying conservation of energy to the nuclear rocket (between points 1 and 3). The equation takes the form:

$$h_{01} + \frac{P_{\text{source}}}{\dot{m}} = c_p T_3 + \frac{u_3^2}{2} \quad (6.6)$$

Since the source power is:

$$P_{\text{source}} = \frac{1}{2} \dot{m} u_3^3 \quad (6.7)$$

and is known for NERVA,  $T_3$  may be calculated.

Finally, the perfect gas law makes it possible to determine the pressure of the working fluid at point 3:

$$p_3 = \rho_3 R_{H_2} T_3 = p_4 \quad (6.8)$$

$R_{H_2}$  : gas constant for  $H_2$

The conditions at points 3 and 4 will be the same (with the exception that the electron temperature of the gas might be different if the electrons could be separately heated in a nonequilibrium fashion. Also, seeding in this area may, in reality, alter conditions between 3 and 4.)

Now, a complete set of thermodynamic conditions (density, temperature, pressure, and velocity) of the fluid are known at the inlet to the generator. The next step is to define a system of equations to solve for the thermodynamic conditions at the generator outlet.

Since the area in the generator remains constant, the continuity equation may be simplified to provide the first equation:

$$\rho_4 u_4 = \rho_5 u_5 \quad (6.9)$$

Next, apply the law of conservation of momentum across the generator. In this calculation, however, it is essential to include the contribution of magnetic pressure:

$$\begin{aligned} \dot{m} \frac{u_4}{wd} + \rho_4 R_{H_2} T_4 + \frac{B_4^2}{2\mu_0} \\ = \dot{m} \frac{u_5}{wd} + \rho_5 R_{H_2} T_5 + \frac{B_5^2}{2\mu_0} \end{aligned} \quad (6.10)$$

B : magnetic field

w : generator plate width

d : generator plate spacing

In the above equation, the magnetic field for the generator has not yet been set. This will come as the result of the power requirements placed on the generator. Assuming some efficiency for the MHD, so that net output power is:

$$P_{gen} = \epsilon_{gen} \left( \frac{1}{2} \dot{m} u_4^2 \right) \quad (6.11)$$

The equation for power production in an MHD generator can then be used to find the necessary value of  $B_4$ :

$$JB_4 du_4 - \frac{J^2}{\sigma} \frac{d}{lw} = P_{gen} \quad (6.12)$$

$J$  : generator current

The amount of current in the generator is set by the current requirements of the load. The necessary current is a function of the thrust requirement, which combines the available source power, the mission delta-v, the attainable exhaust velocity of the thruster, the payload mass, and the specific mass of the propulsion system:

$$F_t = \frac{u_{ex}}{t_{burn}} [(e^{\Delta v/u_{ex}} - 1)(M_{pay} + \beta_{ps} P_{source})] \quad (6.13)$$

Now, the current requirement for the thruster load and the generator may be set:

$$J_{MPD} = J_{MHD} = \sqrt{\frac{F_t}{(\mu_0/4\pi)(\ln r_a/r_c + 3/4)}} \quad (6.14)$$

For the 290 day round-trip mission to Mars, described in Chapter 4, using the magnetoplasmadynamic thruster with and  $I_{sp}$  of 10,000 seconds, the current is calculated to be 210 kA.

The change in the magnetic field across the generator is due to the combined effect of the motion of the individual charge carriers in the plasma. As they move, they generate magnetic fields of their own, which add to the applied field:

$$B_4 + \frac{\mu_0 J}{w} = B_5 \quad (6.15)$$

Another conservation law that may be invoked is the law of conservation of energy. This must include a term representing the energy flowing from the system to drive the load:

$$c_p T_4 + \frac{u_4^2}{2} = c_p T_5 + \frac{u_5^2}{2} + \frac{\epsilon_{mhd} P_{source}}{m} \quad (6.16)$$

$c_p$  : specific heat

Finally, the perfect gas law is used at the generator outlet to relate pressure to temperature and density:

$$p_5 = \rho_5 R_{H2} T_5 \quad (6.17)$$

Now, there is a system of six equations, 6.7-6.8 and 6.10-6.13, to solve for the six unknown quantities:

$$\rho_5, T_5, p_5, u_5, B_4, B_5$$

Solving them results in a complete definition of the thermodynamic conditions at the outlet to the MHD generator, point 5.

Having addressed the unusual situation of the MHD generator, the next step is to continue, using variation of the same conservation equations, and close the NEPTUNE thermodynamic loop. This leads first to an analysis of the adiabatic diffuser that is used to compress the flow to the desired radiator temperature.

Earlier, the conditions which help to define an acceptable radiator temperature were presented and a temperature was set at 1000 K. Using this fact, the mach number of the flow at point 6, just prior to the radiator, can be defined using the stagnation temperature of the fluid:

$$M_6 = \sqrt{\frac{2}{\gamma-1} \left( \frac{T_{06}}{T_6} - 1 \right)} \quad (6.18)$$

As no energy has been exchanged between points 5 and 6, the stagnation temperatures of these two points will be the same. Therefore, the thermodynamic conditions defined at point 5 can be used to determine this stagnation temperature:

$$a_5 = \sqrt{\gamma R_{H2} T_5} \quad (6.19)$$

$$M_5 = \frac{u_5}{a_5} \quad (6.20)$$



$$T_{05} = T_5 \left(1 + \frac{\gamma-1}{2} M_5^2\right) \quad (6.21)$$

Similarly, the stagnation pressure at points 5 and 6 will be the same and can be calculated:

$$p_{05} = p_5 \left(1 + \frac{\gamma-1}{2} M_5^2\right)^{\gamma/\gamma-1} \quad (6.22)$$

The determination of the stagnation pressure makes it possible to solve for the pressure of the fluid at point 6:

$$p_6 = \frac{p_{06}}{\left(1 + \frac{\gamma-1}{2} M_6^2\right)^{\gamma/\gamma-1}} \quad (6.23)$$

Finally, the perfect gas law may be used to find the density of the fluid at point 6:

$$\rho_6 = \frac{p_6}{R_{H2} T_6} \quad (6.24)$$

and, with the local speed of sound, the velocity of the fluid is found at point 6 to complete the thermodynamic definition of the fluid:

$$a_6 = \sqrt{\gamma R_{H2} T_6} \quad (6.25)$$

$$u_6 = M_6 a_6 \quad (6.26)$$

The above analysis has taken one more step along NEPTUNE's thermodynamic cycle. Now, a complete set of thermodynamic conditions in the working fluid has been defined for points 3 through 6. Additionally, the conditions that must exist at the rocket inlet are known. The theory is that an isothermal rejection of heat by the radiator (between point 6 and 1) can lead directly to the inlet conditions required to complete the cycle. Now, it is time to test that theory.

The energy equation for the radiator region is replaced by the assumption that  $T_6 = T_1$ . However, an equation for the conservation of momentum is available and takes the form:

$$\frac{u_6^2}{2} - \frac{u_1^2}{2} = R_{H2} T_6 \ln \frac{p_1}{p_6} \quad (6.27)$$

For complete stagnation of the flow at point 1,  $u_1 = 0$ , as stated earlier. (Note that the heat rejected during this isothermal process is  $\frac{\Delta q}{m} = R_{H2} T_6 \ln \frac{p_1}{p_6}$ .) Again, the perfect gas law may be used to provide the last unknown state variable:

$$p_1 = \rho_1 R_{H2} T_1 \quad (6.28)$$

All that remains is to interpret the results. What will emerge from the analysis of the cycle as it proceeds forward (across the radiator) is a definition of the state of the fluid at the inlet to the reactor. However, from a knowledge of the NERVA outlet and chamber conditions and assumptions of the flow across the reactor, a complete set of thermodynamic conditions that must exist in the fluid at point 1 is already known. Obviously, if the cycle is to be closed, these conditions must agree.

But what if the conditions don't match? Then it is necessary to consider why they have not matched. What characteristics of the cycle can contribute to rectifying the discontinuity?

If the fluid density and pressure can not be returned to their initial value, when the temperature is set, then there must not be enough energy remaining to complete the cycle. The parameter that dictates the amount of energy left in the fluid is the efficiency of the generator. It is likely that the system will be too efficient to work in a closed cycle. In that case, the efficiency should be reduced to accommodate the closed cycle.

The above process was applied to a system with a generator efficiency of 0.5. In this case, the fluid indeed fell short of returning to its inlet conditions. To correct the problem, different generator efficiencies were evaluated until a satisfactory result was reached at an efficiency of 0.38. This efficiency value allowed enough energy to be retained in the flow so that the calculated inlet conditions to the system were closely matched to the required inlet values and the cycle was successfully closed.

Table 6.1 -- Thermodynamic data of NEPTUNE loop

Test Point	Mass Flow (kg/s)	Velocity (m/s)	Density (kg/m <sup>3</sup> x10 <sup>-4</sup> )	Temperature (K)	Pressure (N/m <sup>2</sup> )
1	50	---	1.66	1,000	6.895x10 <sup>5</sup>
2	50	---	0.28	3,000	6.895x10 <sup>6</sup>
3	50	9,810	3.51x10 <sup>-4</sup>	1,000	1,459.7
4	50	9,810	3.51x10 <sup>-4</sup>	1,000 (T <sub>c</sub> = 10,000)	1,459.7
5	50	5,320	6.48x10 <sup>-4</sup>	2,416	6,504
6	50	8,320	7.30x10 <sup>-5</sup>	1,000	303.27

## **CHAPTER VII -- CONCLUSIONS**

This thesis set out to analyze the ability of the NEPTUNE propulsion concept to support a manned Mars venture. A Mars mission is a formidable task. NEPTUNE is an electric propulsion concept, acting in a thrust region normally reserved for chemical, or possibly nuclear thermal systems. This is a thrust region that the multimegawatt NEPTUNE system can potentially reach. However, the analysis is clouded by the fact that the multimegawatt elements that make up NEPTUNE do not exist. Instead, a knowledge about these elements must be implied from a knowledge of their lower power relatives.

The results of the first part of this thesis reflect the fact that NEPTUNE can not support the manned Mars mission, particularly if we simply accept component mass estimates based on direct upscaling of the masses of similar low power components. (Bear in mind that this conclusion also incorporates thrusting times of no more than 2% of the mission time, as a limitation. There is evidence that suggests that thrusting times lasting as long as 5-10 percent of the mission time may still be considered by impulsive analysis.<sup>52</sup>) Therefore, in order to rectify the situation, one of two things must be done. The manned Mars mission must become less demanding, or proof must be provided that multimegawatt extrapolation of the elements which make up NEPTUNE involves more than the direct application of specific mass values for their low power relatives.

Appendix C addresses the possibility of decreasing the delta-v demand of a manned Mars venture, perhaps making it more reachable by NEPTUNE. The second part of the thesis, however, is dedicated to increasing the effectiveness of NEPTUNE. Two primary concepts were discussed -- the nonequilibrium MHD generator to produce electricity for the thruster, and a particle bed nuclear thermal rocket to produce high velocity plasma flow for the generator. The reasons why each device should improve the NEPTUNE system were presented.

The theory behind the elements which would make a Martian voyage possible using NEPTUNE was summarized by a thermodynamic analysis of NEPTUNE which incorporated the improvements. This analysis was intended to demonstrate that if the theories explained could be incorporated into NEPTUNE, the system could act on a closed cycle to meet the power needs of its Mars mission.

For the purpose of a thermodynamic analysis, Chapter 6 assumes a successful nonequilibrium MHD generator. Appendix E takes a closer look at the actual feasibility of a nonequilibrium MHD generator for NEPTUNE based on elevated electron temperature and develops a method to analyze the fluid's ability to sustain a nonequilibrium state ( $T_e \gg T_i$ ).

It is nearly impossible to apply quantitative values defining the effectiveness of the advanced technologies without actual experimental analysis. The intent, however, was to describe the physics behind the developments so that a legitimate claim may be made -- the technologies must work because the laws of physics say they must work. Obviously, solutions don't come that easily. The basic laws of nature are clouded by competing

phenomena along the way. The experimentalist must maintain a belief in physics and know that the device can succeed, so that he or she can develop methods in which the device does succeed.

NEPTUNE capitalizes on several basic ideas which immediately make it a propulsion system worth studying. It is clearly a system which makes an effort to match components that belong together, because of their separate characteristics. It is a system that uses the best known energy source, in terms of power density. Finally, it is a system that capitalizes on natural electromagnetic field forces to employ its power. Together, these components make up an unproven and futuristic system, but the ideas upon which it is based clearly define it as a system representing the direction of space propulsion on the horizon.

## **APPENDIX A**

Computer program MARSTRIP is to calculate the delta-v requirement for a round-trip Mars trajectory, based on an input time of flight constraint. It cycles through all of the time of flight and planetary geometry scenarios reasonable for a manned mission.

The program is written in Fortran and frequent, descriptive comments are contained to outline the flow. The program incorporates some subroutines from the United States Air Force Academy Department of Astronautical Engineering Computer Library.<sup>24</sup>



program marsclp

.....  
\* This program will determine the delta-v required to escape earth  
\* orbit (400 km) and undertake a mission transfer. Upon arrival at  
\* mars, the craft will enter a circular mars orbit for the time the  
\* crew remains on the surface. After stay time, the craft will fire  
\* a third burn to return to earth.  
.....

\* Define variables  
implicit logical (a-z)

```
real*8 on, daysec, tofout, e, deltae, a, p, atofout, nus, ra(1:3), pl  
real*8 rangeloo, cl, musun, vhal(1:3), vgh(1:3), vgal(1:3), rcmag  
real*8 margo, vcmag, vscmag, vbmag, dya, ehypoco, nu00, raddeg  
real*8 evel, c, put, ur, bt, at, mag, nub, tboag, numar, rmarag, rcmagag  
real*8 vmsc, vcmagag, dayco, umars, atay, tofah, c2, rbl(1:3)  
real*8 vgh(1:3), vgh1(1:3), vgh2(1:3), vgh3(1:3), vgh4(1:3), vgh5(1:3)  
real*8 tofobak, atay, margo, nub2, cb2(1:3), vrb2(1:3), vrb3(1:3)  
real*8 vrb1(1:3), vrb2(1:3), vrb3(1:3), vrb4(1:3), vrb5(1:3), vrb6(1:3)  
real*8 vrb7(1:3), vrb8(1:3), vrb9(1:3), vrb10(1:3), vrb11(1:3), vrb12(1:3)  
real*8 vrb13(1:3), vrb14(1:3), vrb15(1:3), vrb16(1:3), vrb17(1:3), vrb18(1:3)  
real*8 vrb19(1:3), vrb20(1:3), vrb21(1:3), vrb22(1:3), vrb23(1:3), vrb24(1:3)  
real*8 vrb25(1:3), vrb26(1:3), vrb27(1:3), vrb28(1:3), vrb29(1:3), vrb30(1:3)  
real*8 vrb31(1:3), vrb32(1:3), vrb33(1:3), vrb34(1:3), vrb35(1:3), vrb36(1:3)  
real*8 vrb37(1:3), vrb38(1:3), vrb39(1:3), vrb40(1:3), vrb41(1:3), vrb42(1:3)  
real*8 vrb43(1:3), vrb44(1:3), vrb45(1:3), vrb46(1:3), vrb47(1:3), vrb48(1:3)  
real*8 vrb49(1:3), vrb50(1:3), vrb51(1:3), vrb52(1:3), vrb53(1:3), vrb54(1:3)  
real*8 vrb55(1:3), vrb56(1:3), vrb57(1:3), vrb58(1:3), vrb59(1:3), vrb60(1:3)  
real*8 vrb61(1:3), vrb62(1:3), vrb63(1:3), vrb64(1:3), vrb65(1:3), vrb66(1:3)  
real*8 vrb67(1:3), vrb68(1:3), vrb69(1:3), vrb70(1:3), vrb71(1:3), vrb72(1:3)  
real*8 vrb73(1:3), vrb74(1:3), vrb75(1:3), vrb76(1:3), vrb77(1:3), vrb78(1:3)  
real*8 vrb79(1:3), vrb80(1:3), vrb81(1:3), vrb82(1:3), vrb83(1:3), vrb84(1:3)  
real*8 vrb85(1:3), vrb86(1:3), vrb87(1:3), vrb88(1:3), vrb89(1:3), vrb90(1:3)  
real*8 vrb91(1:3), vrb92(1:3), vrb93(1:3), vrb94(1:3), vrb95(1:3), vrb96(1:3)  
real*8 vrb97(1:3), vrb98(1:3), vrb99(1:3), vrb100(1:3), vrb101(1:3), vrb102(1:3)  
real*8 vrb103(1:3), vrb104(1:3), vrb105(1:3), vrb106(1:3), vrb107(1:3), vrb108(1:3)  
real*8 vrb109(1:3), vrb110(1:3), vrb111(1:3), vrb112(1:3), vrb113(1:3), vrb114(1:3)  
real*8 vrb115(1:3), vrb116(1:3), vrb117(1:3), vrb118(1:3), vrb119(1:3), vrb120(1:3)  
real*8 vrb121(1:3), vrb122(1:3), vrb123(1:3), vrb124(1:3), vrb125(1:3), vrb126(1:3)  
real*8 vrb127(1:3), vrb128(1:3), vrb129(1:3), vrb130(1:3), vrb131(1:3), vrb132(1:3)  
real*8 vrb133(1:3), vrb134(1:3), vrb135(1:3), vrb136(1:3), vrb137(1:3), vrb138(1:3)  
real*8 vrb139(1:3), vrb140(1:3), vrb141(1:3), vrb142(1:3), vrb143(1:3), vrb144(1:3)  
real*8 vrb145(1:3), vrb146(1:3), vrb147(1:3), vrb148(1:3), vrb149(1:3), vrb150(1:3)  
real*8 vrb151(1:3), vrb152(1:3), vrb153(1:3), vrb154(1:3), vrb155(1:3), vrb156(1:3)  
real*8 vrb157(1:3), vrb158(1:3), vrb159(1:3), vrb160(1:3), vrb161(1:3), vrb162(1:3)  
real*8 vrb163(1:3), vrb164(1:3), vrb165(1:3), vrb166(1:3), vrb167(1:3), vrb168(1:3)  
real*8 vrb169(1:3), vrb170(1:3), vrb171(1:3), vrb172(1:3), vrb173(1:3), vrb174(1:3)  
real*8 vrb175(1:3), vrb176(1:3), vrb177(1:3), vrb178(1:3), vrb179(1:3), vrb180(1:3)  
real*8 vrb181(1:3), vrb182(1:3), vrb183(1:3), vrb184(1:3), vrb185(1:3), vrb186(1:3)  
real*8 vrb187(1:3), vrb188(1:3), vrb189(1:3), vrb190(1:3), vrb191(1:3), vrb192(1:3)  
real*8 vrb193(1:3), vrb194(1:3), vrb195(1:3), vrb196(1:3), vrb197(1:3), vrb198(1:3)  
real*8 vrb199(1:3), vrb200(1:3), vrb201(1:3), vrb202(1:3), vrb203(1:3), vrb204(1:3)  
real*8 vrb205(1:3), vrb206(1:3), vrb207(1:3), vrb208(1:3), vrb209(1:3), vrb210(1:3)  
real*8 vrb211(1:3), vrb212(1:3), vrb213(1:3), vrb214(1:3), vrb215(1:3), vrb216(1:3)  
real*8 vrb217(1:3), vrb218(1:3), vrb219(1:3), vrb220(1:3), vrb221(1:3), vrb222(1:3)  
real*8 vrb223(1:3), vrb224(1:3), vrb225(1:3), vrb226(1:3), vrb227(1:3), vrb228(1:3)  
real*8 vrb229(1:3), vrb230(1:3), vrb231(1:3), vrb232(1:3), vrb233(1:3), vrb234(1:3)  
real*8 vrb235(1:3), vrb236(1:3), vrb237(1:3), vrb238(1:3), vrb239(1:3), vrb240(1:3)  
real*8 vrb241(1:3), vrb242(1:3), vrb243(1:3), vrb244(1:3), vrb245(1:3), vrb246(1:3)  
real*8 vrb247(1:3), vrb248(1:3), vrb249(1:3), vrb250(1:3), vrb251(1:3), vrb252(1:3)  
real*8 vrb253(1:3), vrb254(1:3), vrb255(1:3), vrb256(1:3), vrb257(1:3), vrb258(1:3)  
real*8 vrb259(1:3), vrb260(1:3), vrb261(1:3), vrb262(1:3), vrb263(1:3), vrb264(1:3)  
real*8 vrb265(1:3), vrb266(1:3), vrb267(1:3), vrb268(1:3), vrb269(1:3), vrb270(1:3)  
real*8 vrb271(1:3), vrb272(1:3), vrb273(1:3), vrb274(1:3), vrb275(1:3), vrb276(1:3)  
real*8 vrb277(1:3), vrb278(1:3), vrb279(1:3), vrb280(1:3), vrb281(1:3), vrb282(1:3)  
real*8 vrb283(1:3), vrb284(1:3), vrb285(1:3), vrb286(1:3), vrb287(1:3), vrb288(1:3)  
real*8 vrb289(1:3), vrb290(1:3), vrb291(1:3), vrb292(1:3), vrb293(1:3), vrb294(1:3)  
real*8 vrb295(1:3), vrb296(1:3), vrb297(1:3), vrb298(1:3), vrb299(1:3), vrb300(1:3)  
real*8 vrb301(1:3), vrb302(1:3), vrb303(1:3), vrb304(1:3), vrb305(1:3), vrb306(1:3)  
real*8 vrb307(1:3), vrb308(1:3), vrb309(1:3), vrb310(1:3), vrb311(1:3), vrb312(1:3)  
real*8 vrb313(1:3), vrb314(1:3), vrb315(1:3), vrb316(1:3), vrb317(1:3), vrb318(1:3)  
real*8 vrb319(1:3), vrb320(1:3), vrb321(1:3), vrb322(1:3), vrb323(1:3), vrb324(1:3)  
real*8 vrb325(1:3), vrb326(1:3), vrb327(1:3), vrb328(1:3), vrb329(1:3), vrb330(1:3)  
real*8 vrb331(1:3), vrb332(1:3), vrb333(1:3), vrb334(1:3), vrb335(1:3), vrb336(1:3)  
real*8 vrb337(1:3), vrb338(1:3), vrb339(1:3), vrb340(1:3), vrb341(1:3), vrb342(1:3)  
real*8 vrb343(1:3), vrb344(1:3), vrb345(1:3), vrb346(1:3), vrb347(1:3), vrb348(1:3)  
real*8 vrb349(1:3), vrb350(1:3), vrb351(1:3), vrb352(1:3), vrb353(1:3), vrb354(1:3)  
real*8 vrb355(1:3), vrb356(1:3), vrb357(1:3), vrb358(1:3), vrb359(1:3), vrb360(1:3)  
real*8 vrb361(1:3), vrb362(1:3), vrb363(1:3), vrb364(1:3), vrb365(1:3), vrb366(1:3)  
real*8 vrb367(1:3), vrb368(1:3), vrb369(1:3), vrb370(1:3), vrb371(1:3), vrb372(1:3)  
real*8 vrb373(1:3), vrb374(1:3), vrb375(1:3), vrb376(1:3), vrb377(1:3), vrb378(1:3)  
real*8 vrb379(1:3), vrb380(1:3), vrb381(1:3), vrb382(1:3), vrb383(1:3), vrb384(1:3)  
real*8 vrb385(1:3), vrb386(1:3), vrb387(1:3), vrb388(1:3), vrb389(1:3), vrb390(1:3)  
real*8 vrb391(1:3), vrb392(1:3), vrb393(1:3), vrb394(1:3), vrb395(1:3), vrb396(1:3)  
real*8 vrb397(1:3), vrb398(1:3), vrb399(1:3), vrb400(1:3), vrb401(1:3), vrb402(1:3)  
real*8 vrb403(1:3), vrb404(1:3), vrb405(1:3), vrb406(1:3), vrb407(1:3), vrb408(1:3)  
real*8 vrb409(1:3), vrb410(1:3), vrb411(1:3), vrb412(1:3), vrb413(1:3), vrb414(1:3)  
real*8 vrb415(1:3), vrb416(1:3), vrb417(1:3), vrb418(1:3), vrb419(1:3), vrb420(1:3)  
real*8 vrb421(1:3), vrb422(1:3), vrb423(1:3), vrb424(1:3), vrb425(1:3), vrb426(1:3)  
real*8 vrb427(1:3), vrb428(1:3), vrb429(1:3), vrb430(1:3), vrb431(1:3), vrb432(1:3)  
real*8 vrb433(1:3), vrb434(1:3), vrb435(1:3), vrb436(1:3), vrb437(1:3), vrb438(1:3)  
real*8 vrb439(1:3), vrb440(1:3), vrb441(1:3), vrb442(1:3), vrb443(1:3), vrb444(1:3)  
real*8 vrb445(1:3), vrb446(1:3), vrb447(1:3), vrb448(1:3), vrb449(1:3), vrb450(1:3)  
real*8 vrb451(1:3), vrb452(1:3), vrb453(1:3), vrb454(1:3), vrb455(1:3), vrb456(1:3)  
real*8 vrb457(1:3), vrb458(1:3), vrb459(1:3), vrb460(1:3), vrb461(1:3), vrb462(1:3)  
real*8 vrb463(1:3), vrb464(1:3), vrb465(1:3), vrb466(1:3), vrb467(1:3), vrb468(1:3)  
real*8 vrb469(1:3), vrb470(1:3), vrb471(1:3), vrb472(1:3), vrb473(1:3), vrb474(1:3)  
real*8 vrb475(1:3), vrb476(1:3), vrb477(1:3), vrb478(1:3), vrb479(1:3), vrb480(1:3)  
real*8 vrb481(1:3), vrb482(1:3), vrb483(1:3), vrb484(1:3), vrb485(1:3), vrb486(1:3)  
real*8 vrb487(1:3), vrb488(1:3), vrb489(1:3), vrb490(1:3), vrb491(1:3), vrb492(1:3)  
real*8 vrb493(1:3), vrb494(1:3), vrb495(1:3), vrb496(1:3), vrb497(1:3), vrb498(1:3)  
real*8 vrb499(1:3), vrb500(1:3), vrb501(1:3), vrb502(1:3), vrb503(1:3), vrb504(1:3)  
real*8 vrb505(1:3), vrb506(1:3), vrb507(1:3), vrb508(1:3), vrb509(1:3), vrb510(1:3)  
real*8 vrb511(1:3), vrb512(1:3), vrb513(1:3), vrb514(1:3), vrb515(1:3), vrb516(1:3)  
real*8 vrb517(1:3), vrb518(1:3), vrb519(1:3), vrb520(1:3), vrb521(1:3), vrb522(1:3)  
real*8 vrb523(1:3), vrb524(1:3), vrb525(1:3), vrb526(1:3), vrb527(1:3), vrb528(1:3)  
real*8 vrb529(1:3), vrb530(1:3), vrb531(1:3), vrb532(1:3), vrb533(1:3), vrb534(1:3)  
real*8 vrb535(1:3), vrb536(1:3), vrb537(1:3), vrb538(1:3), vrb539(1:3), vrb540(1:3)  
real*8 vrb541(1:3), vrb542(1:3), vrb543(1:3), vrb544(1:3), vrb545(1:3), vrb546(1:3)  
real*8 vrb547(1:3), vrb548(1:3), vrb549(1:3), vrb550(1:3), vrb551(1:3), vrb552(1:3)  
real*8 vrb553(1:3), vrb554(1:3), vrb555(1:3), vrb556(1:3), vrb557(1:3), vrb558(1:3)  
real*8 vrb559(1:3), vrb560(1:3), vrb561(1:3), vrb562(1:3), vrb563(1:3), vrb564(1:3)  
real*8 vrb565(1:3), vrb566(1:3), vrb567(1:3), vrb568(1:3), vrb569(1:3), vrb570(1:3)  
real*8 vrb571(1:3), vrb572(1:3), vrb573(1:3), vrb574(1:3), vrb575(1:3), vrb576(1:3)  
real*8 vrb577(1:3), vrb578(1:3), vrb579(1:3), vrb580(1:3), vrb581(1:3), vrb582(1:3)  
real*8 vrb583(1:3), vrb584(1:3), vrb585(1:3), vrb586(1:3), vrb587(1:3), vrb588(1:3)  
real*8 vrb589(1:3), vrb590(1:3), vrb591(1:3), vrb592(1:3), vrb593(1:3), vrb594(1:3)  
real*8 vrb595(1:3), vrb596(1:3), vrb597(1:3), vrb598(1:3), vrb599(1:3), vrb600(1:3)  
real*8 vrb601(1:3), vrb602(1:3), vrb603(1:3), vrb604(1:3), vrb605(1:3), vrb606(1:3)  
real*8 vrb607(1:3), vrb608(1:3), vrb609(1:3), vrb610(1:3), vrb611(1:3), vrb612(1:3)  
real*8 vrb613(1:3), vrb614(1:3), vrb615(1:3), vrb616(1:3), vrb617(1:3), vrb618(1:3)  
real*8 vrb619(1:3), vrb620(1:3), vrb621(1:3), vrb622(1:3), vrb623(1:3), vrb624(1:3)  
real*8 vrb625(1:3), vrb626(1:3), vrb627(1:3), vrb628(1:3), vrb629(1:3), vrb630(1:3)  
real*8 vrb631(1:3), vrb632(1:3), vrb633(1:3), vrb634(1:3), vrb635(1:3), vrb636(1:3)  
real*8 vrb637(1:3), vrb638(1:3), vrb639(1:3), vrb640(1:3), vrb641(1:3), vrb642(1:3)  
real*8 vrb643(1:3), vrb644(1:3), vrb645(1:3), vrb646(1:3), vrb647(1:3), vrb648(1:3)  
real*8 vrb649(1:3), vrb650(1:3), vrb651(1:3), vrb652(1:3), vrb653(1:3), vrb654(1:3)  
real*8 vrb655(1:3), vrb656(1:3), vrb657(1:3), vrb658(1:3), vrb659(1:3), vrb660(1:3)  
real*8 vrb661(1:3), vrb662(1:3), vrb663(1:3), vrb664(1:3), vrb665(1:3), vrb666(1:3)  
real*8 vrb667(1:3), vrb668(1:3), vrb669(1:3), vrb670(1:3), vrb671(1:3), vrb672(1:3)  
real*8 vrb673(1:3), vrb674(1:3), vrb675(1:3), vrb676(1:3), vrb677(1:3), vrb678(1:3)  
real*8 vrb679(1:3), vrb680(1:3), vrb681(1:3), vrb682(1:3), vrb683(1:3), vrb684(1:3)  
real*8 vrb685(1:3), vrb686(1:3), vrb687(1:3), vrb688(1:3), vrb689(1:3), vrb690(1:3)  
real*8 vrb691(1:3), vrb692(1:3), vrb693(1:3), vrb694(1:3), vrb695(1:3), vrb696(1:3)  
real*8 vrb697(1:3), vrb698(1:3), vrb699(1:3), vrb700(1:3), vrb701(1:3), vrb702(1:3)  
real*8 vrb703(1:3), vrb704(1:3), vrb705(1:3), vrb706(1:3), vrb707(1:3), vrb708(1:3)  
real*8 vrb709(1:3), vrb710(1:3), vrb711(1:3), vrb712(1:3), vrb713(1:3), vrb714(1:3)  
real*8 vrb715(1:3), vrb716(1:3), vrb717(1:3), vrb718(1:3), vrb719(1:3), vrb720(1:3)  
real*8 vrb721(1:3), vrb722(1:3), vrb723(1:3), vrb724(1:3), vrb725(1:3), vrb726(1:3)  
real*8 vrb727(1:3), vrb728(1:3), vrb729(1:3), vrb730(1:3), vrb731(1:3), vrb732(1:3)  
real*8 vrb733(1:3), vrb734(1:3), vrb735(1:3), vrb736(1:3), vrb737(1:3), vrb738(1:3)  
real*8 vrb739(1:3), vrb740(1:3), vrb741(1:3), vrb742(1:3), vrb743(1:3), vrb744(1:3)  
real*8 vrb745(1:3), vrb746(1:3), vrb747(1:3), vrb748(1:3), vrb749(1:3), vrb750(1:3)  
real*8 vrb751(1:3), vrb752(1:3), vrb753(1:3), vrb754(1:3), vrb755(1:3), vrb756(1:3)  
real*8 vrb757(1:3), vrb758(1:3), vrb759(1:3), vrb760(1:3), vrb761(1:3), vrb762(1:3)  
real*8 vrb763(1:3), vrb764(1:3), vrb765(1:3), vrb766(1:3), vrb767(1:3), vrb768(1:3)  
real*8 vrb769(1:3), vrb770(1:3), vrb771(1:3), vrb772(1:3), vrb773(1:3), vrb774(1:3)  
real*8 vrb775(1:3), vrb776(1:3), vrb777(1:3), vrb778(1:3), vrb779(1:3), vrb780(1:3)  
real*8 vrb781(1:3), vrb782(1:3), vrb783(1:3), vrb784(1:3), vrb785(1:3), vrb786(1:3)  
real*8 vrb787(1:3), vrb788(1:3), vrb789(1:3), vrb790(1:3), vrb791(1:3), vrb792(1:3)  
real*8 vrb793(1:3), vrb794(1:3), vrb795(1:3), vrb796(1:3), vrb797(1:3), vrb798(1:3)  
real*8 vrb799(1:3), vrb800(1:3), vrb801(1:3), vrb802(1:3), vrb803(1:3), vrb804(1:3)  
real*8 vrb805(1:3), vrb806(1:3), vrb807(1:3), vrb808(1:3), vrb809(1:3), vrb810(1:3)  
real*8 vrb811(1:3), vrb812(1:3), vrb813(1:3), vrb814(1:3), vrb815(1:3), vrb816(1:3)  
real*8 vrb817(1:3), vrb818(1:3), vrb819(1:3), vrb820(1:3), vrb821(1:3), vrb822(1:3)  
real*8 vrb823(1:3), vrb824(1:3), vrb825(1:3), vrb826(1:3), vrb827(1:3), vrb828(1:3)  
real*8 vrb829(1:3), vrb830(1:3), vrb831(1:3), vrb832(1:3), vrb833(1:3), vrb834(1:3)  
real*8 vrb835(1:3), vrb836(1:3), vrb837(1:3), vrb838(1:3), vrb839(1:3), vrb840(1:3)  
real*8 vrb841(1:3), vrb842(1:3), vrb843(1:3), vrb844(1:3), vrb845(1:3), vrb846(1:3)  
real*8 vrb847(1:3), vrb848(1:3), vrb849(1:3), vrb850(1:3), vrb851(1:3), vrb852(1:3)  
real*8 vrb853(1:3), vrb854(1:3), vrb855(1:3), vrb856(1:3), vrb857(1:3), vrb858(1:3)  
real*8 vrb859(1:3), vrb860(1:3), vrb861(1:3), vrb862(1:3), vrb863(1:3), vrb864(1:3)  
real*8 vrb865(1:3), vrb866(1:3), vrb867(1:3), vrb868(1:3), vrb869(1:3), vrb870(1:3)  
real*8 vrb871(1:3), vrb872(1:3), vrb873(1:3), vrb874(1:3), vrb875(1:3), vrb876(1:3)  
real*8 vrb877(1:3), vrb878(1:3), vrb879(1:3), vrb880(1:3), vrb881(1:3), vrb882(1:3)  
real*8 vrb883(1:3), vrb884(1:3), vrb885(1:3), vrb886(1:3), vrb887(1:3), vrb888(1:3)  
real*8 vrb889(1:3), vrb890(1:3), vrb891(1:3), vrb892(1:3), vrb893(1:3), vrb894(1:3)  
real*8 vrb895(1:3), vrb896(1:3), vrb897(1:3), vrb898(1:3), vrb899(1:3), vrb900(1:3)  
real*8 vrb901(1:3), vrb902(1:3), vrb903(1:3), vrb904(1:3), vrb905(1:3), vrb906(1:3)  
real*8 vrb907(1:3), vrb908(1:3), vrb909(1:3), vrb910(1:3), vrb911(1:3), vrb912(1:3)  
real*8 vrb913(1:3), vrb914(1:3), vrb915(1:3), vrb916(1:3), vrb917(1:3), vrb918(1:3)  
real*8 vrb919(1:3), vrb920(1:3), vrb921(1:3), vrb922(1:3), vrb923(1:3), vrb924(1:3)  
real*8 vrb925(1:3), vrb926(1:3), vrb927(1:3), vrb928(1:3), vrb929(1:3), vrb930(1:3)  
real*8 vrb931(1:3), vrb932(1:3), vrb933(1:3), vrb934(1:3), vrb935(1:3), vrb936(1:3)  
real*8 vrb937(1:3), vrb938(1:3), vrb939(1:3), vrb940(1:3), vrb941(1:3), vrb942(1:3)  
real*8 vrb943(1:3), vrb944(1:3), vrb945(1:3), vrb946(1:3), vrb947(1:3), vrb948(1:3)  
real*8 vrb949(1:3), vrb950(1:3), vrb951(1:3), vrb952(1:3), vrb953(1:3), vrb954(1:3)  
real*8 vrb955(1:3), vrb956(1:3), vrb957(1:3), vrb958(1:3), vrb959(1:3), vrb960(1:3)  
real*8 vrb961(1:3), vrb962(1:3), vrb963(1:3), vrb964(1:3), vrb965(1:3), vrb966(1:3)  
real*8 vrb967(1:3), vrb968(1:3), vrb969(1:3), vrb970(1:3), vrb971(1:3), vrb972(1:3)  
real*8 vrb973(1:3), vrb974(1:3), vrb975(1:3), vrb976(1:3), vrb977(1:3), vrb978(1:3)  
real*8 vrb979(1:3), vrb980(1:3), vrb981(1:3), vrb982(1:3), vrb983(1:3), vrb984(1:3)  
real*8 vrb985(1:3), vrb986(1:3), vrb987(1:3), vrb988(1:3), vrb989(1:3), vrb990(1:3)  
real*8 vrb991(1:3), vrb992(1:3), vrb993(1:3), vrb994(1:3), vrb995(1:3), vrb996(1:3)  
real*8 vrb997(1:3), vrb998(1:3), vrb999(1:3), vrb1000(1:3), vrb1001(1:3), vrb1002(1:3)  
real*8 vrb1003(1:3), vrb1004(1:3), vrb1005(1:3), vrb1006(1:3), vrb1007(1:3), vrb1008(1:3)  
real*8 vrb1009(1:3), vrb1010(1:3), vrb1011(1:3), vrb1012(1:3), vrb1013(1:3), vrb1014(1:3)  
real*8 vrb1015(1:3), vrb1016(1:3), vrb1017(1:3), vrb1018(1:3), vrb1019(1:3), vrb1020(1:3)  
real*8 vrb1021(1:3), vrb1022(1:3), vrb1023(1:3), vrb1024(1:3), vrb1025(1:3), vrb1026(1:3)  
real*8 vrb1027(1:3), vrb1028(1:3), vrb1029(1:3), vrb1030(1:3), vrb1031(1:3), vrb1032(1:3)  
real*8 vrb1033(1:3), vrb1034(1:3), vrb1035(1:3), vrb1036(1:3), vrb1037(1:3), vrb1038(1:3)  
real*8 vrb1039(1:3), vrb1040(1:3), vrb1041(1:3), vrb1042(1:3), vrb1043(1:3), vrb1044(1:3)  
real*8 vrb1045(1:3), vrb1046(1:3), vrb1047(1:3), vrb1048(1:3), vrb1049(1:3), vrb1050(1:3)  
real*8 vrb1051(1:3), vrb1052(1:3), vrb1053(1:3), vrb1054(1:3), vrb1055(1:3), vrb1056(1:3)  
real*8 vrb1057(1:3), vrb1058(1:3), vrb1059(1:3), vrb1060(1:3), vrb1061(1:3), vrb1062(1:3)  
real*8 vrb1063(1:3), vrb1064(1:3), vrb1065(1:3), vrb1066(1:3), vrb1067(1:3), vrb1068(1:3)  
real*8 vrb1069(1:3), vrb1070(1:3), vrb1071(1:3), vrb1072(1:3), vrb1073(1:3), vrb1074(1:3)  
real*8 vrb1075(1:3), vrb1076(1:3), vrb1077(1:3), vrb1078(1:3), vrb1079(1:3), vrb1080(1:3)  
real*8 vrb1081(1:3), vrb1082(1:3), vrb1083(1:3), vrb1084(1:3), vrb1085(1:3), vrb1086(1:3)  
real*8 vrb1087(1:3), vrb1088(1:3), vrb1089(1:3), vrb1090(1:3), vrb1091(1:3), vrb1092(1:3)  
real*8 vrb1093(1:3), vrb1094(
```



9304/24  
07/07/80

```

dva = dabs(rbmag - vcmag)

* Determine when to apply dva
chyppe = 1.0d0 * (vvel(3)**2.0d0/rcmag/magc)
nu00 = dcos(1.0d0/chyppe)

* Fire thruster at an angle nu00 short of ra direction

* Calculate delta-v from Hartian orbit insertion
* First Hera encounter, find nub
nub = dcos((p-rmag)/(e*rmag))

* Find rbl and vrb1 vectors
rbl(1) = rmag-dcos(nub)
rbl(2) = rmag-dsin(nub)
rbl(3) = mag(rbl)

vrb1(1) = -c1 * dsin(nub)
vrb1(2) = c1 * (e-dcos(nub))
vrb1(3) = mag(vrb1)

* Find vrb1
c2 = dsqrt(massn/rmag)
vrb1(1) = -c2 * dsin(nub)
vrb1(2) = c2 * dcos(nub)
vrb1(3) = mag(vrb1)

* Use vrb1 = vrb1 + vrb1
do 20, i=1,2
  vrb1(i) = vrb1(i) + vrb1(i)
cont'ine
vrb1(3) = mag(vrb1)

20

* Consider a 400 km parking orbit of Hera
vrmag = dsqrt(vrb1(1)**2.0d0 + vrb1(2)**2.0d0)
dvr1 = dabs(vrmag - vcmag)

* Start middle loop
lctay = 10.0d0
cont'ine

* Start inner loop
lctflsh = 70.0d0
cont'ine

14

* Use Gauss to calculate delta-v from return orbit insertion
stcfsh = lctflsh + daysec
lctofsh = lctflsh + dayc

* Define rrb2
stctay = lctay + daysec
mrmag = stctay * mmas
nub2 = nub + mrmag
rbl(1) = rmag + dcos(nub2)
rbl(2) = rmag + dsin(nub2)
rbl(3) = mag(rbl)

* Transfer to HJ
do 22, i=1,3
  aur2(i) = rbl(i) / 1.495965d8
cont'ine

22

* Define ra2

```

tmropt.f

```

nuar2 = (lctofsh + stcfsh + stctay) * vmpo
ra2(1) = raumpo + dcos(nuar2)
ra2(2) = raumpo + dsin(nuar2)
ra2(3) = mag(ra2)

* Transfer to AU
do 24, i=1,3
  aur2(i) = ra2(i) / 1.495965d8
cont'ine

24

* Call Gauss
call gauss(aur2,aur2,dm,totofsh,vrb2a,vrb2a)
call gauss(aur2,aur2,dm,totofsh,vrb2b,vrb2b)

* Put velocities in km/s
do 26, i=1,3
  vrb2a(i) = vrb2a(i) * raumpo / 5.0326737d6
  vrb2b(i) = vrb2b(i) * raumpo / 5.0326737d6
  vrb2i(i) = vrb2i(i) * raumpo / 5.0326737d6
  vrb2f(i) = vrb2f(i) * raumpo / 5.0326737d6
cont'ine

26

* Determine return orbit parameters
call elorb(rb2,vrb2a,p21,d21,m21,aur2a)
call elorb(rb2,vrb2b,p21,d21,m21,aur2b)

* Use vrb2 = vrb2 + vrb2
vrb2(1) = -c2 * dsin(nub2)
vrb2(2) = c2 * dcos(nub2)
vrb2(3) = mag(vrb2)

do 28, i=1,2
  vrb2a(i) = vrb2a(i) + vrb2(i)
  vrb2b(i) = vrb2b(i) + vrb2(i)
cont'ine
vrb2a(3) = mag(vrb2a)
vrb2b(3) = mag(vrb2b)

28

* Calculate delta-v at a from 400 km parking orbit
vrb2a = dsqrt(vrb2a(1)**2 + vrb2a(2)**2)
vrb2b = dsqrt(vrb2b(1)**2 + vrb2b(2)**2)
dvr2a = dabs(vrb2a - vcmag)
dvr2b = dabs(vrb2b - vcmag)

* Calculate total delta-v
drtota = dva + dvr1 + dvr2a
drtot1 = dva + dvr1 + dvr2b

*****
* Calculate total time of flight
ttot = totot + totflsh + lctay
sectof = ttot * 24.0d0 * 3600.0d0
tburn = tfract + sectof

* Find mass flow
nrmag = envel * 1000.0d0
ndrtota = drtota * 1000.0d0
ndotlmpd = 2.0d0 * pchrust / (nrmag*ndrtota)
mprop = ndotlmpd * tburn

* Governing equations
pur = ndrtota/nrmag

```

5300473  
97:07:49

```

t1 = at** (par) - 1.000
alpha = (lmpap / t1) - mpar) / psource) * 1000000.000

* Write to output file
if (alpha .ge. 0.000) then
  write(60,90) t1ot,totout,tatay,totbat,alpha,dva,dvb1,dvb2,
/
  dovb1
endif

* Governing equations
ndvot1 = detot1 * 1000.000
par = ndvot1/ndvot1
t1 = at** (par) - 1.000
alpha = (lmpap / t1) - mpar) / psource) * 1000000.000

* Write to output file
if (alpha .ge. 0.000) then
  write(60,90) t1ot,totout,tatay,totbat,alpha,dva,dvb1,dvb2,
/
  dovb1
endif

* Update return time
totbat = totbat + 20.000
if (totbat .le. 250.000) goto 14

* Update stay time
tatay = tatay + 20.000
if (tatay .le. 110.000) goto 12

* Update time of flight
totout = totout + 20.000
count = count + 1
if (totout .le. 250.000) goto 10

* Format statements
72 format (4n,'source power: ',f12.11)
73 format (4n,'ambient velocity: ',f8.3)
74 format (4n,'burn time fraction: ',f5.3,/)
75 format (5n,'tot',3n,'totat',3n,'tatay',2n,'totbat',8n,'alpha',4n
/
  ,dva1',3n,'dvb1',3n,'dvb2',2n,'detot1'
90 format (4n,f5.1,2n,f5.1,2n,f5.1,2n,f5.1,4n,f6.4,4n
/
  ,f5.1,2n,f5.1,2n,f5.1,2n,f5.1)

stop
end

* Define function mag(v)
real*8 function mag(v)
real*8 v(1:3)
mag = dsqrt(v(1)**2 + v(2)**2 + v(3)**2)
return
end

* Define variables
subroutine eccent (totf,r,p,delta,a)
real*8 totf,r,p,delta,a,ra,rb,ma,ma0,p,arg1,arg2,arg3,nu
real*8 anpnu,ec,anpnu,ltot,halfday
* Define radius at point a (earth) and point b (mars)

```

tmpropt.f

```

ra = 1.49599834e
rb = 1.52540e + ra
ma0nu = 1.3271546e11
halfday = 12.060 + 3600.000

* Set initial eccentricity guess
10 continue
e0 = e
a = ra / (1.000 - e0)
p = a * (1.000 + e0**2)

* Calculate angles nu and ee
arg1 = (p-rb) / (e0*rb)
nu = dcos(arg1)
anpnu = dcos(nu)
arg2 = (anpnu*e0) / (1.000 + (e0*anpnu))
ee = dcos(arg2)
anpee = dsin(ee)

* Calculate new guess time of flight
arg3 = dsqrt(a**3.000/ma0nu)
ltotf = arg3 * (ee - e0 + anpee)

* Compare guess with desired time of flight
if (dabs(ltotf-totf) .gt. halfday) then
  e = e0 + deltae
  goto 10
endif

return
end

* Subroutine findcnds(new,cnew,eneew)
.....
implicit logical (l-1)
real*8 new,cnew,eneew,eqrts,eqrd
if (new .gt. 0.000) then
  eqrts = sqrt(new)
  cnew = (1.000-dcos(eqrts)) / new
  enew = (eqrts-dsin(eqrts)) / (eqrts**3)
else
  eqrd = new**2
  cnew = 9.540 - new/20.000 + eqrd/720.000 -
/
  (eqrd**2)/40320.000
  enew = 1.040/5.000 - new/120.000 + eqrd/3040.000 -
/
  (eqrd**2)/382800.000
endif
return
end

* Subroutine gauss1(r2,dt,time,v1,v2)
.....
* This routine solves the Gauss problem of orbit determination and
* returns the velocity vectors corresponding to the two input position
* vectors.
.....
implicit logical (a-i)
real*8 r1(1:3),r2(1:3),time,v1(1:3),v2(1:3),deta,y,upper,lower
real*8 code1,code2,f,q,qdot,ncld,ncldub,ncld,ncnew,cnew,eneew
real*8 t1,ncnew,small,t1upl,dt,ncag

```

5/24/79  
67:07:49

```

integer i,j
character dm

tloop = 2.0d0 + dacos(-1.0d0)
small = 0.00001d0
tlimnew = -10.0d0
do 10 i = 1,3
  v(1) = 0.0d0
  v(2) = 0.0d0
10 continue
codeltnew = (r(1)*r2(1)+r1(2)*r2(2)) / (r1(3)*r2(3))
if (dm .eq. 'l') then
  vare = -dqrt(r1(3)*r2(3)*(1.0d0+codeltnew))
else
  vare = dqrt(r1(3)*r2(3)*(1.0d0-codeltnew))
endif

* Make initial guess
solid = 0.0d0
cnew = 0.5d0
snew = 1.0d0/6.0d0

* Define boundaries for n-iteration
upper = tloop**2
lower = -2.0d0*tloop

* Ensure orbit is unstable
if (dabs(vare) .gt. small) then
  j = 0
  continue
  if (dabs(tlimnew-tlim) .gt. small) .and. (i .le. 30) then
    y = r1(3)*r2(3)-(vare*(1.0d0-solid*snew)/dqrt(cnew))
    if ((vare .gt. 0.0d0) .and. (y .lt. 0.0d0)) then
      j = j + 1
      continue
    else
      cnew = dqrt(cnew)
      y = r1(3)*r2(3) - (vare*(1.0d0-solid*snew)/dqrt(cnew))
      j = j + 1
      goto 30
    endif
  if (j .gt. 10) then
    write(*,*) 'Iteration failed for Yn in Gauss'
  endif
endif
solid = dqrt(y/cnew)
solidub = solid**3
tlimnew = solidub*snew + vare*dqrt(y)

* Adjust upper and lower bounds
if (tlimnew .lt. tlim) then
  lower = solid
  upper = solid
endif
if (tlimnew .gt. tlim) then
  upper = solid
endif

```

tmnropt.f

```

new = (upper+lower) / 2.0d0

* Ensure first guess isn't too close
if ((dabs(tlimnew-tlim) .lt. small) .and. (i .eq. 0)) then
  tlimnew = -10.0d0
endif

* Find c and a functions
call findcands(new,cnew,snew)
solid = snew
j = j + 1
goto 30
endif

if (i .gt. 30) then
  write(*,*) 'Gauss not converged in 30 iterations'
else
  find val vecs with f and g functions
  f = 3.0d0 - (y/r1(3))
  g = vare*dqrt(y)
  ddot = 1.0d0 - y/r2(3)
  do 40 i = 1,2
    v1(i) = f*r1(i) + g
    v2(i) = (gdot*r2(i) - r1(i)) / g
  40 continue
endif
v1(3) = mag(v1)
v2(3) = mag(v2)
dim
write(*,*) 'Gauss problem cannot be solved'
return
end

*****
subtract line elorbfr,v,p,acc,me,ame)
*****
* This routine finds the classical orbital elements given position and
* velocity vectors at a point in the orbit
*****
implicit logical (a-z)
real*8 r(1:3),v(1:3),p,a,acc,me,c1,rdotv,c3,small,ame
real*8 hbar,elorbfr(1:3),tloop,halfpl,p1,dot,meas
integer i
character*2 typeorbit

* Initialize variables
meas = 1.3271544d11
pl = dacos(-1.0d0)
tloop = 2.0d0 + pl
halfpl = pl / 2.0d0
small = 0.00001d0
infinite = 99999.9d0
underflim = 99999.1d0

* Find h, n, and a vectors
hbar = r(1)*v(2) - r(2)*v(1)
if (dabs(hbar) .gt. small) then
  c1 = v(3)**2 - meas/r(3)
  rdotv = r(1)*v(1) + r(2)*v(2)
  do 10 i = 1,2
    elorbfr(i) = (c1*r(i) - rdotv*v(i)) / meas
  10 continue
  elorbfr(3) = mag(hbar)

```

93/04/29  
07/07/05

51

tmropt.f

```

* Find a, b, and p
a = (r(3)+2/2.0d0) - (mean/r(3))
if (dabs(a) < .qt_small) then
  a = -mean / (2.0d0*me)
else
  a = infinite
endif
ecc = ebar(3)

p = (hbar**2) / meon

* Find true anomaly at epoch
if ((ebar(3)+r(3)) < .qt_small) .and. (ecc < .qt_small) then
  nu = dectoebar((r(1) + ebar(2)+r(2)) / (ebar(3)+r(3)))
  if (dabs(nu - 0.0d0) < .qt_small) then
    nu = twopi - nu
  endif
else
  nu = undefined
endif
else
  p = undefined
  a = undefined
  ecc = undefined
  nu = undefined
  me = undefined
endif
return
end
```

## **APPENDIX B**

This section contains the two output files generated by program MARSTRIP, contained in Appendix A. The scenario is based on an input exhaust velocity of 98.1 km/s. The output files represent the same outbound Martain trajectory and differ in the direction of their return trajectory. The data in these files was used to generate the graphs contained in Chapter IV of the thesis.

330423  
07:20:39

SHORT OPTION

source power: 100000000.0  
exhaust velocity: 90.100  
burn time fraction: 0.010

ref	test	total	thrust	alpha	delta1	delta2	delta3
210.0	70.0	10.0	130.0	0.8336	0.7	17.3	10.6
230.0	70.0	10.0	150.0	4.0706	0.7	17.3	9.0
250.0	70.0	10.0	170.0	7.4722	0.7	17.3	7.6
270.0	70.0	10.0	190.0	1.7494	0.7	17.3	12.1
290.0	70.0	10.0	210.0	5.2360	0.7	17.3	10.1
310.0	70.0	10.0	230.0	8.9043	0.7	17.3	8.4
330.0	70.0	10.0	250.0	2.6720	0.7	17.3	13.5
350.0	70.0	10.0	270.0	6.4167	0.7	17.3	11.1
370.0	70.0	10.0	290.0	3.5374	0.7	17.3	14.7
390.0	70.0	10.0	310.0	0.4555	0.7	17.3	11.9
410.0	70.0	10.0	330.0	4.5434	0.7	17.3	13.7
430.0	70.0	10.0	350.0	0.3192	0.7	17.3	10.7
450.0	70.0	10.0	370.0	1.7097	0.7	17.3	18.6
470.0	70.0	10.0	390.0	5.2030	0.7	17.3	16.2
490.0	70.0	10.0	410.0	1.0032	0.7	17.3	14.2
510.0	70.0	10.0	430.0	4.1404	0.7	17.3	12.0
530.0	70.0	10.0	450.0	8.7060	0.7	17.3	10.0
550.0	70.0	10.0	470.0	13.6110	0.7	17.3	8.3
570.0	70.0	10.0	490.0	19.2350	0.7	17.3	6.3
590.0	70.0	10.0	510.0	6.1017	0.7	17.3	4.0
610.0	70.0	10.0	530.0	4.6957	0.7	17.3	2.6
630.0	70.0	10.0	550.0	15.1217	0.7	17.3	1.6
650.0	70.0	10.0	570.0	0.9516	0.7	17.3	0.3
670.0	70.0	10.0	590.0	6.3296	0.7	17.3	2.2
690.0	70.0	10.0	610.0	5.2732	0.7	17.3	1.6
710.0	70.0	10.0	630.0	10.6592	0.7	17.3	1.4
730.0	70.0	10.0	650.0	16.5039	0.7	17.3	1.3
750.0	70.0	10.0	670.0	0.6096	0.7	17.3	0.9
770.0	70.0	10.0	690.0	2.5207	0.7	17.3	0.6
790.0	70.0	10.0	710.0	0.6105	0.7	17.3	0.4
810.0	70.0	10.0	730.0	11.7047	0.7	17.3	0.3
830.0	70.0	10.0	750.0	0.0354	0.7	17.3	0.2
850.0	70.0	10.0	770.0	1.9711	0.7	17.3	0.1
870.0	70.0	10.0	790.0	4.2070	0.7	17.3	0.1
890.0	70.0	10.0	810.0	0.9631	0.7	17.3	0.1
910.0	70.0	10.0	830.0	12.0450	0.7	17.3	0.1
930.0	70.0	10.0	850.0	1.4205	0.7	17.3	0.1
950.0	70.0	10.0	870.0	3.5622	0.7	17.3	0.1
970.0	70.0	10.0	890.0	6.0705	0.7	17.3	0.1
990.0	70.0	10.0	910.0	1.3995	0.7	17.3	0.1
1010.0	70.0	10.0	930.0	7.4727	0.7	17.3	0.1
1030.0	70.0	10.0	950.0	0.8711	0.7	17.3	0.1
1050.0	70.0	10.0	970.0	2.9274	0.7	17.3	0.1
1070.0	70.0	10.0	990.0	5.2001	0.7	17.3	0.1
1090.0	70.0	10.0	1010.0	8.0064	0.7	17.3	0.1
1110.0	70.0	10.0	1030.0	3.6770	0.7	17.3	0.1
1130.0	70.0	10.0	1050.0	9.3777	0.7	17.3	0.1
1150.0	70.0	10.0	1070.0	15.6974	0.7	17.3	0.1
1170.0	70.0	10.0	1090.0	27.6046	0.7	17.3	0.1
1190.0	70.0	10.0	1110.0	1.1191	0.7	17.3	0.1
1210.0	70.0	10.0	1130.0	3.1955	0.7	17.3	0.1
1230.0	70.0	10.0	1150.0	5.7025	0.7	17.3	0.1
1250.0	70.0	10.0	1170.0	8.7990	0.7	17.3	0.1
1270.0	70.0	10.0	1190.0	14.5788	0.7	17.3	0.1

attofi

290.0	110.0	30.0	150.0	24.0544	4.0	6.9	11.7	25.4
310.0	110.0	30.0	170.0	0.4911	4.0	6.9	41.7	55.4
330.0	110.0	30.0	190.0	2.4628	4.0	6.9	40.3	53.9
350.0	110.0	30.0	210.0	4.2517	4.0	6.9	38.5	52.1
370.0	110.0	30.0	230.0	3.8259	4.0	6.9	24.2	37.9
390.0	110.0	30.0	250.0	10.1359	4.0	6.9	19.3	33.0
410.0	110.0	30.0	270.0	17.5933	4.0	6.9	15.5	29.2
430.0	110.0	30.0	290.0	0.2536	4.0	6.9	42.7	56.3
450.0	110.0	30.0	310.0	2.1409	4.0	6.9	41.2	54.9
470.0	110.0	30.0	330.0	4.3156	4.0	6.9	39.5	52.2
490.0	110.0	30.0	350.0	6.8444	4.0	6.9	37.5	51.2
510.0	110.0	30.0	370.0	10.8946	4.0	6.9	26.7	40.0
530.0	110.0	30.0	390.0	18.7479	4.0	6.9	16.4	30.1
550.0	110.0	30.0	410.0	1.6066	4.0	6.9	47.3	55.9
570.0	110.0	30.0	430.0	3.6497	4.0	6.9	40.6	54.3
590.0	110.0	30.0	450.0	6.0960	4.0	6.9	38.7	52.4
610.0	110.0	30.0	470.0	8.5089	4.0	6.9	36.5	50.2
630.0	110.0	30.0	490.0	4.4191	4.0	6.9	28.2	41.9
650.0	110.0	30.0	510.0	11.7989	4.0	6.9	21.9	35.6
670.0	110.0	30.0	530.0	1.0737	4.0	6.9	43.4	57.1
690.0	110.0	30.0	550.0	3.0488	4.0	6.9	41.8	55.4
710.0	110.0	30.0	570.0	5.3555	4.0	6.9	39.9	53.5
730.0	110.0	30.0	590.0	8.0250	4.0	6.9	37.7	51.4
750.0	110.0	30.0	610.0	11.1395	4.0	6.9	35.4	49.0
770.0	110.0	30.0	630.0	4.8992	4.0	6.9	29.9	43.6
790.0	110.0	30.0	650.0	12.7385	4.0	6.9	22.9	36.6
810.0	110.0	30.0	670.0	2.3342	4.0	6.9	44.1	56.7
830.0	110.0	30.0	690.0	7.3538	4.0	6.9	41.1	54.8
850.0	110.0	30.0	710.0	4.5973	4.0	6.9	39.0	52.7
870.0	110.0	30.0	730.0	7.1586	4.0	6.9	36.7	50.3
890.0	110.0	30.0	750.0	10.1281	4.0	6.9	34.1	47.8
910.0	110.0	30.0	770.0	13.5892	4.0	6.9	31.6	45.0
930.0	110.0	30.0	790.0	0.2286	4.2	6.7	26.6	37.5
950.0	110.0	30.0	810.0	6.5543	4.2	6.7	21.3	32.2
970.0	110.0	30.0	830.0	13.6221	4.2	6.7	17.4	28.3
990.0	110.0	30.0	850.0	21.6017	4.2	6.7	14.2	25.1
1010.0	110.0	30.0	870.0	30.4110	4.2	6.7	11.6	22.5
1030.0	110.0	30.0	890.0	0.2395	4.2	6.7	43.0	53.9
1050.0	110.0	30.0	910.0	6.1015	4.2	6.7	40.4	51.3
1070.0	110.0	30.0	930.0	2.0708	4.2	6.7	38.6	49.5
1090.0	110.0	30.0	950.0	6.4433	4.2	6.7	36.6	47.7
1110.0	110.0	30.0	970.0	13.4942	4.2	6.7	34.7	45.7
1130.0	110.0	30.0	990.0	22.5140	4.2	6.7	32.2	43.2
1150.0	110.0	30.0	1010.0	1.5901	4.2	6.7	29.9	40.9
1170.0	110.0	30.0	1030.0	5.4158	4.2	6.7	27.7	38.6
1190.0	110.0	30.0	1050.0	8.9301	4.2	6.7	25.3	36.4
1210.0	110.0	30.0	1070.0	0.5783	4.2	6.7	23.0	34.2
1230.0	110.0	30.0	1090.0	14.2453	4.2	6.7	20.5	31.4
1250.0	110.0	30.0	1110.0	21.6112	4.2	6.7	18.3	29.2
1270.0	110.0	30.0	1130.0	1.0810	4.2	6.7	16.3	27.2
1290.0	110.0	30.0	1150.0	3.0378	4.2	6.7	14.7	25.4
1310.0	110.0	30.0	1170.0	5.2684	4.2	6.7	13.3	23.6
1330.0	110.0	30.0	1190.0	7.8569	4.2	6.7	12.1	21.7
1350.0	110.0	30.0	1210.0	10.8907	4.2	6.7	11.0	20.0
1370.0	110.0	30.0	1230.0	13.4774	4.2	6.7	9.9	18.5
1390.0	110.0	30.0	1250.0	16.6209	4.2	6.7	8.9	17.1
1410.0	110.0	30.0	1270.0	19.3657	4.2	6.7	8.0	15.8
1430.0	110.0	30.0	1290.0	21.7076	4.2	6.7	7.2	14.6
1450.0	110.0	30.0	1310.0	24.6485	4.2	6.7	6.5	13.5
1470.0	110.0	30.0	1330.0	27.1919	4.2	6.7	5.9	12.5
1490.0	110.0	30.0	1350.0	29.4375	4.2	6.7	5.4	11.6
1510.0	110.0	30.0	1370.0	31.3861	4.2	6.7	4.9	10.8
1530.0	110.0	30.0	1390.0	33.0397	4.2	6.7	4.5	10.0
1550.0	110.0	30.0	1410.0	34.3994	4.2	6.7	4.1	9.3
1570.0	110.0	30.0	1430.0	35.4653	4.2	6.7	3.7	8.7
1590.0	110.0	30.0	1450.0	36.2377	4.2	6.7	3.4	8.1
1610.0	110.0	30.0	1470.0	36.7167	4.2	6.7	3.1	7.6
1630.0	110.0	30.0	1490.0	36.9025	4.2	6.7	2.8	7.1
1650.0	110.0	30.0	1510.0	36.7960	4.2	6.7	2.6	6.7
1670.0	110.0	30.0	1530.0	36.3979	4.2	6.7	2.4	6.3
1690.0	110.0	30.0	1550.0	35.7018	4.2	6.7	2.2	5.9
1710.0	110.0	30.0	1570.0	34.7076	4.2	6.7	2.0	5.6
1730.0	110.0	30.0	1590.0	33.4194	4.2	6.7	1.8	5.2
1750.0	110.0	30.0	1610.0	31.8372	4.2	6.7	1.6	4.8
1770.0	110.0	30.0	1630.0	30.0	4.2	6.7	1.5	4.5

1

930429  
07:20:39

2

attofl

450.0	130.0	70.0	230.0	13.3064	4.2	6.7	35.6	46.5	450.0	150.0	90.0	210.0	12.4802	3.9	5.1	38.4	47.4
310.0	130.0	90.0	110.0	7.2323	4.2	6.7	29.6	40.5	470.0	150.0	90.0	230.0	16.2579	3.9	5.1	36.0	45.0
330.0	130.0	90.0	110.0	16.1719	4.2	6.7	22.0	33.7	490.0	150.0	90.0	250.0	20.7160	3.9	5.1	33.3	42.4
350.0	130.0	90.0	110.0	1.6617	4.2	6.7	42.9	55.0	490.0	150.0	110.0	70.0	70.7160	3.9	5.1	32.3	42.4
370.0	130.0	90.0	110.0	3.0189	4.2	6.7	42.9	55.0	350.0	150.0	110.0	90.0	10.2744	3.9	5.1	42.5	52.5
390.0	130.0	90.0	110.0	6.2727	4.2	6.7	41.3	52.2	370.0	150.0	110.0	110.0	0.1917	3.9	5.1	49.8	58.9
410.0	130.0	90.0	110.0	8.9700	4.2	6.7	36.9	47.8	390.0	150.0	110.0	130.0	2.7837	3.9	5.1	46.9	55.9
430.0	130.0	90.0	250.0	12.1890	4.2	6.7	36.9	47.8	410.0	150.0	110.0	150.0	5.3760	3.9	5.1	44.5	53.5
450.0	130.0	90.0	250.0	15.9502	4.2	6.7	34.4	45.3	430.0	150.0	110.0	170.0	8.1573	3.9	5.1	42.2	51.2
470.0	130.0	90.0	250.0	7.7904	4.2	6.7	31.0	41.9	450.0	150.0	110.0	190.0	11.2872	3.9	5.1	39.8	48.9
350.0	130.0	110.0	110.0	17.2464	4.2	6.7	23.6	34.5	470.0	150.0	110.0	210.0	14.9015	3.9	5.1	37.3	46.4
370.0	130.0	110.0	130.0	6.6960	4.2	6.7	46.9	57.0	490.0	150.0	110.0	230.0	19.1360	3.9	5.1	34.7	43.8
390.0	130.0	110.0	150.0	2.9390	4.2	6.7	42.7	55.6	510.0	150.0	110.0	250.0	24.1365	3.9	5.1	32.0	41.0
410.0	130.0	110.0	170.0	5.3335	4.2	6.7	42.7	53.6	250.0	170.0	10.0	70.0	2.1985	3.0	4.0	32.4	40.1
430.0	130.0	110.0	190.0	8.0102	4.2	6.7	40.5	51.4	270.0	170.0	10.0	90.0	10.3852	3.0	4.0	25.2	32.9
450.0	130.0	110.0	210.0	11.0853	4.2	6.7	30.7	46.1	290.0	170.0	10.0	110.0	19.6017	3.0	4.0	20.0	27.7
470.0	130.0	110.0	230.0	14.6705	4.2	6.7	30.7	46.6	310.0	170.0	10.0	130.0	30.9661	3.0	4.0	15.9	23.7
490.0	130.0	110.0	250.0	18.0613	4.2	6.7	33.1	44.0	330.0	170.0	10.0	150.0	0.8575	3.0	4.0	44.9	52.6
290.0	150.0	10.0	70.0	1.4222	3.9	5.1	29.6	38.6	350.0	170.0	10.0	170.0	2.7464	3.0	4.0	43.8	51.5
250.0	150.0	10.0	90.0	8.7335	3.9	5.1	23.3	32.3	370.0	170.0	10.0	190.0	4.6363	3.0	4.0	42.5	50.2
270.0	150.0	10.0	110.0	17.0742	3.9	5.1	18.7	27.7	390.0	170.0	10.0	210.0	7.2334	3.0	4.0	41.0	48.7
290.0	150.0	10.0	130.0	26.6621	3.9	5.1	15.1	24.1	410.0	170.0	10.0	230.0	10.0785	3.0	4.0	39.2	46.9
310.0	150.0	10.0	150.0	0.7312	3.9	5.1	43.9	52.9	430.0	170.0	10.0	250.0	13.3253	3.0	4.0	37.1	44.0
330.0	150.0	10.0	170.0	2.5784	3.9	5.1	42.0	51.0	450.0	170.0	10.0	270.0	1.6342	3.0	4.0	35.4	43.3
350.0	150.0	10.0	190.0	4.6807	3.9	5.1	41.4	50.5	470.0	170.0	10.0	290.0	10.3409	3.0	4.0	27.2	35.0
370.0	150.0	10.0	210.0	7.1206	3.9	5.1	39.0	48.9	490.0	170.0	10.0	310.0	20.4069	3.0	4.0	21.3	29.0
390.0	150.0	10.0	230.0	9.9643	3.9	5.1	37.9	47.0	510.0	170.0	10.0	330.0	32.1382	3.0	4.0	16.4	24.3
410.0	150.0	10.0	250.0	1.0042	3.9	5.1	33.0	42.0	350.0	170.0	30.0	90.0	2.0743	3.0	4.0	45.0	52.7
250.0	150.0	30.0	70.0	0.6460	3.9	5.1	25.6	34.6	370.0	170.0	30.0	170.0	4.1595	3.0	4.0	43.6	51.3
270.0	150.0	30.0	90.0	17.4811	3.9	5.1	20.2	29.2	390.0	170.0	30.0	190.0	6.4784	3.0	4.0	42.1	49.8
290.0	150.0	30.0	110.0	27.6534	3.9	5.1	16.1	25.1	410.0	170.0	30.0	210.0	9.1441	3.0	4.0	40.3	48.0
310.0	150.0	30.0	130.0	0.1954	3.9	5.1	44.9	54.0	430.0	170.0	30.0	230.0	12.2630	3.0	4.0	38.3	46.8
330.0	150.0	30.0	150.0	2.0376	3.9	5.1	43.0	52.0	450.0	170.0	30.0	250.0	15.9483	3.0	4.0	36.0	43.7
350.0	150.0	30.0	170.0	4.0749	3.9	5.1	42.4	51.5	470.0	170.0	30.0	270.0	1.6532	3.0	4.0	34.0	42.6
370.0	150.0	30.0	190.0	6.4036	3.9	5.1	40.9	49.9	490.0	170.0	30.0	290.0	10.4192	3.0	4.0	29.4	36.8
390.0	150.0	30.0	210.0	9.1149	3.9	5.1	36.9	46.1	510.0	170.0	30.0	310.0	21.1664	3.0	4.0	22.4	30.2
410.0	150.0	30.0	230.0	12.3040	3.9	5.1	34.9	44.0	350.0	170.0	50.0	110.0	1.1744	3.0	4.0	46.7	54.4
430.0	150.0	50.0	250.0	0.7544	3.9	5.1	36.1	45.1	370.0	170.0	50.0	130.0	3.3513	3.0	4.0	45.0	52.7
450.0	150.0	50.0	270.0	2.0376	3.9	5.1	34.9	43.9	390.0	170.0	50.0	150.0	5.6610	3.0	4.0	43.3	51.0
470.0	150.0	50.0	290.0	4.0749	3.9	5.1	31.5	39.5	410.0	170.0	50.0	170.0	8.2432	3.0	4.0	41.5	49.2
490.0	150.0	50.0	310.0	6.0805	3.9	5.1	28.0	36.6	430.0	170.0	50.0	190.0	11.2194	3.0	4.0	39.5	47.2
310.0	150.0	50.0	110.0	1.1030	3.9	5.1	45.0	54.0	450.0	170.0	50.0	210.0	14.7082	3.0	4.0	37.2	45.0
330.0	150.0	50.0	130.0	3.4145	3.9	5.1	43.4	52.6	470.0	170.0	50.0	230.0	18.0381	3.0	4.0	34.0	42.6
350.0	150.0	50.0	150.0	5.6721	3.9	5.1	40.7	49.2	490.0	170.0	50.0	250.0	11.6432	3.0	4.0	31.0	40.7
370.0	150.0	50.0	170.0	8.2610	3.9	5.1	38.1	47.1	510.0	170.0	50.0	270.0	13.0482	3.0	4.0	30.5	38.7
390.0	150.0	50.0	190.0	11.7825	3.9	5.1	35.6	44.9	350.0	170.0	70.0	130.0	22.1587	3.0	4.0	25.3	31.1
410.0	150.0	50.0	210.0	14.6621	3.9	5.1	33.9	42.9	370.0	170.0	70.0	150.0	4.3015	3.0	4.0	46.9	54.6
430.0	150.0	70.0	230.0	0.6822	3.9	5.1	28.3	36.3	390.0	170.0	70.0	170.0	7.2942	3.0	4.0	44.8	52.8
450.0	150.0	70.0	250.0	10.9415	3.9	5.1	22.6	31.6	410.0	170.0	70.0	190.0	16.1574	3.0	4.0	42.5	50.6
470.0	150.0	70.0	270.0	0.5127	3.9	5.1	48.0	51.0	430.0	170.0	70.0	210.0	13.4884	3.0	4.0	38.4	46.3
490.0	150.0	70.0	290.0	2.6317	3.9	5.1	45.0	54.0	450.0	170.0	70.0	230.0	17.3993	3.0	4.0	36.1	43.9
310.0	150.0	70.0	110.0	4.0800	3.9	5.1	43.2	52.3	470.0	170.0	70.0	250.0	22.0307	3.0	4.0	33.4	41.3
330.0	150.0	70.0	130.0	7.3906	3.9	5.1	41.4	50.6	490.0	170.0	70.0	270.0	1.7937	3.0	4.0	43.1	50.9
350.0	150.0	70.0	150.0	10.2713	3.9	5.1	39.3	48.6	510.0	170.0	70.0	290.0	11.6704	3.0	4.0	31.8	39.3
370.0	150.0	70.0	170.0	13.4525	3.9	5.1	37.1	46.1	350.0	170.0	90.0	90.0	0.8237	3.0	4.0	49.8	57.5
390.0	150.0	70.0	190.0	17.4330	3.9	5.1	34.6	43.7	370.0	170.0	90.0	110.0	3.4927	3.0	4.0	46.9	54.6
410.0	150.0	90.0	210.0	0.1718	3.9	5.1	41.4	50.6	390.0	170.0	90.0	130.0	6.1571	3.0	4.0	44.5	52.3
430.0	150.0	90.0	230.0	9.4057	3.9	5.1	30.8	39.0	410.0	170.0	90.0	150.0	9.0217	3.0	4.0	42.3	50.0
450.0	150.0	90.0	250.0	15.9616	3.9	5.1	23.5	32.5	430.0	170.0	90.0	170.0	12.7480	3.0	4.0	40.0	47.7
470.0	150.0	90.0	270.0	1.4165	3.9	5.1	46.9	55.9	450.0	170.0	90.0	190.0	15.7480	3.0	4.0	37.5	45.3
490.0	150.0	90.0	290.0	3.9555	3.9	5.1	44.8	53.8	470.0	170.0	90.0	210.0	20.3767	3.0	4.0	34.9	42.7
310.0	150.0	90.0	110.0	6.4535	3.9	5.1	42.0	51.0	490.0	170.0	90.0	230.0	25.5811	3.0	4.0	32.0	40.0
330.0	150.0	90.0	130.0	9.2532	3.9	5.1	40.7	49.7	510.0	170.0	110.0	250.0	2.0968	3.0	4.0	45.0	52.7

9300429  
07:20:30

3

atofl

170.0	170.0	110.0	90.0	12.4771	3.0	4.0	32.0	40.5	490.0	190.0	110.0	190.0	11.0920	3.7	3.7	38.1	44.9
180.0	170.0	110.0	110.0	1.8323	3.0	4.0	50.0	57.0	510.0	190.0	110.0	210.0	22.7353	3.7	3.7	35.3	42.1
190.0	170.0	110.0	130.0	4.7666	3.0	4.0	40.0	54.5	530.0	190.0	110.0	230.0	28.4632	3.7	3.7	32.4	39.2
200.0	170.0	110.0	150.0	7.7276	3.0	4.0	48.1	51.0	550.0	190.0	110.0	250.0	35.2719	3.7	3.7	29.4	36.2
210.0	170.0	110.0	170.0	10.9300	3.0	4.0	41.6	49.3	290.0	210.0	10.0	70.0	2.0003	3.6	2.6	38.0	44.2
220.0	170.0	110.0	190.0	14.5494	3.0	4.0	39.0	46.0	310.0	210.0	10.0	90.0	12.5708	3.6	2.6	35.0	41.2
230.0	170.0	110.0	210.0	18.7074	3.0	4.0	36.4	44.1	330.0	210.0	10.0	110.0	24.0203	3.6	2.6	32.0	38.2
240.0	170.0	110.0	230.0	23.6074	3.0	4.0	33.6	41.3	350.0	210.0	10.0	130.0	1.9661	3.6	2.6	29.2	35.5
250.0	170.0	110.0	250.0	29.5435	3.0	4.0	30.7	38.5	370.0	210.0	10.0	150.0	6.2372	3.6	2.6	26.2	32.5
260.0	170.0	110.0	270.0	2.6562	3.7	3.2	35.2	42.0	390.0	210.0	10.0	170.0	6.6258	3.6	2.6	23.2	29.5
270.0	170.0	110.0	290.0	11.6146	3.7	3.2	27.0	33.0	410.0	210.0	10.0	190.0	9.3009	3.6	2.6	20.2	26.5
280.0	170.0	110.0	310.0	22.1746	3.7	3.2	21.1	26.0	430.0	210.0	10.0	210.0	12.3921	3.6	2.6	17.2	23.5
290.0	170.0	110.0	330.0	34.6549	3.7	3.2	16.7	23.5	450.0	210.0	10.0	230.0	16.0270	3.6	2.6	14.2	20.5
300.0	170.0	110.0	350.0	2.5777	3.7	3.2	45.0	51.0	470.0	210.0	10.0	250.0	20.3460	3.6	2.6	11.2	17.5
310.0	170.0	110.0	370.0	4.7001	3.7	3.2	43.6	50.5	490.0	210.0	10.0	270.0	2.7791	3.6	2.6	8.2	14.5
320.0	170.0	110.0	390.0	7.0643	3.7	3.2	42.1	48.9	510.0	210.0	10.0	290.0	12.0592	3.6	2.6	5.2	11.5
330.0	170.0	110.0	410.0	9.7050	3.7	3.2	40.4	47.2	330.0	210.0	30.0	90.0	76.9010	3.6	2.6	2.2	8.5
340.0	170.0	110.0	430.0	12.9738	3.7	3.2	38.1	45.2	350.0	210.0	30.0	110.0	3.1423	3.6	2.6	30.3	36.5
350.0	170.0	110.0	450.0	16.7490	3.7	3.2	36.1	43.0	370.0	210.0	30.0	130.0	24.9010	3.6	2.6	27.2	33.4
360.0	170.0	110.0	470.0	2.4020	3.7	3.2	28.0	35.9	390.0	210.0	30.0	150.0	5.6306	3.6	2.6	24.2	30.4
370.0	170.0	110.0	490.0	11.7637	3.7	3.2	22.3	29.1	410.0	210.0	30.0	170.0	8.2099	3.6	2.6	21.2	27.4
380.0	170.0	110.0	510.0	22.0651	3.7	3.2	22.3	29.1	430.0	210.0	30.0	190.0	11.2000	3.6	2.6	18.2	24.4
390.0	170.0	110.0	530.0	1.6573	3.7	3.2	45.0	51.0	450.0	210.0	30.0	210.0	14.7401	3.6	2.6	15.2	21.4
400.0	170.0	110.0	550.0	3.0755	3.7	3.2	45.0	51.0	470.0	210.0	30.0	230.0	19.0292	3.6	2.6	12.2	18.4
410.0	170.0	110.0	570.0	6.2289	3.7	3.2	41.6	48.9	490.0	210.0	30.0	250.0	23.0644	3.6	2.6	9.2	15.4
420.0	170.0	110.0	590.0	8.0625	3.7	3.2	38.7	45.5	510.0	210.0	30.0	270.0	13.0190	3.6	2.6	6.2	12.4
430.0	170.0	110.0	610.0	11.4132	3.7	3.2	35.4	42.5	330.0	210.0	50.0	110.0	4.3662	3.6	2.6	3.2	9.4
440.0	170.0	110.0	630.0	15.0076	3.7	3.2	35.4	42.5	350.0	210.0	50.0	130.0	7.1230	3.6	2.6	4.2	10.4
450.0	170.0	110.0	650.0	19.7076	3.7	3.2	32.0	39.1	370.0	210.0	50.0	150.0	10.0932	3.6	2.6	5.2	11.4
460.0	170.0	110.0	670.0	22.1356	3.7	3.2	30.7	37.2	390.0	210.0	50.0	170.0	13.4457	3.6	2.6	6.2	12.4
470.0	170.0	110.0	690.0	24.8122	3.7	3.2	28.2	34.7	410.0	210.0	50.0	190.0	16.0932	3.6	2.6	7.2	13.4
480.0	170.0	110.0	710.0	2.0000	3.7	3.2	46.5	53.1	430.0	210.0	50.0	210.0	19.3391	3.6	2.6	8.2	14.4
490.0	170.0	110.0	730.0	5.2510	3.7	3.2	44.8	51.7	450.0	210.0	50.0	230.0	21.9337	3.6	2.6	9.2	15.4
500.0	170.0	110.0	750.0	7.0705	3.7	3.2	42.9	49.7	470.0	210.0	50.0	250.0	24.0033	3.6	2.6	10.2	16.4
510.0	170.0	110.0	770.0	10.0134	3.7	3.2	40.9	47.7	490.0	210.0	50.0	270.0	3.1131	3.6	2.6	11.2	17.4
520.0	170.0	110.0	790.0	14.2190	3.7	3.2	38.7	45.5	510.0	210.0	50.0	290.0	14.1059	3.6	2.6	12.2	18.4
530.0	170.0	110.0	810.0	18.2740	3.7	3.2	36.3	43.1	330.0	210.0	70.0	110.0	2.0273	3.6	2.6	9.2	15.4
540.0	170.0	110.0	830.0	2.4416	3.7	3.2	42.9	49.7	350.0	210.0	70.0	130.0	5.0704	3.6	2.6	6.2	12.4
550.0	170.0	110.0	850.0	12.7102	3.7	3.2	42.9	49.7	370.0	210.0	70.0	150.0	8.7401	3.6	2.6	7.2	13.4
560.0	170.0	110.0	870.0	1.2945	3.7	3.2	31.6	38.5	390.0	210.0	70.0	170.0	12.0639	3.6	2.6	8.2	14.4
570.0	170.0	110.0	890.0	1.2945	3.7	3.2	31.6	38.5	410.0	210.0	70.0	190.0	15.0290	3.6	2.6	9.2	15.4
580.0	170.0	110.0	910.0	4.0090	3.7	3.2	46.9	53.7	430.0	210.0	70.0	210.0	18.0290	3.6	2.6	10.2	16.4
590.0	170.0	110.0	930.0	6.7264	3.7	3.2	46.9	53.7	450.0	210.0	70.0	230.0	21.0290	3.6	2.6	11.2	17.4
600.0	170.0	110.0	950.0	9.6491	3.7	3.2	44.6	51.4	470.0	210.0	70.0	250.0	24.0290	3.6	2.6	12.2	18.4
610.0	170.0	110.0	970.0	12.9457	3.7	3.2	42.4	49.2	490.0	210.0	70.0	270.0	3.3230	3.6	2.6	13.2	19.4
620.0	170.0	110.0	990.0	16.7693	3.7	3.2	40.1	46.9	510.0	210.0	70.0	290.0	6.1223	3.6	2.6	14.2	20.4
630.0	170.0	110.0	1010.0	21.2744	3.7	3.2	37.7	44.5	330.0	210.0	90.0	70.0	10.3230	3.6	2.6	15.2	21.4
640.0	170.0	110.0	1030.0	26.6275	3.7	3.2	35.1	41.9	350.0	210.0	90.0	90.0	13.7264	3.6	2.6	16.2	22.4
650.0	170.0	110.0	1050.0	3.2111	3.7	3.2	44.0	51.6	370.0	210.0	90.0	110.0	17.0036	3.6	2.6	17.2	23.4
660.0	170.0	110.0	1070.0	13.4900	3.7	3.2	44.0	51.6	390.0	210.0	90.0	130.0	20.3060	3.6	2.6	18.2	24.4
670.0	170.0	110.0	1090.0	19.5919	3.7	3.2	40.0	48.5	410.0	210.0	90.0	150.0	23.4727	3.6	2.6	19.2	25.4
680.0	170.0	110.0	1110.0	26.6275	3.7	3.2	37.7	44.5	430.0	210.0	90.0	170.0	26.4727	3.6	2.6	20.2	26.4
690.0	170.0	110.0	1130.0	3.2051	3.7	3.2	50.0	56.0	450.0	210.0	90.0	190.0	29.2666	3.6	2.6	21.2	27.4
700.0	170.0	110.0	1150.0	5.3009	3.7	3.2	44.2	51.0	470.0	210.0	90.0	210.0	32.2700	3.6	2.6	22.2	28.4
710.0	170.0	110.0	1170.0	8.0221	3.7	3.2	41.7	48.5	490.0	210.0	90.0	230.0	35.2700	3.6	2.6	23.2	29.4
720.0	170.0	110.0	1190.0	11.5919	3.7	3.2	39.1	46.0	510.0	210.0	90.0	250.0	38.2700	3.6	2.6	24.2	30.4
730.0	170.0	110.0	1210.0	15.2927	3.7	3.2	36.5	43.3	330.0	210.0	110.0	70.0	4.0056	3.6	2.6	25.2	31.4
740.0	170.0	110.0	1230.0	19.5937	3.7	3.2	36.5	43.3	350.0	210.0	110.0	90.0	8.0000	3.6	2.6	26.2	32.4
750.0	170.0	110.0	1250.0	24.6477	3.7	3.2	33.9	40.6	370.0	210.0	110.0	110.0	11.0000	3.6	2.6	27.2	33.4
760.0	170.0	110.0	1270.0	30.1005	3.7	3.2	30.9	37.9	390.0	210.0	110.0	130.0	14.0000	3.6	2.6	28.2	34.4
770.0	170.0	110.0	1290.0	3.1352	3.7	3.2	46.3	53.1	410.0	210.0	110.0	150.0	17.0000	3.6	2.6	29.2	35.4
780.0	170.0	110.0	1310.0	8.3937	3.7	3.2	50.1	56.9	430.0	210.0	110.0	170.0	20.0000	3.6	2.6	30.2	36.4
790.0	170.0	110.0	1330.0	13.8716	3.7	3.2	46.5	53.4	450.0	210.0	110.0	190.0	23.0000	3.6	2.6	31.2	37.4
800.0	170.0	110.0	1350.0	19.0651	3.7	3.2	43.5	50.4	470.0	210.0	110.0	210.0	26.0000	3.6	2.6	32.2	38.4
810.0	170.0	110.0	1370.0	24.0651	3.7	3.2	40.8	47.7	490.0	210.0	110.0	230.0	29.0000	3.6	2.6	33.2	39.4
820.0	170.0	110.0	1390.0	29.0651	3.7	3.2	40.8	47.7	510.0	210.0	110.0	250.0	32.0000	3.6	2.6	34.2	40.4
830.0	170.0	110.0	1410.0	34.0651	3.7	3.2	40.8	47.7	330.0	210.0	130.0	70.0	35.0000	3.6	2.6	35.2	41.4
840.0	170.0	110.0	1430.0	39.0651	3.7	3.2	40.8	47.7	350.0	210.0	130.0	90.0	38.0000	3.6	2.6	36.2	42.4
850.0	170.0	110.0	1450.0	44.0651	3.7	3.2	40.8	47.7	370.0	210.0	130.0	110.0	41.0000	3.6	2.6	37.2	43.4
860.0	170.0	110.0	1470.0	49.0651	3.7	3.2	40.8	47.7	390.0	210.0	130.0	130.0	44.0000	3.6	2.6	38.2	44.4
870.0	170.0</																



5/10/75  
9/20/75

110.0	230.0	10.0	70.0	2.9463	3.6	2.3	40.5	46.5	430.0	230.0	10.0	170.0	10.6715	3.6	2.1	42.2	47.9
110.0	230.0	10.0	90.0	13.1948	3.6	2.3	30.3	36.2	430.0	230.0	10.0	190.0	14.1885	3.6	2.1	39.8	45.5
110.0	230.0	10.0	110.0	25.5317	3.6	2.3	21.2	27.1	430.0	230.0	10.0	210.0	18.7804	3.6	2.1	37.4	43.1
110.0	230.0	10.0	130.0	3.1461	3.6	2.3	44.8	52.7	430.0	230.0	10.0	230.0	23.1183	3.6	2.1	34.7	40.4
110.0	230.0	10.0	150.0	8.5785	3.6	2.3	44.8	50.7	430.0	230.0	10.0	250.0	28.8887	3.6	2.1	32.0	37.7
110.0	230.0	10.0	170.0	11.6097	3.6	2.3	42.9	48.8	430.0	230.0	10.0	270.0	3.1040	3.6	2.1	45.2	50.9
110.0	230.0	10.0	190.0	15.1339	3.6	2.3	38.7	44.6	430.0	230.0	10.0	290.0	14.4349	3.6	2.1	33.9	38.6
110.0	230.0	10.0	210.0	18.7903	3.6	2.3	36.3	42.7	430.0	230.0	10.0	310.0	2.8758	3.6	2.1	50.1	55.8
110.0	230.0	10.0	230.0	24.2387	3.6	2.3	31.7	39.6	430.0	230.0	10.0	330.0	6.0385	3.6	2.1	48.7	52.4
110.0	230.0	10.0	250.0	3.0303	3.6	2.3	47.9	48.7	430.0	230.0	10.0	350.0	9.2445	3.6	2.1	44.0	49.7
110.0	230.0	10.0	270.0	13.7607	3.6	2.3	31.6	37.5	430.0	230.0	10.0	370.0	12.7774	3.6	2.1	41.5	47.2
110.0	230.0	10.0	290.0	1.7753	3.6	2.3	49.0	55.6	430.0	230.0	10.0	390.0	16.6826	3.6	2.1	38.9	44.6
110.0	230.0	10.0	310.0	4.5815	3.6	2.3	46.9	52.8	430.0	230.0	10.0	410.0	21.2950	3.6	2.1	36.2	41.9
110.0	230.0	10.0	330.0	7.3824	3.6	2.3	44.6	50.4	430.0	230.0	10.0	430.0	26.7567	3.6	2.1	33.4	39.1
110.0	230.0	10.0	350.0	10.3968	3.6	2.3	42.4	48.2	430.0	230.0	10.0	450.0	33.2777	3.6	2.1	30.5	36.2
110.0	230.0	10.0	370.0	13.8068	3.6	2.3	40.1	46.0	430.0	230.0	10.0	470.0	3.5807	3.6	2.1	46.6	52.3
110.0	230.0	10.0	390.0	17.7485	3.6	2.3	37.7	43.5	430.0	230.0	10.0	490.0	0.2797	3.6	2.1	55.3	61.0
110.0	230.0	10.0	410.0	22.4885	3.6	2.3	35.1	41.0	430.0	230.0	10.0	510.0	4.0136	3.6	2.1	44.5	50.2
110.0	230.0	10.0	430.0	28.0265	3.6	2.3	32.4	38.7	430.0	230.0	10.0	530.0	7.5084	3.6	2.1	40.5	46.3
110.0	230.0	10.0	450.0	3.2864	3.6	2.3	44.7	50.6	430.0	230.0	10.0	550.0	11.0847	3.6	2.1	43.4	49.1
110.0	230.0	10.0	470.0	14.5379	3.6	2.3	32.7	38.5	430.0	230.0	10.0	570.0	14.9973	3.6	2.1	40.6	46.3
110.0	230.0	10.0	490.0	2.8163	3.6	2.3	58.0	55.9	430.0	230.0	10.0	590.0	19.4541	3.6	2.1	37.8	43.4
110.0	230.0	10.0	510.0	5.9034	3.6	2.3	44.2	50.0	430.0	230.0	10.0	610.0	24.6631	3.6	2.1	34.9	40.6
110.0	230.0	10.0	530.0	9.0199	3.6	2.3	44.2	50.0	430.0	230.0	10.0	630.0	30.8404	3.6	2.1	32.0	37.7
110.0	230.0	10.0	550.0	12.3976	3.6	2.3	41.7	47.5	430.0	230.0	10.0	650.0	38.2221	3.6	2.1	29.8	36.7
110.0	230.0	10.0	570.0	16.2260	3.6	2.3	39.2	45.0	430.0	230.0	10.0	670.0	4.2030	3.6	2.1	47.3	53.4
110.0	230.0	10.0	590.0	20.6904	3.6	2.3	36.5	42.4	430.0	230.0	10.0	690.0	1.1982	3.6	2.1	55.4	61.2
110.0	230.0	10.0	610.0	25.9680	3.6	2.3	33.0	39.6	430.0	230.0	10.0	710.0	5.2524	3.6	2.1	46.0	51.7
110.0	230.0	10.0	630.0	32.7481	3.6	2.3	30.9	36.8	430.0	230.0	10.0	730.0	9.1202	3.6	2.1	40.5	46.3
110.0	230.0	10.0	650.0	3.7654	3.6	2.3	46.2	52.1	430.0	230.0	10.0	750.0	13.1233	3.6	2.1	38.5	44.3
110.0	230.0	10.0	670.0	10.2760	3.6	2.3	35.2	41.1	430.0	230.0	10.0	770.0	17.5210	3.6	2.1	32.5	38.2
110.0	230.0	10.0	690.0	15.0131	3.6	2.3	33.1	39.0	430.0	230.0	10.0	790.0	22.5531	3.6	2.1	30.3	36.2
110.0	230.0	10.0	710.0	2.1341	3.6	2.3	46.6	52.4	430.0	230.0	10.0	810.0	28.4420	3.6	2.1	28.4	34.1
110.0	230.0	10.0	730.0	7.6095	3.6	2.3	43.5	49.5	430.0	230.0	10.0	830.0	35.4465	3.6	2.1	26.4	32.1
110.0	230.0	10.0	750.0	12.6095	3.6	2.3	40.8	46.7	430.0	230.0	10.0	850.0	42.8187	3.6	2.1	23.7	29.1
110.0	230.0	10.0	770.0	18.9138	3.6	2.3	38.1	44.0	430.0	230.0	10.0	870.0	2.7787	3.6	2.1	49.7	55.4
110.0	230.0	10.0	790.0	25.9159	3.6	2.3	35.1	41.1	430.0	230.0	10.0	890.0	8.4113	3.6	2.1	43.4	49.1
110.0	230.0	10.0	810.0	3.2719	3.6	2.3	50.1	56.0	430.0	230.0	10.0	910.0	10.9047	3.6	2.1	41.7	47.4
110.0	230.0	10.0	830.0	7.1341	3.6	2.3	46.6	52.4	430.0	230.0	10.0	930.0	13.3846	3.6	2.1	38.4	44.1
110.0	230.0	10.0	850.0	12.6095	3.6	2.3	43.5	49.5	430.0	230.0	10.0	950.0	16.0390	3.6	2.1	35.2	40.9
110.0	230.0	10.0	870.0	18.9138	3.6	2.3	40.8	46.7	430.0	230.0	10.0	970.0	22.7706	3.6	2.1	32.8	37.7
110.0	230.0	10.0	890.0	25.9159	3.6	2.3	38.1	44.0	430.0	230.0	10.0	990.0	26.0390	3.6	2.1	30.4	36.3
110.0	230.0	10.0	910.0	3.2719	3.6	2.3	50.1	56.0	430.0	230.0	10.0	1010.0	32.7706	3.6	2.1	28.0	34.5
110.0	230.0	10.0	930.0	7.1341	3.6	2.3	46.6	52.4	430.0	230.0	10.0	1030.0	40.6669	3.6	2.1	25.7	31.4
110.0	230.0	10.0	950.0	12.6095	3.6	2.3	43.5	49.5	430.0	230.0	10.0	1050.0	50.1741	3.6	2.1	23.1	28.8
110.0	230.0	10.0	970.0	18.9138	3.6	2.3	40.8	46.7	430.0	230.0	10.0	1070.0	8.1210	3.6	2.1	49.2	54.9
110.0	230.0	10.0	990.0	25.9159	3.6	2.3	38.1	44.0	430.0	230.0	10.0	1090.0	12.8976	3.6	2.1	44.5	50.2
110.0	230.0	10.0	1010.0	3.2719	3.6	2.3	50.1	56.0	430.0	230.0	10.0	1110.0	17.9333	3.6	2.1	40.6	46.3
110.0	230.0	10.0	1030.0	7.1341	3.6	2.3	46.6	52.4	430.0	230.0	10.0	1130.0	23.5326	3.6	2.1	37.1	42.8
110.0	230.0	10.0	1050.0	12.6095	3.6	2.3	43.5	49.5	430.0	230.0	10.0	1150.0	29.9824	3.6	2.1	33.7	39.4
110.0	230.0	10.0	1070.0	18.9138	3.6	2.3	40.8	46.7	430.0	230.0	10.0	1170.0	37.5720	3.6	2.1	30.4	36.1
110.0	230.0	10.0	1090.0	25.9159	3.6	2.3	38.1	44.0	430.0	230.0	10.0	1190.0	46.6119	3.6	2.1	27.1	32.8
110.0	230.0	10.0	1110.0	3.2719	3.6	2.3	50.1	56.0	430.0	230.0	10.0	1210.0	57.4284	3.6	2.1	24.0	29.7
110.0	230.0	10.0	1130.0	7.1341	3.6	2.3	46.6	52.4	430.0	230.0	10.0	1230.0					
110.0	230.0	10.0	1150.0	12.6095	3.6	2.3	43.5	49.5	430.0	230.0	10.0	1250.0					
110.0	230.0	10.0	1170.0	18.9138	3.6	2.3	40.8	46.7	430.0	230.0	10.0	1270.0					
110.0	230.0	10.0	1190.0	25.9159	3.6	2.3	38.1	44.0	430.0	230.0	10.0	1290.0					
110.0	230.0	10.0	1210.0	3.2719	3.6	2.3	50.1	56.0	430.0	230.0	10.0	1310.0					
110.0	230.0	10.0	1230.0	7.1341	3.6	2.3	46.6	52.4	430.0	230.0	10.0	1330.0					
110.0	230.0	10.0	1250.0	12.6095	3.6	2.3	43.5	49.5	430.0	230.0	10.0	1350.0					
110.0	230.0	10.0	1270.0	18.9138	3.6	2.3	40.8	46.7	430.0	230.0	10.0	1370.0					
110.0	230.0	10.0	1290.0	25.9159	3.6	2.3	38.1	44.0	430.0	230.0	10.0	1390.0					
110.0	230.0	10.0	1310.0	3.2719	3.6	2.3	50.1	56.0	430.0	230.0	10.0	1410.0					
110.0	230.0	10.0	1330.0	7.1341	3.6	2.3	46.6	52.4	430.0	230.0	10.0	1430.0					
110.0	230.0	10.0	1350.0	12.6095	3.6	2.3	43.5	49.5	430.0	230.0	10.0	1450.0					
110.0	230.0	10.0	1370.0	18.9138	3.6	2.3	40.8	46.7	430.0	230.0	10.0	1470.0					
110.0	230.0	10.0	1390.0	25.9159	3.6	2.3	38.1	44.0	430.0	230.0	10.0	1490.0					
110.0	230.0	10.0	1410.0	3.2719	3.6	2.3	50.1	56.0	430.0	230.0	10.0	1510.0					
110.0	230.0	10.0	1430.0	7.1341	3.6	2.3	46.6	52.4	430.0	230.0	10.0	1530.0					
110.0	230.0	10.0	1450.0	12.6095	3.6	2.3	43.5	49.5	430.0	230.0	10.0	1550.0					
110.0	230.0	10.0	1470.0	18.9138	3.6	2.3	40.8	46.7	430.0	230.0	10.0	1570.0					
110.0	230.0	10.0	1490.0	25.9159	3.6	2.3	38.1	44.0	430.0	230.0	10.0	1590.0					
110.0	230.0	10.0	1510.0	3.2719	3.6	2.3	50.1	56.0	430.0	230.0	10.0	1610.0					
110.0	230.0	10.0	1530.0	7.1341	3.6	2.3	46.6	52.4	430.0	230.0	10.0</						



L/MC OPTION

source power: 100000000.0  
exhaust velocity: 90.100  
burn time fraction: 0.010

tol	test	test	test	alpha	beta	gamma	delta	epsilon
270.0	70.0	10.0	190.0	31.0470	0.7	17.3	6.4	32.3
290.0	70.0	10.0	210.0	14.7405	0.7	17.3	5.2	31.2
310.0	70.0	10.0	230.0	10.4791	0.7	17.3	4.3	30.3
330.0	70.0	10.0	250.0	22.0312	0.7	17.3	3.5	29.6
350.0	70.0	30.0	190.0	12.7446	0.7	17.3	5.9	32.0
310.0	70.0	30.0	210.0	16.6990	0.7	17.3	5.6	31.5
190.0	70.0	30.0	230.0	20.6410	0.7	17.3	4.5	30.3
350.0	70.0	30.0	250.0	24.2042	0.7	17.3	3.8	29.8
310.0	70.0	50.0	190.0	10.3536	0.7	17.3	9.0	35.0
190.0	70.0	50.0	210.0	14.4099	0.7	17.3	7.2	33.3
350.0	70.0	50.0	230.0	22.8953	0.7	17.3	5.8	31.0
310.0	70.0	50.0	250.0	27.8345	0.7	17.3	4.7	30.7
190.0	70.0	70.0	190.0	11.0647	0.7	17.3	4.0	30.0
190.0	70.0	70.0	210.0	16.7112	0.7	17.3	3.6	33.6
350.0	70.0	70.0	230.0	20.7449	0.7	17.3	6.0	32.0
310.0	70.0	70.0	250.0	25.0509	0.7	17.3	4.8	30.8
190.0	70.0	90.0	190.0	8.0962	0.7	17.3	12.6	30.6
350.0	70.0	90.0	210.0	13.4329	0.7	17.3	10.0	30.0
310.0	70.0	90.0	230.0	18.1271	0.7	17.3	7.9	33.9
190.0	70.0	90.0	250.0	22.8526	0.7	17.3	6.2	32.1
350.0	70.0	90.0	270.0	27.2717	0.7	17.3	4.9	30.9
310.0	70.0	90.0	290.0	30.5731	0.7	17.3	4.5	30.4
190.0	70.0	110.0	190.0	16.2232	0.7	17.3	13.2	39.1
350.0	70.0	110.0	210.0	15.0674	0.7	17.3	10.3	36.3
310.0	70.0	110.0	230.0	20.0567	0.7	17.3	8.1	34.0
190.0	70.0	110.0	250.0	25.0163	0.7	17.3	6.3	32.2
350.0	70.0	110.0	270.0	29.4540	0.7	17.3	5.1	31.0
310.0	70.0	110.0	290.0	32.2270	0.7	17.3	4.9	30.9
190.0	70.0	130.0	190.0	25.0753	0.0	12.1	6.8	24.9
350.0	70.0	130.0	210.0	31.0914	0.0	12.1	5.3	23.6
310.0	70.0	130.0	230.0	37.2072	0.0	12.1	4.5	22.6
190.0	70.0	130.0	250.0	42.0430	0.0	12.1	3.8	21.9
350.0	70.0	130.0	270.0	46.9733	0.0	12.1	3.0	21.1
310.0	70.0	130.0	290.0	50.9733	0.0	12.1	2.1	20.1
190.0	70.0	150.0	190.0	40.1710	0.0	12.1	4.7	22.0
350.0	70.0	150.0	210.0	45.0496	0.0	12.1	4.0	22.1
310.0	70.0	150.0	230.0	49.8883	0.0	12.1	3.2	21.3
190.0	70.0	150.0	250.0	54.7270	0.0	12.1	2.5	20.5
350.0	70.0	150.0	270.0	59.5657	0.0	12.1	1.8	19.7
310.0	70.0	150.0	290.0	64.4041	0.0	12.1	1.1	18.9
190.0	70.0	170.0	190.0	48.7041	0.0	12.1	3.0	21.9
350.0	70.0	170.0	210.0	53.5428	0.0	12.1	2.3	21.3
310.0	70.0	170.0	230.0	58.3815	0.0	12.1	1.6	20.6
190.0	70.0	170.0	250.0	63.2202	0.0	12.1	1.0	19.8
350.0	70.0	170.0	270.0	68.0589	0.0	12.1	0.3	19.0
310.0	70.0	170.0	290.0	72.8976	0.0	12.1	0.2	18.2
190.0	70.0	190.0	190.0	57.1970	0.0	12.1	1.9	21.9
350.0	70.0	190.0	210.0	62.0357	0.0	12.1	1.2	21.2
310.0	70.0	190.0	230.0	66.8744	0.0	12.1	0.6	20.4
190.0	70.0	190.0	250.0	71.7131	0.0	12.1	0.4	19.6
350.0	70.0	190.0	270.0	76.5518	0.0	12.1	0.2	18.8
310.0	70.0	190.0	290.0	81.3905	0.0	12.1	0.1	18.0
190.0	70.0	210.0	190.0	65.6899	0.0	12.1	1.1	20.9
350.0	70.0	210.0	210.0	70.5286	0.0	12.1	0.7	20.2
310.0	70.0	210.0	230.0	75.3673	0.0	12.1	0.4	19.4
190.0	70.0	210.0	250.0	80.2060	0.0	12.1	0.2	18.6
350.0	70.0	210.0	270.0	85.0447	0.0	12.1	0.1	17.8
310.0	70.0	210.0	290.0	89.8834	0.0	12.1	0.0	17.0
190.0	70.0	230.0	190.0	74.1818	0.0	12.1	0.8	20.7
350.0	70.0	230.0	210.0	79.0205	0.0	12.1	0.5	19.9
310.0	70.0	230.0	230.0	83.8592	0.0	12.1	0.3	19.1
190.0	70.0	230.0	250.0	88.6979	0.0	12.1	0.1	18.3
350.0	70.0	230.0	270.0	93.5366	0.0	12.1	0.0	17.5
310.0	70.0	230.0	290.0	98.3753	0.0	12.1	0.0	16.7
190.0	70.0	250.0	190.0	82.6737	0.0	12.1	0.9	20.4
350.0	70.0	250.0	210.0	87.5124	0.0	12.1	0.6	19.6
310.0	70.0	250.0	230.0	92.3511	0.0	12.1	0.4	18.8
190.0	70.0	250.0	250.0	97.1898	0.0	12.1	0.2	18.0
350.0	70.0	250.0	270.0	102.0285	0.0	12.1	0.1	17.2
310.0	70.0	250.0	290.0	106.8672	0.0	12.1	0.0	16.4
190.0	70.0	270.0	190.0	91.1656	0.0	12.1	1.0	20.1
350.0	70.0	270.0	210.0	96.0043	0.0	12.1	0.7	19.3
310.0	70.0	270.0	230.0	100.8430	0.0	12.1	0.5	18.5
190.0	70.0	270.0	250.0	105.6817	0.0	12.1	0.3	17.7
350.0	70.0	270.0	270.0	110.5204	0.0	12.1	0.1	16.9
310.0	70.0	270.0	290.0	115.3591	0.0	12.1	0.0	16.1
190.0	70.0	290.0	190.0	99.6575	0.0	12.1	1.1	19.8
350.0	70.0	290.0	210.0	104.4962	0.0	12.1	0.8	19.0
310.0	70.0	290.0	230.0	109.3349	0.0	12.1	0.6	18.2
190.0	70.0	290.0	250.0	114.1736	0.0	12.1	0.4	17.4
350.0	70.0	290.0	270.0	119.0123	0.0	12.1	0.2	16.6
310.0	70.0	290.0	290.0	123.8510	0.0	12.1	0.1	15.8
190.0	70.0	310.0	190.0	108.1494	0.0	12.1	1.2	19.5
350.0	70.0	310.0	210.0	112.9881	0.0	12.1	0.9	18.7
310.0	70.0	310.0	230.0	117.8268	0.0	12.1	0.7	17.9
190.0	70.0	310.0	250.0	122.6655	0.0	12.1	0.5	17.1
350.0	70.0	310.0	270.0	127.5042	0.0	12.1	0.3	16.3
310.0	70.0	310.0	290.0	132.3429	0.0	12.1	0.1	15.5
190.0	70.0	330.0	190.0	117.1810	0.0	12.1	1.3	19.2
350.0	70.0	330.0	210.0	122.0197	0.0	12.1	1.0	18.4
310.0	70.0	330.0	230.0	126.8584	0.0	12.1	0.8	17.6
190.0	70.0	330.0	250.0	131.6971	0.0	12.1	0.6	16.8
350.0	70.0	330.0	270.0	136.5358	0.0	12.1	0.4	16.0
310.0	70.0	330.0	290.0	141.3745	0.0	12.1	0.2	15.2
190.0	70.0	350.0	190.0	126.1116	0.0	12.1	1.4	18.9
350.0	70.0	350.0	210.0	130.9503	0.0	12.1	1.1	18.1
310.0	70.0	350.0	230.0	135.7890	0.0	12.1	0.9	17.3
190.0	70.0	350.0	250.0	140.6277	0.0	12.1	0.7	16.5
350.0	70.0	350.0	270.0	145.4664	0.0	12.1	0.5	15.7
310.0	70.0	350.0	290.0	150.3051	0.0	12.1	0.3	14.9
190.0	70.0	370.0	190.0	135.0412	0.0	12.1	1.5	18.6
350.0	70.0	370.0	210.0	139.8799	0.0	12.1	1.2	17.8
310.0	70.0	370.0	230.0	144.7186	0.0	12.1	1.0	17.0
190.0	70.0	370.0	250.0	149.5573	0.0	12.1	0.8	16.2
350.0	70.0	370.0	270.0	154.3960	0.0	12.1	0.6	15.4
310.0	70.0	370.0	290.0	159.2347	0.0	12.1	0.4	14.6
190.0	70.0	390.0	190.0	143.9098	0.0	12.1	1.6	18.3
350.0	70.0	390.0	210.0	148.7485	0.0	12.1	1.3	17.5
310.0	70.0	390.0	230.0	153.5872	0.0	12.1	1.1	16.7
190.0	70.0	390.0	250.0	158.4259	0.0	12.1	0.9	15.9
350.0	70.0	390.0	270.0	163.2646	0.0	12.1	0.7	15.1
310.0	70.0	390.0	290.0	168.1033	0.0	12.1	0.5	14.3
190.0	70.0	410.0	190.0	152.7784	0.0	12.1	1.7	18.0
350.0	70.0	410.0	210.0	157.6171	0.0	12.1	1.4	17.2
310.0	70.0	410.0	230.0	162.4558	0.0	12.1	1.2	16.4
190.0	70.0	410.0	250.0	167.2945	0.0	12.1	1.0	15.6
350.0	70.0	410.0	270.0	172.1332	0.0	12.1	0.8	14.8
310.0	70.0	410.0	290.0	176.9719	0.0	12.1	0.6	14.0
190.0	70.0	430.0	190.0	161.6470	0.0	12.1	1.8	17.7
350.0	70.0	430.0	210.0	166.4857	0.0	12.1	1.5	16.9
310.0	70.0	430.0	230.0	171.3244	0.0	12.1	1.3	16.1
190.0	70.0	430.0	250.0	176.1631	0.0	12.1	1.1	15.3
350.0	70.0	430.0	270.0	181.0018	0.0	12.1	0.9	14.5
310.0	70.0	430.0	290.0	185.8405	0.0	12.1	0.7	13.7

attor2



20.9540	6.0	12.1	10.6	20.7
22.0403	6.0	12.1	8.2	26.2
45.1713	6.0	12.1	8.2	24.4
51.9702	6.0	12.1	8.2	21.3
54.3705	6.0	12.1	8.2	23.6
30.7214	4.8	8.9	5.9	22.6
38.7212	4.8	8.9	7.2	20.9
47.2802	4.8	8.9	5.0	19.4
50.2103	4.8	8.9	4.6	18.3
84.4165	4.8	8.9	3.9	17.6
27.3009	4.8	8.9	9.4	23.1
41.3302	4.8	8.9	7.5	21.2
60.0312	4.8	8.9	6.0	19.7
67.9122	4.8	8.9	4.0	18.5
25.0456	4.8	8.9	4.1	17.0
34.5085	4.8	8.9	9.9	23.6
44.1289	4.8	8.9	7.6	21.5
54.2371	4.8	8.9	6.1	19.8
63.9570	4.8	8.9	4.9	18.6
70.9944	4.8	8.9	4.4	17.1
74.5549	4.8	8.9	4.5	18.1
24.3212	4.8	8.9	10.2	23.9
33.5106	4.8	8.9	8.0	21.7
51.9794	4.8	8.9	6.2	19.9
57.9193	4.8	8.9	5.6	18.4
73.9193	4.8	8.9	4.8	17.2
78.9193	4.8	8.9	10.3	24.2
80.9193	4.8	8.9	8.1	20.0
86.9193	4.8	8.9	6.3	18.9
91.9193	4.8	8.9	5.3	18.0
94.9193	4.8	8.9	3.9	16.9
97.9193	4.8	8.9	3.7	16.0
99.9193	4.8	8.9	3.7	15.0
100.9193	4.8	8.9	3.7	14.0
101.9193	4.8	8.9	3.7	13.0
102.9193	4.8	8.9	3.7	12.0
103.9193	4.8	8.9	3.7	11.0
104.9193	4.8	8.9	3.7	10.0
105.9193	4.8	8.9	3.7	9.0
106.9193	4.8	8.9	3.7	8.0
107.9193	4.8	8.9	3.7	7.0
108.9193	4.8	8.9	3.7	6.0
109.9193	4.8	8.9	3.7	5.0
110.9193	4.8	8.9	3.7	4.0
111.9193	4.8	8.9	3.7	3.0
112.9193	4.8	8.9	3.7	2.0
113.9193	4.8	8.9	3.7	1.0
114.9193	4.8	8.9	3.7	0.0
115.9193	4.8	8.9	3.7	-1.0
116.9193	4.8	8.9	3.7	-2.0
117.9193	4.8	8.9	3.7	-3.0
118.9193	4.8	8.9	3.7	-4.0
119.9193	4.8	8.9	3.7	-5.0
120.9193	4.8	8.9	3.7	-6.0
121.9193	4.8	8.9	3.7	-7.0
122.9193	4.8	8.9	3.7	-8.0
123.9193	4.8	8.9	3.7	-9.0
124.9193	4.8	8.9	3.7	-10.0
125.9193	4.8	8.9	3.7	-11.0
126.9193	4.8	8.9	3.7	-12.0
127.9193	4.8	8.9	3.7	-13.0
128.9193	4.8	8.9	3.7	-14.0
129.9193	4.8	8.9	3.7	-15.0
130.9193	4.8	8.9	3.7	-16.0
131.9193	4.8	8.9	3.7	-17.0
132.9193	4.8	8.9	3.7	-18.0
133.9193	4.8	8.9	3.7	-19.0
134.9193	4.8	8.9	3.7	-20.0
135.9193	4.8	8.9	3.7	-21.0
136.9193	4.8	8.9	3.7	-22.0
137.9193	4.8	8.9	3.7	-23.0
138.9193	4.8	8.9	3.7	-24.0
139.9193	4.8	8.9	3.7	-25.0
140.9193	4.8	8.9	3.7	-26.0
141.9193	4.8	8.9	3.7	-27.0
142.9193	4.8	8.9	3.7	-28.0
143.9193	4.8	8.9	3.7	-29.0
144.9193	4.8	8.9	3.7	-30.0
145.9193	4.8	8.9	3.7	-31.0
146.9193	4.8	8.9	3.7	-32.0
147.9193	4.8	8.9	3.7	-33.0
148.9193	4.8	8.9	3.7	-34.0
149.9193	4.8	8.9	3.7	-35.0
150.9193	4.8	8.9	3.7	-36.0
151.9193	4.8	8.9	3.7	-37.0
152.9193	4.8	8.9	3.7	-38.0
153.9193	4.8	8.9	3.7	-39.0
154.9193	4.8	8.9	3.7	-40.0
155.9193	4.8	8.9	3.7	-41.0
156.9193	4.8	8.9	3.7	-42.0
157.9193	4.8	8.9	3.7	-43.0
158.9193	4.8	8.9	3.7	-44.0
159.9193	4.8	8.9	3.7	-45.0
160.9193	4.8	8.9	3.7	-46.0
161.9193	4.8	8.9	3.7	-47.0
162.9193	4.8	8.9	3.7	-48.0
163.9193	4.8	8.9	3.7	-49.0
164.9193	4.8	8.9	3.7	-50.0
165.9193	4.8	8.9	3.7	-51.0
166.9193	4.8	8.9	3.7	-52.0
167.9193	4.8	8.9	3.7	-53.0
168.9193	4.8	8.9	3.7	-54.0
169.9193	4.8	8.9	3.7	-55.0
170.9193	4.8	8.9	3.7	-56.0
171.9193	4.8	8.9	3.7	-57.0
172.9193	4.8	8.9	3.7	-58.0
173.9193	4.8	8.9	3.7	-59.0
174.9193	4.8	8.9	3.7	-60.0
175.9193	4.8	8.9	3.7	-61.0
176.9193	4.8	8.9	3.7	-62.0
177.9193	4.8	8.9	3.7	-63.0
178.9193	4.8	8.9	3.7	-64.0
179.9193	4.8	8.9	3.7	-65.0
180.9193	4.8	8.9	3.7	-66.0
181.9193	4.8	8.9	3.7	-67.0
182.9193	4.8	8.9	3.7	-68.0
183.9193	4.8	8.9	3.7	-69.0
184.9193	4.8	8.9	3.7	-70.0
185.9193	4.8	8.9	3.7	-71.0
186.9193	4.8	8.9	3.7	-72.0
187.9193	4.8	8.9	3.7	-73.0
188.9193	4.8	8.9	3.7	-74.0
189.9193	4.8	8.9	3.7	-75.0
190.9193	4.8	8.9	3.7	-76.0
191.9193	4.8	8.9	3.7	-77.0
192.9193	4.8	8.9	3.7	-78.0
193.9193	4.8	8.9	3.7	-79.0
194.9193	4.8	8.9	3.7	-80.0
195.9193	4.8	8.9	3.7	-81.0
196.9193	4.8	8.9	3.7	-82.0
197.9193	4.8	8.9	3.7	-83.0
198.9193	4.8	8.9	3.7	-84.0
199.9193	4.8	8.9	3.7	-85.0
200.9193	4.8	8.9	3.7	-86.0
201.9193	4.8	8.9	3.7	-87.0
202.9193	4.8	8.9	3.7	-88.0
203.9193	4.8	8.9	3.7	-89.0
204.9193	4.8	8.9	3.7	-90.0
205.9193	4.8	8.9	3.7	-91.0
206.9193	4.8	8.9	3.7	-92.0
207.9193	4.8	8.9	3.7	-93.0
208.9193	4.8	8.9	3.7	-94.0
209.9193	4.8	8.9	3.7	-95.0
210.9193	4.8	8.9	3.7	-96.0
211.9193	4.8	8.9	3.7	-97.0
212.9193	4.8	8.9	3.7	-98.0
213.9193	4.8	8.9	3.7	-99.0
214.9193	4.8	8.9	3.7	-100.0
215.9193	4.8	8.9	3.7	-101.0
216.9193	4.8	8.9	3.7	-102.0
217.9193	4.8	8.9	3.7	-103.0
218.9193	4.8	8.9	3.7	-104.0
219.9193	4.8	8.9	3.7	-105.0
220.9193	4.8	8.9	3.7	-106.0
221.9193	4.8	8.9	3.7	-107.0
222.9193	4.8	8.9	3.7	-108.0
223.9193	4.8	8.9	3.7	-109.0
224.9193	4.8	8.9	3.7	-110.0
225.9193	4.8	8.9	3.7	-111.0
226.9193	4.8	8.9	3.7	-112.0
227.9193	4.8	8.9	3.7	-113.0
228.9193	4.8	8.9	3.7	-114.0
229.9193	4.8	8.9	3.7	-115.0
230.9193	4.8	8.9	3.7	-116.0
231.9193	4.8	8.9	3.7	-117.0
232.9193	4.8	8.9	3.7	-118.0
233.9193	4.8	8.9	3.7	-119.0
234.9193	4.8	8.9	3.7	-120.0
235.9193	4.8	8.9	3.7	-121.0
236.9193	4.8	8.9	3.7	-122.0
237.9193	4.8	8.9	3.7	-123.0
238.9193	4.8	8.9	3.7	-124.0
239.9193	4.8	8.9	3.7	-125.0
240.9193	4.8	8.9	3.7	-126.0
241.9193	4.8	8.9	3.7	-127.0
242.9193	4.8	8.9	3.7	-128.0
243.9193	4.8	8.9	3.7	-129.0
244.9193	4.8	8.9	3.7	-130.0
245.9193	4.8	8.9	3.7	-131.0
246.9193	4.8	8.9	3.7	-132.0
247.9193	4.8	8.9	3.7	-133.0
248.9193	4.8	8.9	3.7	-134.0
249.9193	4.8	8.9	3.7	-135.0
250.9193	4.8	8.9	3.7	-136.0
251.9193	4.8	8.9	3.7	-137.0
252.9193	4.8	8.9	3.7	-138.0
253.9193	4.8	8.9	3.7	-139.0
254.9193	4.8	8.9	3.7	-140.0
255.9193	4.8	8.9	3.7	-141.0
256.9193	4.8	8.9	3.7	-142.0
257.9193	4.8	8.9	3.7	-143.0
258.9193	4.8	8.9	3.7	-144.0
259.9193	4.8	8.9	3.7	-145.0
260.9193	4.8	8.9	3.7	-146.0
261.9193	4.8	8.9	3.7	-147.0
262.9193	4.8	8.9	3.7	-148.0
263.9193	4.8	8.9	3.7	-149.0
264.9193	4.8	8.9	3.7	-150.0
265.9193	4.8	8.9	3.7	-151.0
266.9193	4.8	8.9	3.7	-152.0
267.9193	4.8	8.9	3.7	-153.0
268.9193	4.8	8.9	3.7	-154.0
269.9193	4.8	8.9	3.7	-155.0
270.9193	4.8	8.9	3.7	-156.0
271.9193	4.8	8.9	3.7	-157.0
272.9193	4.8	8.9	3.7	-158.0
273.9193	4.8	8.9	3.7	-159.0
274.9193	4.8	8.9	3.7	-160.0
275.9193	4.8	8.9	3.7	-161.0
276.9193	4.8	8.9	3.7	-162.0
277.9193	4.8	8.9	3.7	-163.0
278.9193	4.8	8.9	3.7	-164.0
279.9193	4.8	8.9	3.7	-165.0
280.9193	4.8	8.9	3.7	-166.0
281.9193	4.8	8.9	3.7	-167.0
282.9193	4.8	8.9	3.7	-168.0
283.9193	4.8	8.9	3.7	-169.0
284.9193	4.8	8.9	3.7	-170.0
285.9193	4.8	8.9	3.7	-171.0
286.9193	4.8	8.9	3.7	-172.0
287.9193	4.8	8.9	3.7	-173.0
288.9193	4.8	8.9	3.7	-174.0
289.9193	4.8	8.9	3.7	-175.0
290.9193	4.8	8.9	3.7	-176.0
291.9193	4.8	8.9	3.7	-177.0
292.9193	4.8	8.9	3.7	-178.0
293.9193	4.8	8.9	3.7	-179.0
294.9193	4.8	8.9	3.7	-180.0
295.9193	4.8	8.9	3.7	-181.0
296.9193	4.8	8.9	3.7	-182.0
297.9193	4.8	8.9	3.7	-183.0
298.9193	4.8	8.9	3.7	-184.0
299.9193	4.8	8.9	3.7	-185.0
300.9193	4.8	8.9	3.7	-186.0
301.9193	4.8	8.9	3.7	-187.0
302.9193	4.8	8.9	3.7	-188.0
303.9193	4.8	8.9	3.7	-189.0
304.9193	4.8	8.9	3.7	-190.0
305.9193	4.8	8.9	3.7	-191.0
306.9193	4.8	8.9	3.7	-192.0
307.9193	4.8	8.9	3.7	-193.0
308.9193	4.8	8.9	3.7	-194.0
309.9193	4.8	8.9	3.7	-195.0
310.9193	4.8	8.9	3.7	-196.0
311.9193	4.8	8.9	3.7	-197.0
312.9193	4.8	8.9	3.7	-198.0
313.9193	4.8	8.		

438.0	130.0	70.0	250.0	4.2	6.7	5.2	16.1	390.0	170.0	30.0	190.0	3.0	4.0	0.1	13.1
439.0	130.0	90.0	130.0	4.2	6.7	17.7	20.6	410.0	170.0	30.0	210.0	3.0	4.0	0.1	13.1
440.0	130.0	90.0	130.0	4.2	6.7	17.7	20.6	430.0	170.0	30.0	230.0	3.0	4.0	0.1	13.1
441.0	130.0	90.0	130.0	4.2	6.7	10.2	24.7	450.0	170.0	30.0	250.0	3.0	4.0	0.1	13.1
442.0	130.0	90.0	130.0	4.2	6.7	12.0	21.6	470.0	170.0	30.0	270.0	3.0	4.0	0.1	13.1
443.0	130.0	90.0	130.0	4.2	6.7	6.2	19.1	490.0	170.0	30.0	290.0	3.0	4.0	0.1	13.1
444.0	130.0	90.0	130.0	4.2	6.7	6.2	19.1	510.0	170.0	30.0	310.0	3.0	4.0	0.1	13.1
445.0	130.0	90.0	130.0	4.2	6.7	6.2	19.1	530.0	170.0	30.0	330.0	3.0	4.0	0.1	13.1
446.0	130.0	90.0	130.0	4.2	6.7	6.2	19.1	550.0	170.0	30.0	350.0	3.0	4.0	0.1	13.1
447.0	130.0	90.0	130.0	4.2	6.7	6.2	19.1	570.0	170.0	30.0	370.0	3.0	4.0	0.1	13.1
448.0	130.0	90.0	130.0	4.2	6.7	6.2	19.1	590.0	170.0	30.0	390.0	3.0	4.0	0.1	13.1
449.0	130.0	90.0	130.0	4.2	6.7	6.2	19.1	610.0	170.0	30.0	410.0	3.0	4.0	0.1	13.1
450.0	130.0	90.0	130.0	4.2	6.7	6.2	19.1	630.0	170.0	30.0	430.0	3.0	4.0	0.1	13.1
451.0	130.0	90.0	130.0	4.2	6.7	6.2	19.1	650.0	170.0	30.0	450.0	3.0	4.0	0.1	13.1
452.0	130.0	90.0	130.0	4.2	6.7	6.2	19.1	670.0	170.0	30.0	470.0	3.0	4.0	0.1	13.1
453.0	130.0	90.0	130.0	4.2	6.7	6.2	19.1	690.0	170.0	30.0	490.0	3.0	4.0	0.1	13.1
454.0	130.0	90.0	130.0	4.2	6.7	6.2	19.1	710.0	170.0	30.0	510.0	3.0	4.0	0.1	13.1
455.0	130.0	90.0	130.0	4.2	6.7	6.2	19.1	730.0	170.0	30.0	530.0	3.0	4.0	0.1	13.1
456.0	130.0	90.0	130.0	4.2	6.7	6.2	19.1	750.0	170.0	30.0	550.0	3.0	4.0	0.1	13.1
457.0	130.0	90.0	130.0	4.2	6.7	6.2	19.1	770.0	170.0	30.0	570.0	3.0	4.0	0.1	13.1
458.0	130.0	90.0	130.0	4.2	6.7	6.2	19.1	790.0	170.0	30.0	590.0	3.0	4.0	0.1	13.1
459.0	130.0	90.0	130.0	4.2	6.7	6.2	19.1	810.0	170.0	30.0	610.0	3.0	4.0	0.1	13.1
460.0	130.0	90.0	130.0	4.2	6.7	6.2	19.1	830.0	170.0	30.0	630.0	3.0	4.0	0.1	13.1
461.0	130.0	90.0	130.0	4.2	6.7	6.2	19.1	850.0	170.0	30.0	650.0	3.0	4.0	0.1	13.1
462.0	130.0	90.0	130.0	4.2	6.7	6.2	19.1	870.0	170.0	30.0	670.0	3.0	4.0	0.1	13.1
463.0	130.0	90.0	130.0	4.2	6.7	6.2	19.1	890.0	170.0	30.0	690.0	3.0	4.0	0.1	13.1
464.0	130.0	90.0	130.0	4.2	6.7	6.2	19.1	910.0	170.0	30.0	710.0	3.0	4.0	0.1	13.1
465.0	130.0	90.0	130.0	4.2	6.7	6.2	19.1	930.0	170.0	30.0	730.0	3.0	4.0	0.1	13.1
466.0	130.0	90.0	130.0	4.2	6.7	6.2	19.1	950.0	170.0	30.0	750.0	3.0	4.0	0.1	13.1
467.0	130.0	90.0	130.0	4.2	6.7	6.2	19.1	970.0	170.0	30.0	770.0	3.0	4.0	0.1	13.1
468.0	130.0	90.0	130.0	4.2	6.7	6.2	19.1	990.0	170.0	30.0	790.0	3.0	4.0	0.1	13.1
469.0	130.0	90.0	130.0	4.2	6.7	6.2	19.1	1010.0	170.0	30.0	810.0	3.0	4.0	0.1	13.1
470.0	130.0	90.0	130.0	4.2	6.7	6.2	19.1	1030.0	170.0	30.0	830.0	3.0	4.0	0.1	13.1
471.0	130.0	90.0	130.0	4.2	6.7	6.2	19.1	1050.0	170.0	30.0	850.0	3.0	4.0	0.1	13.1
472.0	130.0	90.0	130.0	4.2	6.7	6.2	19.1	1070.0	170.0	30.0	870.0	3.0	4.0	0.1	13.1
473.0	130.0	90.0	130.0	4.2	6.7	6.2	19.1	1090.0	170.0	30.0	890.0	3.0	4.0	0.1	13.1
474.0	130.0	90.0	130.0	4.2	6.7	6.2	19.1	1110.0	170.0	30.0	910.0	3.0	4.0	0.1	13.1
475.0	130.0	90.0	130.0	4.2	6.7	6.2	19.1	1130.0	170.0	30.0	930.0	3.0	4.0	0.1	13.1
476.0	130.0	90.0	130.0	4.2	6.7	6.2	19.1	1150.0	170.0	30.0	950.0	3.0	4.0	0.1	13.1
477.0	130.0	90.0	130.0	4.2	6.7	6.2	19.1	1170.0	170.0	30.0	970.0	3.0	4.0	0.1	13.1
478.0	130.0	90.0	130.0	4.2	6.7	6.2	19.1	1190.0	170.0	30.0	990.0	3.0	4.0	0.1	13.1
479.0	130.0	90.0	130.0	4.2	6.7	6.2	19.1	1210.0	170.0	30.0	1010.0	3.0	4.0	0.1	13.1
480.0	130.0	90.0	130.0	4.2	6.7	6.2	19.1	1230.0	170.0	30.0	1030.0	3.0	4.0	0.1	13.1
481.0	130.0	90.0	130.0	4.2	6.7	6.2	19.1	1250.0	170.0	30.0	1050.0	3.0	4.0	0.1	13.1
482.0	130.0	90.0	130.0	4.2	6.7	6.2	19.1	1270.0	170.0	30.0	1070.0	3.0	4.0	0.1	13.1
483.0	130.0	90.0	130.0	4.2	6.7	6.2	19.1	1290.0	170.0	30.0	1090.0	3.0	4.0	0.1	13.1
484.0	130.0	90.0	130.0	4.2	6.7	6.2	19.1	1310.0	170.0	30.0	1110.0	3.0	4.0	0.1	13.1
485.0	130.0	90.0	130.0	4.2	6.7	6.2	19.1	1330.0	170.0	30.0	1130.0	3.0	4.0	0.1	13.1
486.0	130.0	90.0	130.0	4.2	6.7	6.2	19.1	1350.0	170.0	30.0	1150.0	3.0	4.0	0.1	13.1
487.0	130.0	90.0	130.0	4.2	6.7	6.2	19.1	1370.0	170.0	30.0	1170.0	3.0	4.0	0.1	13.1
488.0	130.0	90.0	130.0	4.2	6.7	6.2	19.1	1390.0	170.0	30.0	1190.0	3.0	4.0	0.1	13.1
489.0	130.0	90.0	130.0	4.2	6.7	6.2	19.1	1410.0	170.0	30.0	1210.0	3.0	4.0	0.1	13.1
490.0	130.0	90.0	130.0	4.2	6.7	6.2	19.1	1430.0	170.0	30.0	1230.0	3.0	4.0	0.1	13.1
491.0	130.0	90.0	130.0	4.2	6.7	6.2	19.1	1450.0	170.0	30.0	1250.0	3.0	4.0	0.1	13.1
492.0	130.0	90.0	130.0	4.2	6.7	6.2	19.1	1470.0	170.0	30.0	1270.0	3.0	4.0	0.1	13.1
493.0	130.0	90.0	130.0	4.2	6.7	6.2	19.1	1490.0	170.0	30.0	1290.0	3.0	4.0	0.1	13.1
494.0	130.0	90.0	130.0	4.2	6.7	6.2	19.1	1510.0	170.0	30.0	1310.0	3.0	4.0	0.1	13.1
495.0	130.0	90.0	130.0	4.2	6.7	6.2	19.1	1530.0	170.0	30.0	1330.0	3.0	4.0	0.1	13.1
496.0	130.0	90.0	130.0	4.2	6.7	6.2	19.1	1550.0	170.0	30.0	1350.0	3.0	4.0	0.1	13.1
497.0	130.0	90.0	130.0	4.2	6.7	6.2	19.1	1570.0	170.0	30.0	1370.0	3.0	4.0	0.1	13.1
498.0	130.0	90.0	130.0	4.2	6.7	6.2	19.1	1590.0	170.0	30.0	1390.0	3.0	4.0	0.1	13.1
499.0	130.0	90.0	130.0	4.2	6.7	6.2	19.1	1610.0	170.0	30.0	1410.0	3.0	4.0	0.1	13.1
500.0	130.0	90.0	130.0	4.2	6.7	6.2	19.1	1630.0	170.0	30.0	1430.0	3.0	4.0	0.1	13.1
501.0	130.0	90.0	130.0	4.2	6.7	6.2	19.1	1650.0	170.0	30.0	1450.0	3.0	4.0	0.1	13.1
502.0	130.0	90.0	130.0	4.2	6.7	6.2	19.1	1670.0	170.0	30.0	1470.0	3.0	4.0	0.1	13.1
503.0	130.0	90.0	130.0	4.2	6.7	6.2	19.1	1690.0	170.0	30.0	1490.0	3.0	4.0	0.1	13.1
504.0	130.0	90.0	130.0	4.2	6.7	6.2	19.1	1710.0	170.0	30.0	1510.0	3.0	4.0	0.1	13.1
505.0	130.0	90.0	130.0	4.2	6.7	6.2	19.1	1730.0	170.0	30.0	1530.0	3.0	4.0	0.1	13.1
506.0	130.0	90.0	130.0	4.2	6.7	6.2	19.1	1750.0	170.0	30.0	1550.0	3.0	4.0	0.1	13.1
507.0	130.0	90.0	130.0	4.2	6.7	6.2	19.1	1770.0	170.0	30.0	1570.0	3.0	4.0	0.1	13.1
508.0	130.0	90.0	130.0	4.2	6.7	6.2	19.1	1790.0	170.0	30.0	1590.0	3.0	4.0	0.1	13.1
509.0	130.0	90.0	130.0	4.2	6.7	6.2	19.1	1810.0	170.0	30.0	1610.0	3.0	4.0	0.1	13.1
510.0	130.0	90.0	130.0	4.2	6.7	6.2	19.1	1830.0	170.0	30.0	1630.0	3.0	4.0	0.1	13.1
511.0	130.0	90.0	130.0	4.2	6.7	6.2	19.1	1850.0	170.0	30.0	1650.0	3.0	4.0	0.1	13.1
512.0	130.0	90.0	130.0	4.2	6.7	6.2	19.1	1870.0	170.0	30.0	1670.0	3.0	4.0	0.1	13.1
513.0	130.0	90.0	130.0	4.2	6.7	6.2	19.1	1890.0	170.0	30.0	1690.0	3.0	4.0	0.1	13.1
514.0	130.0	90.0	130.0	4.2	6.7	6.2	19.1	1910.0	170.0	30.0	1710.0	3.0	4.0	0.1	13.1
515.0	130.0	90.0	130.0	4.2	6.7	6.2	19.1	1930.0	170.0	30.0	1730.0	3.0	4.0	0.1	13.1
516.0	130.0	90.0	130.0	4.2	6.7	6.2	19.1	1950.0	170.0	30.0	1750.0	3.0	4.0	0.1	13.1
517.0	130.0	90.0	130.0	4.2	6.7	6.2	19.1	1970.0	170.0	30.0	1770.0	3.0	4.0	0.1	13.1
518.0	130.0	90.0	130.0	4.2	6.7	6.2	19.1	1990.0	170.0	30.0	1790.0	3.0	4.0	0.1	13.1
519.0	130.0	90.0	130.0	4.2	6.7	6.2	19.1	2010.0	170.0	30.0	1810.0	3.0	4.0	0.1	13.1
520.0	130.0	90.0	130.0	4.2	6.7	6.2	19.1	2030.0	170.0	30.0	1830.0	3.0	4.0	0.1	13.1

attol2

190.0	190.0	90.0	110.0	20.0	4299	3.7	3.2	24.6	31.4	550.0	210.0	110.0	230.0	110.3089	3.6	2.6	9.9	16.1
410.0	190.0	90.0	130.0	10.0	4191	3.7	3.2	10.7	25.5	570.0	210.0	110.0	250.0	70.3935	3.6	2.6	10.7	24.3
430.0	190.0	90.0	150.0	0.0	4071	3.7	3.2	14.3	21.1	590.0	230.0	10.0	110.0	0.7060	3.6	2.3	49.4	55.2
450.0	190.0	90.0	170.0	0.0	4061	3.7	3.2	10.8	17.6	570.0	230.0	10.0	130.0	40.3019	3.6	2.3	10.0	23.0
470.0	190.0	90.0	190.0	0.0	3711	3.7	3.2	8.7	15.0	590.0	230.0	10.0	150.0	58.2935	3.6	2.3	12.9	19.0
490.0	190.0	90.0	210.0	0.0	3729	3.7	3.2	6.6	13.4	410.0	230.0	10.0	170.0	79.8244	3.6	2.3	10.7	16.6
510.0	190.0	90.0	230.0	0.0	3394	3.7	3.2	6.8	13.6	430.0	230.0	10.0	190.0	105.1642	3.6	2.3	6.2	14.1
530.0	190.0	90.0	250.0	0.0	4039	3.7	3.2	10.4	17.2	450.0	230.0	10.0	210.0	132.2794	3.6	2.3	6.4	12.7
550.0	190.0	90.0	270.0	0.0	4039	3.7	3.2	33.5	40.3	470.0	230.0	10.0	230.0	151.4194	3.6	2.3	5.5	11.4
570.0	190.0	90.0	290.0	0.0	4039	3.7	3.2	25.0	31.8	490.0	230.0	10.0	250.0	143.3000	3.6	2.3	6.5	12.4
590.0	190.0	90.0	310.0	0.0	4039	3.7	3.2	18.9	25.7	510.0	230.0	10.0	270.0	26.7256	3.6	2.3	24.0	29.8
610.0	190.0	90.0	330.0	0.0	4039	3.7	3.2	14.3	21.1	530.0	230.0	10.0	290.0	42.3954	3.6	2.3	10.4	24.3
630.0	190.0	90.0	350.0	0.0	4039	3.7	3.2	10.7	17.5	550.0	230.0	10.0	310.0	61.3701	3.6	2.3	14.1	20.0
650.0	190.0	90.0	370.0	0.0	4039	3.7	3.2	8.1	15.0	570.0	230.0	10.0	330.0	84.2692	3.6	2.3	10.0	16.7
670.0	190.0	90.0	390.0	0.0	4039	3.7	3.2	6.9	13.7	590.0	230.0	10.0	350.0	111.0400	3.6	2.3	6.2	14.1
690.0	190.0	90.0	410.0	0.0	4039	3.7	3.2	8.0	14.9	610.0	230.0	10.0	370.0	138.0791	3.6	2.3	6.4	12.3
710.0	190.0	90.0	430.0	0.0	4039	3.7	3.2	13.4	20.6	630.0	230.0	10.0	390.0	151.3250	3.6	2.3	6.0	11.0
730.0	190.0	90.0	450.0	0.0	4039	3.7	3.2	17.4	22.6	650.0	230.0	10.0	410.0	130.3129	3.6	2.3	8.1	13.9
750.0	190.0	90.0	470.0	0.0	4039	3.7	3.2	13.6	19.0	670.0	230.0	10.0	430.0	20.1720	3.6	2.3	24.6	30.4
770.0	190.0	90.0	490.0	0.0	4039	3.7	3.2	10.5	16.0	690.0	230.0	10.0	450.0	44.7161	3.6	2.3	10.7	24.6
790.0	190.0	90.0	510.0	0.0	4039	3.7	3.2	8.2	14.4	710.0	230.0	10.0	470.0	64.8430	3.6	2.3	10.3	20.1
810.0	190.0	90.0	530.0	0.0	4039	3.7	3.2	6.3	12.5	730.0	230.0	10.0	490.0	89.1040	3.6	2.3	10.8	16.7
830.0	190.0	90.0	550.0	0.0	4039	3.7	3.2	5.3	11.7	750.0	230.0	10.0	510.0	117.2369	3.6	2.3	8.2	14.0
850.0	190.0	90.0	570.0	0.0	4039	3.7	3.2	5.5	11.7	770.0	230.0	10.0	530.0	142.9036	3.6	2.3	6.5	12.4
870.0	190.0	90.0	590.0	0.0	4039	3.7	3.2	49.4	55.6	790.0	230.0	10.0	550.0	146.0002	3.6	2.3	6.8	12.6
890.0	190.0	90.0	610.0	0.0	4039	3.7	3.2	18.0	24.2	810.0	230.0	10.0	570.0	112.5145	3.6	2.3	10.3	16.2
910.0	190.0	90.0	630.0	0.0	4039	3.7	3.2	13.9	20.1	830.0	230.0	10.0	590.0	29.3130	3.6	2.3	23.5	30.8
930.0	190.0	90.0	650.0	0.0	4039	3.7	3.2	10.7	17.0	850.0	230.0	10.0	610.0	79.8051	3.6	2.3	10.9	24.2
950.0	190.0	90.0	670.0	0.0	4039	3.7	3.2	8.2	14.4	870.0	230.0	10.0	630.0	47.3406	3.6	2.3	10.3	20.1
970.0	190.0	90.0	690.0	0.0	4039	3.7	3.2	6.5	12.5	890.0	230.0	10.0	650.0	60.7202	3.6	2.3	10.3	20.1
990.0	190.0	90.0	710.0	0.0	4039	3.7	3.2	4.5	11.7	910.0	230.0	10.0	670.0	94.5476	3.6	2.3	10.7	16.8
1010.0	190.0	90.0	730.0	0.0	4039	3.7	3.2	4.5	11.7	930.0	230.0	10.0	690.0	123.5045	3.6	2.3	8.1	14.0
1030.0	190.0	90.0	750.0	0.0	4039	3.7	3.2	14.1	20.4	950.0	230.0	10.0	710.0	152.4530	3.6	2.3	6.8	12.7
1050.0	190.0	90.0	770.0	0.0	4039	3.7	3.2	10.6	17.0	970.0	230.0	10.0	730.0	136.7230	3.6	2.3	8.0	13.9
1070.0	190.0	90.0	790.0	0.0	4039	3.7	3.2	8.1	15.0	990.0	230.0	10.0	750.0	91.4944	3.6	2.3	13.7	19.6
1090.0	190.0	90.0	810.0	0.0	4039	3.7	3.2	6.4	12.6	1010.0	230.0	10.0	770.0	16.4829	3.6	2.3	34.0	39.9
1110.0	190.0	90.0	830.0	0.0	4039	3.7	3.2	6.4	12.6	1030.0	230.0	10.0	790.0	31.7900	3.6	2.3	25.2	31.1
1130.0	190.0	90.0	850.0	0.0	4039	3.7	3.2	8.0	14.7	1050.0	230.0	10.0	810.0	56.2941	3.6	2.3	10.9	24.0
1150.0	190.0	90.0	870.0	0.0	4039	3.7	3.2	24.5	30.8	1070.0	230.0	10.0	830.0	73.0055	3.6	2.3	10.6	16.3
1170.0	190.0	90.0	890.0	0.0	4039	3.7	3.2	18.7	24.9	1090.0	230.0	10.0	850.0	100.3484	3.6	2.3	9.1	14.0
1190.0	190.0	90.0	910.0	0.0	4039	3.7	3.2	14.3	20.5	1110.0	230.0	10.0	870.0	129.3995	3.6	2.3	14.2	20.1
1210.0	190.0	90.0	930.0	0.0	4039	3.7	3.2	10.6	17.0	1130.0	230.0	10.0	890.0	144.7015	3.6	2.3	10.4	24.3
1230.0	190.0	90.0	950.0	0.0	4039	3.7	3.2	8.2	14.4	1150.0	230.0	10.0	910.0	120.9357	3.6	2.3	10.6	15.0
1250.0	190.0	90.0	970.0	0.0	4039	3.7	3.2	6.6	12.0	1170.0	230.0	10.0	930.0	71.0787	3.6	2.3	10.4	24.3
1270.0	190.0	90.0	990.0	0.0	4039	3.7	3.2	6.6	12.0	1190.0	230.0	10.0	950.0	4.9802	3.6	2.3	40.3	54.1
1290.0	190.0	90.0	1010.0	0.0	4039	3.7	3.2	6.7	12.9	1210.0	230.0	10.0	970.0	18.0330	3.6	2.3	30.4	40.3
1310.0	190.0	90.0	1030.0	0.0	4039	3.7	3.2	10.2	16.5	1230.0	230.0	10.0	990.0	33.9476	3.6	2.3	25.3	31.2
1330.0	190.0	90.0	1050.0	0.0	4039	3.7	3.2	13.4	19.7	1250.0	230.0	10.0	1010.0	53.5442	3.6	2.3	10.9	24.7
1350.0	190.0	90.0	1070.0	0.0	4039	3.7	3.2	24.9	31.2	1270.0	230.0	10.0	1030.0	77.6997	3.6	2.3	14.1	19.9
1370.0	190.0	90.0	1090.0	0.0	4039	3.7	3.2	18.9	25.1	1290.0	230.0	10.0	1050.0	106.4081	3.6	2.3	10.5	16.3
1390.0	190.0	90.0	1110.0	0.0	4039	3.7	3.2	14.3	20.5	1310.0	230.0	10.0	1070.0	134.1309	3.6	2.3	9.2	14.1
1410.0	190.0	90.0	1130.0	0.0	4039	3.7	3.2	10.7	16.9	1330.0	230.0	10.0	1090.0	138.7802	3.6	2.3	8.3	14.2
1430.0	190.0	90.0	1150.0	0.0	4039	3.7	3.2	8.1	14.4	1350.0	230.0	10.0	1110.0	100.8249	3.6	2.3	13.0	18.0
1450.0	190.0	90.0	1170.0	0.0	4039	3.7	3.2	6.4	13.0	1370.0	230.0	10.0	1130.0	54.6530	3.6	2.3	23.9	29.8
1470.0	190.0	90.0	1190.0	0.0	4039	3.7	3.2	7.9	14.2	1390.0	230.0	10.0	1150.0	26.6705	3.6	2.3	24.2	29.9
1490.0	190.0	90.0	1210.0	0.0	4039	3.7	3.2	13.6	19.8	1410.0	230.0	10.0	1170.0	42.5409	3.6	2.1	18.5	24.2
1510.0	190.0	90.0	1230.0	0.0	4039	3.7	3.2	25.2	31.4	1430.0	230.0	10.0	1190.0	61.8932	3.6	2.1	14.2	19.9
1530.0	190.0	90.0	1250.0	0.0	4039	3.7	3.2	10.6	17.0	1450.0	230.0	10.0	1210.0	85.1150	3.6	2.1	10.6	16.5
1550.0	190.0	90.0	1270.0	0.0	4039	3.7	3.2	8.1	15.0	1470.0	230.0	10.0	1230.0	112.7052	3.6	2.1	8.2	13.9
1570.0	190.0	90.0	1290.0	0.0	4039	3.7	3.2	6.5	12.5	1490.0	230.0	10.0	1250.0	139.8404	3.6	2.1	5.5	12.2
1590.0	190.0	90.0	1310.0	0.0	4039	3.7	3.2	14.2	20.4	1510.0	230.0	10.0	1270.0	150.8284	3.6	2.1	4.2	21.9
1610.0	190.0	90.0	1330.0	0.0	4039	3.7	3.2	10.6	17.0	1530.0	230.0	10.0	1290.0	125.2382	3.6	2.1	8.6	14.3
1630.0	190.0	90.0	1350.0	0.0	4039	3.7	3.2	8.1	14.8	1550.0	230.0	10.0	1310.0	38.2161	3.6	2.1	24.7	30.5
1650.0	190.0	90.0	1370.0	0.0	4039	3.7	3.2	7.3	13.6	1570.0	230.0	10.0	1330.0	45.0074	3.6	2.1	10.6	24.5

330423  
07:10:00

4

attof2

430.0	230.0	30.0	150.0	65.5162	3.6	2.1	14.3	20.0
450.0	230.0	30.0	170.0	90.4208	3.6	2.1	10.8	16.5
470.0	230.0	30.0	190.0	119.0287	3.6	2.1	8.2	13.9
490.0	230.0	30.0	210.0	144.2500	3.6	2.1	6.6	12.3
510.0	230.0	30.0	230.0	164.8138	3.6	2.1	7.1	12.0
530.0	230.0	30.0	250.0	184.6569	3.6	2.1	11.2	16.9
550.0	230.0	50.0	90.0	15.4823	3.6	2.1	33.6	39.3
570.0	230.0	50.0	110.0	29.9440	3.6	2.1	25.0	30.7
590.0	230.0	50.0	130.0	47.7487	3.6	2.1	18.9	24.6
610.0	230.0	50.0	150.0	69.5452	3.6	2.1	14.3	20.0
630.0	230.0	50.0	170.0	95.9763	3.6	2.1	10.7	16.4
650.0	230.0	50.0	190.0	125.3221	3.6	2.1	8.1	13.8
670.0	230.0	50.0	210.0	146.1375	3.6	2.1	7.0	12.7
690.0	230.0	50.0	230.0	132.9169	3.6	2.1	8.5	14.2
710.0	230.0	50.0	250.0	95.3870	3.6	2.1	14.9	20.6
730.0	230.0	70.0	90.0	16.7155	3.6	2.1	34.2	39.9
750.0	230.0	70.0	110.0	32.0106	3.6	2.1	25.3	31.0
770.0	230.0	70.0	130.0	50.6696	3.6	2.1	18.9	24.6
790.0	230.0	70.0	150.0	73.9843	3.6	2.1	14.2	19.9
810.0	230.0	70.0	170.0	101.9112	3.6	2.1	10.6	16.3
830.0	230.0	70.0	190.0	131.0592	3.6	2.1	8.1	13.8
850.0	230.0	70.0	210.0	153.9426	3.6	2.1	7.4	13.3
870.0	230.0	70.0	230.0	115.5033	3.6	2.1	10.7	16.4
890.0	230.0	90.0	70.0	82.5264	3.6	2.1	20.0	23.7
910.0	230.0	90.0	90.0	14.4599	3.6	2.1	48.5	54.2
930.0	230.0	90.0	110.0	18.1379	3.6	2.1	34.5	40.2
950.0	230.0	90.0	130.0	34.7636	3.6	2.1	25.3	31.0
970.0	230.0	90.0	150.0	54.1924	3.6	2.1	18.9	24.6
990.0	230.0	90.0	170.0	78.0795	3.6	2.1	14.0	19.7
1010.0	230.0	90.0	190.0	108.0736	3.6	2.1	10.4	16.1
1030.0	230.0	90.0	210.0	135.3102	3.6	2.1	8.3	14.0
1050.0	230.0	90.0	230.0	136.1466	3.6	2.1	8.7	14.4
1070.0	230.0	90.0	250.0	94.5315	3.6	2.1	14.1	19.8
1090.0	230.0	110.0	70.0	5.8031	3.6	2.1	25.4	31.1
1110.0	230.0	110.0	90.0	12.7139	3.6	2.1	49.8	50.7
1130.0	230.0	110.0	110.0	36.7317	3.6	2.1	34.6	40.3
1150.0	230.0	110.0	130.0	57.9007	3.6	2.1	25.3	31.0
1170.0	230.0	110.0	150.0	84.0560	3.6	2.1	18.7	24.4
1190.0	230.0	110.0	170.0	114.1618	3.6	2.1	13.8	19.3
1210.0	230.0	110.0	190.0	136.7373	3.6	2.1	10.3	16.0
1230.0	230.0	110.0	210.0	122.0957	3.6	2.1	8.7	14.4
1250.0	230.0	110.0	230.0	73.7301	3.6	2.1	10.5	16.2
1270.0	230.0	110.0	250.0	42.6963	3.6	2.1	18.7	24.4
1290.0	230.0	110.0	270.0		3.6	2.1	29.9	35.5

## APPENDIX C -- FEASIBILITY OF SCHWING TRAJECTORY FOR NEPTUNE

There are two ways that a spacecraft is manipulated as it follows a trajectory. The most obvious is through the use of its on board propulsion system. Obviously, this has its costs. For the energy to be used, it must first be carried in some state and processed into another. The second force is far simpler. It results from the body forces of the massive objects in range which assert their influence. Swingbys capitalize upon this attraction to obtain "free" delta-v's or delta-v's of convenience. If the spacecraft passes close to the surface of a much larger body, the body will have the effect of perturbing the trajectory of the vehicle even if it continues to revolve on the larger scale around another larger body. In other words, this body can exert influence without actually capturing the craft.

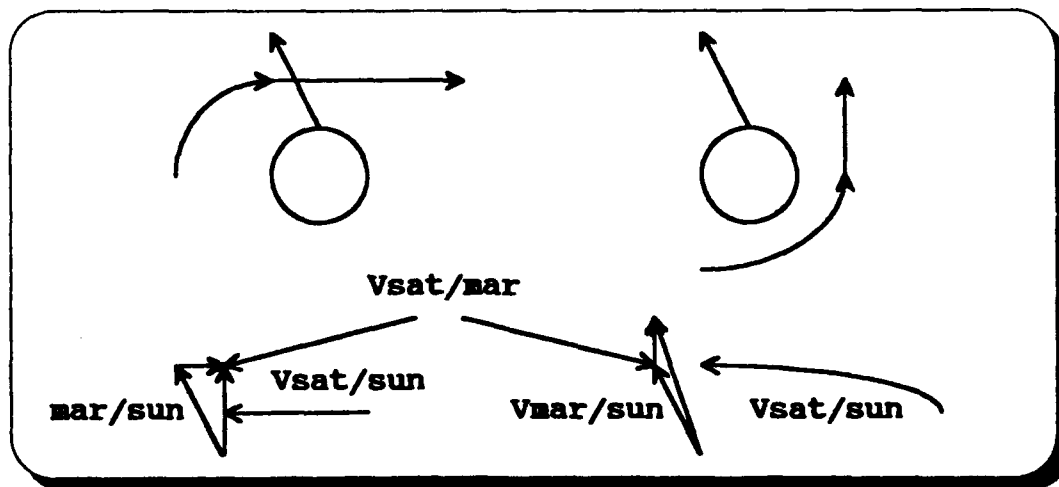


Figure C1 -- Swingby velocity savings

Just by looking at the geometry of the problem, it can be seen that a craft passing in front of the direction of motion of the larger body will experience a delta-v that serves to slow its global velocity with respect to the larger central body. Conversely, if it passes behind the path of the perturbing body, its velocity with respect the central body will increase. (This may be seen by comparing the magnitude of the vector  $v_{sat/sun}$  in the two cases shown in the diagram.)

Schwing was developed to reduce the delta-v requirement for a round-trip mission to Mars. It benefits from the fact that the transfer craft never has to enter a Martian orbit. After following a fairly high energy outbound transfer, the spacecraft drops a manned landing payload off at an initial Mars encounter. The proximity of this encounter will vary, but will be well within the Martian sphere of influence. As shown above, the trajectory of the spacecraft is perturbed by Mars. The key is to perturb the trajectory appropriately to align the new trajectory with a Martian reencounter at about the same time the landing party is ready for departure.

However, the savings are not complete. At the second Martian encounter, the transfer vehicle is conveniently aligned to use Mars again. The purpose this time is to align the return trajectory so that a smaller delta-v is necessary to meet earth after the return time passes.

The mathematics involved in dealing with planetary swingbys are greatly simplified if the problem is broken down into the appropriate reference frames. As the spacecraft approaches Mars, it feels no attraction from the planet and follows a completely heliocentric trajectory. Then at the point where the spacecraft is first able to feel the

gravitational attraction of Mars, call it  $r_{\infty}$ , we define the beginning of a hyperbolic trajectory about Mars. The velocity at this point in the heliocentric trajectory can be considered  $(v_{sat/sun})_{\infty}$ , or the velocity of the satellite with respect to the sun. In order to find this  $(v_{sat/mars})_{\infty}$ , simply use the relation:

$$(v_{sat/mars})_{\infty} = (v_{sat/sun})_{\infty} - v_{mars/sun} \quad (C1)$$

$(v_{sat/mars})_{\infty}$  : velocity of craft with respect to Mars at initial point of influence

The next step is to find the eccentricity of this hyperbolic swingby orbit about Mars. In order to do this, the minimum swingby altitude must be known. Obviously, the closer the craft gets to the surface, the stronger the force of the gravitational attraction which acts to deflect the trajectory and the larger the deflection. With this parameter defined, the eccentricity is:

$$e_H = 1 + \frac{(v_{sat/mars})_{\infty}^2 r_{per}}{\mu_{mars}} \quad (C2)$$

$r_{per}$  : radius of periapsis

This eccentricity makes it possible to solve for the deflection angle in the hyperbolic orbit caused by the gravitational acceleration of the planet. This formula for this calculation is:

$$\sin\left(\frac{\delta}{2}\right) = \frac{1}{e} \quad (C3)$$

Knowing the deflection angle, it is possible to determine the velocity vector of the spacecraft with respect to Mars as it leaves the Martian sphere of influence. The magnitude of this vector will remain as it was at the point of entrance into the sphere of influence, however the direction of the vector will be a simple rotation through the angle  $\delta$  from the direction of entrance. As it turns out, the deflection angle will be the same



whether the craft passes in front of or behind the path of the planet. The difference will be in the direction of the rotation of the velocity vector.

Once the vector velocity of the craft with respect to Mars is known, the heliocentric velocity of the vehicle at that point where it departs the Martian sphere of influence is found with simple vector addition:

$$(v_{sat/sun})_{\infty} = (v_{sat/mars})_{\infty} + v_{mars/sun} \quad (C4)$$

The key to using Schwing properly is to determine what magnitude and direction of velocity is desired in a heliocentric sense upon leaving the planetary sphere of influence. In the case of the first passage, the desired velocity vector is one that places the satellite close to the position of Mars after the surface stay time has passed in a time of flight relatively close to that surface stay time. The second swingby is intended to leave the craft with a velocity vector enabling it to conveniently intercept earth's orbital distance from the sun at that time when the earth will be there.

Ideally, Schwing would make it necessary to burn only once for the entire round trip mission to Mars. After the burn to initiate the outbound trajectory, the craft would proceed to Mars where it would swing into a new trajectory reintercepting Mars after the surface stay is complete. Then, it would swing into a final return orbit to rendez-vous with the earth. Obviously, the gravitational perturbing effect of Mars is insufficient to act alone in steering and accelerating the craft with respect to the sun, but it is extremely useful in reducing the amount of input the thrusters must have to complete the mission.

## **APPENDIX D**

Computer program SCHWING is to calculate the delta-v requirement of a round-trip Mars Schwing trajectory. It is set up to define the delta-v for a single time of flight input, rather than cycle through all possible time of flight and planetary geometry scenarios, as in program MARSTRIP.

This program is written in Fortran and contains frequent, descriptive comments to outline the flow. It also contains some subroutines taken from the USAFA Department of Astronautical Engineering Computer Library.<sup>24</sup>



030729  
070330

```

* First Mars encounter, find neb
rhuag = rhuag
web1 = decos((p-rhuag)/(a*rhuag))

* Find r0 and v0 from vectors
r01(1) = rhuag*dcos(nub1)
r01(2) = rhuag*dsin(nub1)
r01(3) = mag(r01)

v01(1) = -c1 * dsin(nub1)
v01(2) = c1 * dcos(nub1)
v01(3) = mag(v01)

* Find v0 from
c2 = dsqrt(rhuag/rhuag)
v01(1) = -c2 * dsin(nub1)
v01(2) = c2 * dcos(nub1)
v01(3) = mag(v01)

* Determine how far Mars will move in tstay
marsmag = omars * tstay

* Calculate position vector to Mars at reencounter
r02(1) = rhuag*dcos(nub1+marsmag)
r02(2) = rhuag*dsin(nub1+marsmag)
r02(3) = mag(r02)

.....
* Attempt to reduce the delta-v to be applied at point c by
* employing a swingby of Mars on the initial passage.
* Sample different times (less than Mars stay time)
* at which to calculate a spacecraft position vector. Perform
* the Gauss routine to calculate the velocity vector necessary for
* the satellite to encounter Mars its position vector after the
* stay time. Calculate the necessary delta-v to meet Mars.
.....

test = 0.000
* Input altitude of initial swing-by
write('i') 'Input swing-by altitude (km): '
read('i',*) altphyp
rphyp = altphyp * 3280.000

* Input altitude of second swing-by
write('i') 'Input second swing-by altitude (km): '
read('i',*) altphyp3
rphyp3 = altphyp3 * 3280.000
15 continue
tutact = days * test

* Use v01(1) = v01(1) + v01(1)
* No initial swingby calculations
do 20, i=1,2
v01(i) = v01(i) + v01(i)
20 continue
v01(3) = mag(v01)

* Find eccentricity of hyperbolic swingby orbit
eccenpar = 1.000 (rphyp - v01(3)**2)/0.001/mumar
do 30, i=1,2
v01(i) = dsin(i,0.001/eccenpar)
call rot3(v01,deftab,v01(3))

* No calculations for passing in back as well
call rot(v01,-deftab,v01(3))

```

2

# swing3.f

```

* Find new v0 from
do 25, i=1,2
v0b2f(i) = v0b2f(i) + v01(i)
25 continue
v0b2f(3) = mag(v0b2f)

* Do calculations for passing on opposite side
do 30, i=1,2
v0b2b(i) = v0b2b(i) + v01(i)
30 continue
v0b2b(3) = mag(v0b2b)

do 35, i=1,3
aorb1(i) = hmas + r01(i)
aorb2(i) = hmas + r02(i)
av0b2f(i) = hmasau + v0b2f(i)
av0b2b(i) = hmasau + v0b2b(i)
35 continue

* Propagate pos and v0 vectors forward along transfer path
call kopier(aorb1,av0b2f,tutact,deutf,av0b2f)

* Use Gauss to determine new transfer parameters
tcb2 = tstay - test
tutcb2 = tcb2 * days
satm = 'a'
call gauss(aorb1f,aorb2,satm,tutcb2,v0b2f,v0b2f)

* Put new velocities in km/s
do 40, i=1,3
v0b2f(i) = v0b2f(i) / hmasau
v0b2b(i) = v0b2b(i) / hmasau
v0b2f(3) = av0b2f(i) / hmasau
40 continue

* Calculate delta-v at c
do 45, i=1,2
dvcf(i) = v0b2f(i) - v0b2b(i)
45 continue
dvcf(3) = mag(dvcf)

.....
* Upon Martian reencounter, attempt a second swing-by to reduce
* the delta-v at b2 necessary. Then, solve the Gaussian problem
* to connect the position vector of Mars at the time of
* reencounter to the position vector to the earth after the return
* time of flight has passed.
.....

* Do second swingby calculations
* Define v0b3
v0b3(1) = -c2 * dsin(nub3+marsmag)
v0b3(2) = c2 * dcos(nub3)
v0b3(3) = mag(v0b3)

* Use v0b3f/b = v0b3f/b + v0b3
do 55, i=1,2
v0b3f(i) = v0b3f(i) + v0b3(i)
55 continue
v0b3f(3) = mag(v0b3f)

rphyp3f = 1.000 * (rphyp3 + v0b3f(3)**2)/mumar
deftabf = 2.000 * dsin(i,0.001/eccenpar)

```



### swing3.f

```

.....
real*8 function mag(v)
    real*8 v(1:3)
    mag = dsqrt(v(1)**2 + v(2)**2 + v(3)**2)
return
end
.....

real*8 function cot(angle)
    implicit logical (a-z)
    real*8 angle
    if (atan(angle) .le. 0.00001d00) then
        cot = 0.000
    else
        cot = 1.000 / atan(angle)
    endif
return
end
.....

subroutine rec3(rec,angle,outvec)
    implicit logical (a-z)
    real*8 rec(1:3),angle,outvec(1:3),mag,temp,c,s
    temp = sec(2)
    c = cos(angle)
    s = sin(angle)
    outvec(3) = c*rec(2) - s*sec(1)
    outvec(1) = c*rec(1) + s*temp
    outvec(2) = mag(outvec)
return
end
.....

subroutine eccent (tof,a,p,delta,e)
* Define variables
    real*8 tof,a,delta,e,rh,massm,ed,p,arg1,arg2,arg3,nr
    real*8 argms,ee,angex,ltof,halfday
* Halfine radius at point a (earth) and point b (mars)
    rh = 1.4959965e8
    rb = 1.325d0 * ra
    massm = 1.3773546e11
    halfday = 12.000 * 3600.000
* Set initial eccentricity guess
    ee = e
    e = ra / (1.000 - ed)
    p = a * (1.000 - (ed**2))
* Calculate angles nu and ee
    arg1 = (p-rb) / (ed*rb)
    nr = dsqrt(arg1)
.....

```

# swing3.f

```

    anspe = dcos(nu)
    arg2 = (anspe+e0) / (1.000 + (e0*anspe))
    ee = dcos(arg2)
    anspe = dln(tee)

    * Calculate new guess time of flight
    arg3 = degt((a**3.000)/musun)
    ltof = arg3 * (ee - e0 + anspe)

    * Compute guess with desired time of flight
    if (dabs(ltof-lot).gt. halfday) then
        e0 = e0 + deltee
        goto 10
    endif

    return
end

subroutine findcands(traw,cnew,snew)
.....
    implicit logical (a-z)
    real*8 snew,cnew,snew,segt,s,segrd
    if (snew.gt. 0.000) then
        segt = segrd(snew)
        cnew = (1.000-dcos(segt)) / snew
        snew = (segt-dln(segt)) / (segt**3)
    else
        segt = snew**2
        cnew = 0.548 - snew/24.000 + segrd/720.000 -
            (segrd**2)/6320.000
        snew = 1.000/6.000 - snew/120.000 + segrd/3040.000 -
            (segrd**2)/362000.000
    endif
    return
end

subroutine elorb(r,v,p,e,cc,nu,ans)
.....
    * This routine finds the classical orbital elements given position and
    * velocity vectors at a point in the orbit
    .....
    implicit logical (a-z)
    real*8 r(1:3),v(1:3),p,e,cc,nu,c1,rdec,c3,small,ans
    real*8 hbar,abar(1:3),temp,halfpi,phi,dot,musun
    integer i
    character*2 typenrhit

    * Initialize variables
    musun = 1.327156401
    p1 = dcos(-1.000)
    temp1 = 2.000
    halfpi = pi / 2.000
    small = 0.0000100
    infinite = 99999.900
    undefine = 99999.100

    * Find h, e, and a vectors
    hbar = r(1)*v(2) - r(2)*v(1)

```

```

    if (dabs(hbar).gt. small) then
        c1 = v(3)**2 - musun/r(3)
        rdec = r(1)*v(1) + r(2)*v(2)
        do 10 i=1,2
            abar(i) = (c1*r(i) - rdec*v(i)) / musun
        continue
        abar(3) = mag(abar)

    * Find a, e, and p
    ans = (v(3)**2/2.000) - (musun/r(3))
    if (dabs(ans).gt. small) then
        a = -musun / (2.000*ans)
    else
        a = infinite
    endif
    ecc = abar(3)
    p = (hbar**2) / musun

    * Find true anomaly at epoch
    if ((abar(3)*r(3)).gt. small) .and. (ecc.gt. small) then
        nu = dacos((abar(1)*r(1) + abar(2)*r(2)) / (abar(3)*r(3)))
        if (rdec.lt. 0.000) then
            nu = twopi - nu
        endif
    else
        nu = undefined
    endif
    else
        p = undefined
        a = undefined
        ecc = undefined
        nu = undefined
        ans = undefined
    endif
    return
end

subroutine kepler(r0,v0,tlim,r,v)
.....
    implicit logical (a-z)
    real*8 r0(1:3),v0(1:3),tlim,r(1:3),v(1:3),f,g,fdot,gdot,deltat
    real*8 soid,soidgrd,answ,answgrd,snew,cnew,snew,tlimnew,rdec
    real*8 a,alpha,ans,period,a,v,temp,small,twopi,halfpi,dot,cot
    integer i

    * Initialize variables
    halfpi = dacos(-1.000) / 2.000
    twopi = 2.000 * dacos(-1.000)
    infinite = 99999.900
    small = 0.0000100
    tlimnew = -10.000
    rdec = (r0(1)*v0(1) + r0(2)*v0(2))
    do 5 i=1,3
        v(i) = 0.000
    continue

    * Find ans, alpha, and a
    ans = (v0(3)**2 / 2.000) - (1.000/r0(3))
    alpha = -ans*2.000
    if (dabs(ans).gt. small) then

```

```

    sold = new
    goto 10
endif
if (i - st, 15) then
    write*, 'Repier not covered in 15 iterations'
else

```

```

a = -1.000 / (2.000*mp)
else
  a = infinite
endif

if (dabs(alpha) .lt. small) then
  alpha = 0.000
endif

* Make initial guess for a
* Circle and ellipse
  if (alpha .gt. small) then
    period = (cmpl + dgrt(dabs(a)))
    if (dabs(t) .gt. dabs(period)) then
      time = dabs(t) + period
    endif
    if (dabs(alpha) .gt. small) then
      aold = time + alpha
    else
      aold = time*alpha*0.9700
    endif
  else
    aold = time*alpha*0.9700
  endif

* Parabola
  if (dabs(alpha) .lt. small) then
    a = 0.500 + (halfp) - dabs(3.000*dgrt(1.000/
      / (r(3)-a)))
    w = dabs(a)
    aold = dgrt(r(3)) + (2.000*sqrt(2.000*w))
  else
    temp = -2.000 + time / (a*(dabs(a) + sign(1.000,time) +
      / dgrt(-a)*(1.000-r(3)/a)))
    aold = sign(1.000,time) + dgrt(-a) + dlog(temp)
  endif

* Hyperbola
  i = 1
  continue
  if (dabs(time-temp) .gt. 0.000100) .and. (i.le.15)) then
    aold = aold + temp
    anew = aold + alpha
  else
    temp = -2.000 + time / (a*(dabs(a) + sign(1.000,time) +
      / dgrt(-a)*(1.000-r(3)/a)))
    aold = sign(1.000,time) + dgrt(-a) + dlog(temp)
  endif

* Find c and a functions
  call findcands(aold,anew,cnew,snew)

* Use Newton iteration for new values
  / timeold = aold + aold*anew + r(3)*aold*cnew +
  / r(3)*aold*(1.000 - snew*snew)
  / dclat = aold + aold*cnew + r(3)*aold*(1.000-snew*snew) +
  / r(3)*(1.000 - snew*cnew)

* Calculate new value for a
  anew = aold + (time-timeold) / dclat

* Check to see if the step size must be changed
  / if (a .gt. 0.000) .and. (abs(anew) .gt. temp*dgrt(a))
  / .and. (abs(.lt. 0.000)) then
    anew = aold + (time-timeold) / dclat*10.000
  endif

* Write out iterations (take out later)
  write(*,60) i,aold,timeold,dclat,anew,snew,cnew,snew
  i = i + 1

```



9306/25  
9730330

```

* Define boundaries for s-iteration
upper = temp1+2
lower = -2.000*temp1

* Ensure orbit is possible
if (abs(upper) < .01, small) then
  continue
  i = 0
  continue
  if (abs((tnew-time) - .01, small)) and, (i .le. 30) then
    v = r1(3) + r2(3) - (vars*(1.000-sold*snew)/degt(cnew))
    if ((vars < .01, 0.000) and, (y .lt. 0.000)) then
      j = 1
      continue
      if (y .lt. 0.000) and, (j .lt. 10) then
        snew = 0.500*(1.000/snew)*(1.000 - (r1(3)+r2(3))
          *degt(cnew)/vars)
        j = j + 1
        goto 30
      endif
      if (j .ge. 10) then
        write(*,*) 'Iteration failed for Yn in Gauss'
        endif
      endif
      sold = degt(y/cnew)
      soldnew = sold**3
      tnewnew = soldnew*vars*degt(y)

* Adjust upper and lower bounds
      if (tnewnew .lt. time) then
        lower = sold
        if (tnewnew .gt. time) then
          upper = sold
        endif
        if (tnewnew .gt. time) then
          upper = sold
        endif
        snew = (upper+lower) / 2.000

* Ensure first guess isn't too close
        if ((abs(tnewnew-time) .lt. small) and, (1.eq.0)) then
          endif

* Find c and s functions
        call findcands(tnew, cnew, snew)
        sold = snew
        lower = sold
        v = r1(3) + r2(3) - (vars*(1.000-sold*snew)/
          *degt(cnew))
        j = j + 1
        goto 30
      endif
      if (j .ge. 10) then
        write(*,*) 'Iteration failed for Yn in Gauss'
        endif
      endif
      sold = degt(y/cnew)
      soldnew = sold**3
      tnewnew = soldnew*vars*degt(y)

* Adjust upper and lower bounds
      if (tnewnew .lt. time) then
        lower = sold
        if (tnewnew .gt. time) then
          upper = sold
        endif
        if (tnewnew .gt. time) then
          upper = sold
        endif
        snew = (upper+lower) / 2.000

* Ensure first guess isn't too close
        if ((abs(tnewnew-time) .lt. small) and, (1.eq.0)) then
          endif

* Find c and s functions
        call findcands(tnew, cnew, snew)
        sold = snew
        lower = sold
        v = r1(3) + r2(3) - (vars*(1.000-sold*snew)/
          *degt(cnew))
        j = j + 1
        goto 30
      endif
      if (j .ge. 10) then
        write(*,*) 'Gauss not converged in 30 iterations'
        else
          write(*,*) 'Gauss not converged in 30 iterations'
          v = 1.000 - (y/r1(3))
          s = vars*degt(y)
          snew = 1.000 - y/r2(3)
          do 40 i = 1, 2

```

swing3.f

```

40
      v1(1) = (r2(1) - f*(1(1)) / g
      v2(1) = (goc*r2(1) - r1(1)) / g
      continue
    endif
    v1(3) = sde(r1)
    v2(3) = sde(r2)
  else
    write(*,*) 'Gauss problem cannot be solved'
    return
  end
end

```

17

## APPENDIX E – FEASIBILITY OF A NONEQUILIBRIUM MHD FOR NEPTUNE

The ability to create and sustain a nonequilibrium state (with electron temperature  $\gg$  heavy particle temperature) throughout the MHD generator is highly dependent upon the density of the gas at the entrance to the generator. This is due to the fact that a more dense gas will have more collisions and tend to equilibrate more quickly. This analysis will determine if the density of the working fluid leaving the NERVA nozzle is low enough to sustain a nonequilibrium state through the generator.

The characteristics of NERVA described in Chapter 6 explained that for a nozzle exit area of  $14.5 \text{ m}^2$ , the density of the working fluid leaving the system would be  $3.51 \times 10^{-4} \text{ kg/m}^3$ . With hydrogen gas as the working fluid, this translates to a number density of  $1.058 \times 10^{17} \text{ cm}^{-3}$ .

Return now to the inequality derived in Chapter 5. It explained the conditions that would have to exist in the gas in order to sustain a nonequilibrium state in the generator:

$$\frac{(n_e)^2 T_e}{j^2} \leq \frac{(5.04 \times 10^{-4}) A}{k Z_e^2 Z(A_e)^{1/2}} \quad (\text{E1})$$

Recall that the right side is completely defined by the working fluid. For hydrogen gas, the inequality may be rewritten:

$$\frac{(n_e)^2 T_e}{j^2} \leq 7.33 \times 10^{13} \quad (\text{E2})$$

Now, apply the same constraints used to define the thermodynamic cycle in Chapter 6. Additionally, substitute  $n_e = \alpha n$ , and solve for the required number density that must exist in the gas for a nonequilibrium condition to be sustained.

$$n^2 \leq \frac{J^2 (7.33 \times 10^{13})}{(hw)^2 T_e \alpha^2} \quad (E3)$$

J : MHD current

The current required to support the mission analyzed thermodynamically in Chapter 6 is 210 kA.

For reasons explained in Chapter 5, the desired degree of ionization in the gas is at least  $10^{-3}$ . The Saha equation is useful in defining the electron temperature necessary to achieve that degree of ionization in a hydrogen working fluid. It reveals that electron temperatures in excess of 10,000 K will be required to sustain the desired degree of ionization at this density.

The only parameter left undefined in the inequality is the channel length of the generator and the width of the generator plates. First, consider a case where the width of the plates and the plate spacing is equal. Since the cross-sectional area of the nozzle inlet is known from NERVA (4.3 m), the width is defined at 2.07 m. Additionally, consider a channel length of 1 m. Inputting these values into the inequality sets the maximum number density for the gas at  $8.29 \times 10^{12} \text{ cm}^{-3}$ .

Comparing this figure to the actual number density at NERVA exit, it is apparent that the gas is considerably too dense (four orders of magnitude) to sustain a nonequilibrium state in the generator. However, looking again at the inequality, the geometrical dimensions of the generator itself can contribute to its ability to sustain nonequilibrium.

It is obviously advantageous to create a generator with short channel length and small plate width. In other words, the generator plate area should remain small, leading to a large current density and more resistive heating. In order to create a small plate width, the plate spacing must grow to retain the same cross-sectional area.

Consider a second case where the channel length is reduced to 0.1 m. Also, let the plate width be a quarter of the plate spacing,  $w = 1.04$  m. Now, the maximum number density increases to  $1.73 \times 10^{14} \text{ cm}^{-3}$ . Still, however, there is more than a two order of magnitude differential between the required and actual densities.

In order to illustrate the significance of this differential, an exit area requirement on the nozzle of NERVA which would result in the desired density, may be calculated.

Since the working fluid may be considered completely recombined into  $\text{H}_2$  at the original nozzle exit, the equations for an adiabatic expansion through a nozzle apply beyond this point. Using the law of conservation of mass and holding the velocity at the nozzle exit constant at 9810 m/s:

$$A_{\text{required}} = \frac{m}{m_{\text{H}_2} n_{\text{required}} u} \quad (\text{E4})$$

The area of a nozzle which produces flow rarefied enough to sustain nonequilibrium in the MHD generator is  $6390 \text{ m}^2$ . This is an outlet radius of 45 meters.

This is obviously an unfortunate result, as it would represent tremendous savings to be able to use a nonequilibrium MHD generator in NEPTUNE. However, an alternative method of achieving the necessary conductivity in the working fluid would be to seed the fluid with liquid metal droplets (e.g. lithium). This can increase the conductivity of the working fluid without making extreme temperatures necessary.

Additionally, different generator geometry could be used. Creating a series of smaller generators, combining to support the load, is a possibility. The small generators would have high current densities and more power, via resistive heating, would be input to the working fluid.

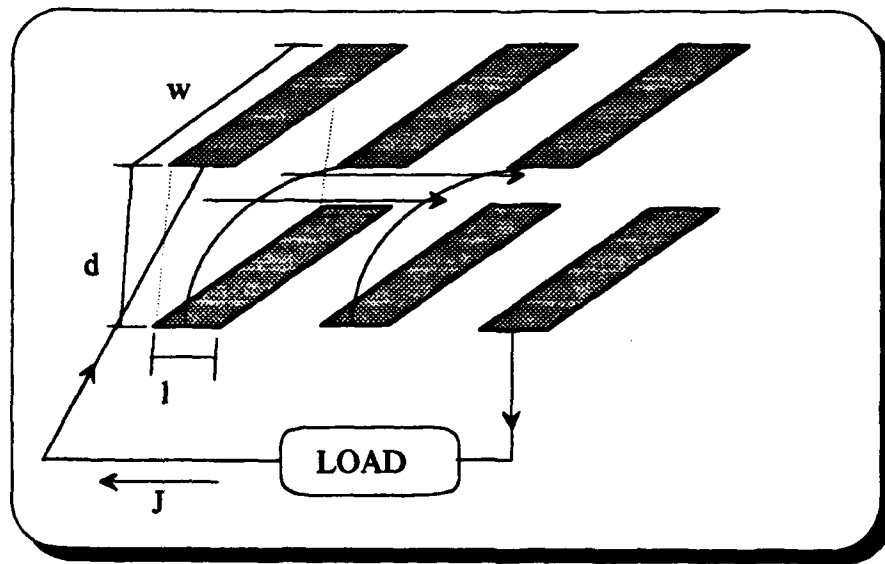


Figure E1 -- Series of MHD Generators

## LIST OF REFERENCES

- <sup>1</sup>Peter J. Turchi, Nuclear Electric Propulsion Using NERVA (NEPTUNE) (Pasadena, CA: Proceedings of Nuclear Electric Propulsion Workshop, Jet Propulsion Laboratory, 19-22 June, 1990), JPL D-9512, May 1992, Vol. I, pp. 2-33.
- <sup>2</sup>Stanley K. Borowski, Solid and Gaseous Core Nuclear Thermal Rockets (Cleveland, OH: Advanced Space Analysis Office, Lewis Research Center), pp. 1-4.
- <sup>3</sup>James T. Walton, System Model Development for Nuclear Thermal Propulsion (Washington D.C.: 43rd Congress of the International Astronautical Federation, 1992), IAF Paper 92-0568.
- <sup>4</sup>Richard J. Rosa, Magnetohydrodynamic Energy Conversion (New York: McGraw-Hill Book Company, 1968), pp. 17-35, 91-110.
- <sup>5</sup>G.J. Womack, MHD Power Generation (London: Chapman and Hall LTD, 1969), pp. 5-60.
- <sup>6</sup>Peter J. Turchi, Design of an MPD Arcjet for Operation at Gigawatt Power Levels (Viareggio, Italy: 22nd International Electric Propulsion Conference Proceedings, 1991), Paper No. 91-058.
- <sup>7</sup>Ernst Stuhlinger, Ion Propulsion for Space Flight (New York: McGraw-Hill Book Company, 1964), p. 279.
- <sup>8</sup>Overview Study of SP Power Technologies for the Advanced Energetic Program (Bellevue, WA: Math Sciences NW, Inc.), NASA CR-165269, pp. 2/19-2/214.
- <sup>9</sup>Roger R. Bate, Donald D. Mueller, and Jerry E. White, Fundamentals of Astrodynamics (New York: Dover Publications, Inc., 1971), pp. 51-271, 357-384.
- <sup>10</sup>Frank Kreith and Mark S. Bohn, Principles of Heat Transfer (New York: Harper Collins Publishers, 1986), p. 18.
- <sup>11</sup>James H. Gilland and Steven R. Oleson, Combined High and Low Propulsion for Fast Piloted Mars Missions (Cleveland, OH: Conference on Advanced SEI Technologies, September, 1991), AIAA Paper 91-2346.

<sup>12</sup>K. J. Hack, et al., Evolutionary Use of Nuclear Electric Propulsion (Cleveland, OH: Conference on Advanced SEI Technologies, September, 1991), AIAA Paper 90-3821.

<sup>13</sup>Roger M. Myers, Maris A. Manteniaks, and Michael R. LaPointe, MPD Thruster Technology (Cleveland, OH: Conference on Advanced SEI Technologies, 1991), AIAA Paper 91-3568.

<sup>14</sup>G. R. Seikel and L. D. Nichols, The Potential of Nuclear MHD Electric Power Systems (Cleveland, OH: NASA Lewis Research Center), pp. 1-5.

<sup>15</sup>Robert G. Jahn, Physics of Electric Propulsion (New York: McGraw-Hill Book Company, 1968), pp.12-83.

<sup>16</sup>Phillip G. Hill and Carl R. Peterson, Mechanics and Thermodynamics of Propulsion (Reading, MA: Addison-Wesley Publishing Company, 1965), pp.102-123.

<sup>17</sup>Lyman Spitzer, Jr., Physics of Fully Ionized Gases (New York: Interscience Publishers, Inc., 1956), pp.65-86.

<sup>18</sup>Private Communication with Roger Myers, Sverdrup Technology, NASA Lewis Research Center, Cleveland, OH.

<sup>19</sup>James Dillon Cobine, Gaseous Conductors (New York: McGraw-Hill Book Company, Inc., 1941) pp.29-56, 205-368.

<sup>20</sup>Merle N. Hirsh and H.J. Oskam, ed., Gaseous Electronics (New York: Academic Press, 1978), pp.173-215, 291-390.

<sup>21</sup>Private Communication with Space Nuclear Thermal Propulsion Program (Albuquerque, NM: Air Force Phillips Laboratory, 1992).

<sup>22</sup>H.W. Liepmann and A. Roshko, Elements of Gasdynamics (New York: John Wiley and Sons, Inc., 1957), pp. 1-34, 124-142.

<sup>23</sup>Robert M. Zubrin, The Use of Low Power Dual Mode Nuclear Thermal Rocket Engines to Support Space Exploration Missions (Denver, CO: Martin Marietta Astronautics Group, 1991), AIAA 91-3406.

<sup>24</sup>David Vallado, Department of Astronautical Engineering Computer Library (Colorado Springs, CO: United States Air Force Academy, 30 August, 1988).

<sup>25</sup>George P. Sutton, Rocket Propulsion Elements (New York: Wiley-Interscience Publishers, 1986), pp.35-65.

- <sup>26</sup>R. Bunde et al., MHD Power Generation (Berlin: Springer-Verlag, 1975), pp.5-38.
- <sup>27</sup>George W. Sutton and Arthur Sherman, Engineering Magnetohydrodynamics (New York: McGraw-Hill Book Company, 1965), pp.15-67,447-468.
- <sup>28</sup>A. D. MacDonald, Microwave Breakdown in Gases (New York: John Wiley and Sons, Inc., 1966), pp.14-33.
- <sup>29</sup>Sanborn C. Brown, Basic Data of Plasma Physics, 1966 (Cambridge, MA: The M.I.T. Press, 1967), pp.13-44.
- <sup>30</sup>Ovid W. Eshbach and Mott Souders, ed., Handbook of Engineering Fundamentals (New York: John Wiley and Sons, 1975), pp.856-863.
- <sup>31</sup>Walter G. Vincenti and Charles H. Kruger, Jr., Introduction to Physical Gas Dynamics (Malabar, FL: Robert E. Krieger Publishing Company, 1965), pp.375-433.
- <sup>32</sup>Robert Rhodes and Dennis Keefer, Numerical Modeling of an RF Plasma in Argon (Tullahoma, TN: University of Tennessee Space Institute, [1988]), AIAA Paper 88-0726.
- <sup>33</sup>G. R. Seikel and L. D. Nichols, The Potential of Nuclear MHD Power Systems (Cleveland: NASA Lewis Research Center) pp.1-10.
- <sup>34</sup>R. R. Holman and S. Way, Exploring a Closed Brayton Cycle MHD Power System Applying NERVA Technology (Pittsburg, PA: Westinghouse Electric Corporation), AIAA Paper 89-2770.
- <sup>35</sup>Overview Study of Space Power Technologies for the Advanced Energetics Program (Bellevue, WA: Math Sciences NW, Inc., [1969]) pp.ch 2, 19-214.
- <sup>36</sup>John Anderson, High Temperature Gas Dynamics (New York: McGraw-Hill Book Company, 1989) pp.364-609.
- <sup>37</sup>Ali Bulent Cambel, Plasma Physics and Magnetofluid-Mechanics (New York: McGraw-Hill Book Company, 1963) pp.80-99.
- <sup>38</sup>Joseph T. Verdeyen, Laser Electronics (Englewood Cliffs, NJ: Prentice-Hall, Inc.) pp. 304-343.
- <sup>39</sup>Space Nuclear Thermal Propulsion (SNTTP) Presentation to Defense Science Board (Draper Laboratory, Boston, MA, 8 May 1992).



<sup>40</sup>John D. Kraus, Electromagnetics (New York: McGraw-Hill, Inc., 1992) pp.39-103.

<sup>41</sup>William C. Reynolds and Henry C. Perkins, Engineering Thermodynamics, (New York: McGraw-Hill, Inc., 1977), pp. 284-362.

<sup>42</sup>Bill Smith, AIAA Brownbag Luncheon (Reston, VA: NASA Space Station Program Office, 1991).

<sup>43</sup>K. J. Hack, J. A. George, and L. A. Dudzinski, Nuclear Electric Propulsion Mission Performance for Fast Piloted Mars Missions (Cleveland, OH: Conference on Advanced SEI Technologies, 1991), AIAA Paper 91-3488.

<sup>44</sup>R. L. Burton, K. E. Clark, and R. G. Jahn, Measured Performance of a Multimegawatt MPD Thruster (Princeton, NJ: Princeton University, 1983), AIAA Paper 81-0684.

<sup>45</sup>M. J. Boyle, K. E. Clark, and R. G. Jahn, Flowfield Characteristics and Performance Limitations of Quasi-Steady Magnetoplasmadynamic Accelerators (Princeton, NJ: AIAA Journal, Vol. 14, No. 7, July, 1976), pp. 955-961.

<sup>46</sup>J. E. Polk and T. J. Pivrotto, Alkali Metal Propellants for MPD Thrusters (Cleveland, OH: Conference on Advanced SEI Technologies, 1991), AIAA Paper 91-3572.

<sup>47</sup>D. Q. King, R. G. Jahn, and K. E. Clark, Effect of Thrust Chamber Configuration on MPD Arcjet Performance (Princeton, NJ: Journal of Applied Physics, Vol. 51, January, 1980), pp. 109-117.

<sup>48</sup>James H. Gilland, NER Mission Sensitivities to System Performance (Cleveland, OH: Lewis Research Center), NASA Contractor Report 189059.

<sup>49</sup>R. R. Holman and S. Way, Exploring a Closed Brayton Cycle MHD Power System Applying NERVA Reactor Technology (Philadelphia, PA: Proceedings of the 22nd Intersociety Energy Conversion Conference, Vol. 4, 1987), pp. 1-6.

<sup>50</sup>S. Sandler and R. Feddersen, Particle Bed Reactor Technology (Huntsville, AL: AIAA Space Program and Technologies Conference, March 24-26, 1992), AIAA Paper 92-1493.

<sup>51</sup>Joel C. Sercel, Multimegawatt Nuclear Electric Propulsion First Order System Design and Performance Evaluation (Pasadena, CA: Jet Propulsion Laboratory, January 19, 1987), JPL D-3898, pp. 1-47.